August 1, 2019

# A First Course in Hydraulics

John D. Fenton

Institute of Hydraulic Engineering and Water Resources Management
Vienna University of Technology, Karlsplatz 13/222,
1040 Vienna, Austria

**URL:** *http://johndfenton.com/*
**URL:** *mailto:JohnDFenton@gmail.com*

### Abstract

This course of lectures is an introduction to hydraulics, the traditional name for fluid mechanics in civil and environmental engineering where sensible and convenient approximations to apparently-complex situations are made. An attempt is made to obtain physical understanding and insight into the subject by emphasising that we are following a *modelling* process, where simplicity, insight, and adequacy go hand-in-hand. We hope to include all important physical considerations, and to exclude those that are not important, but with understanding of what is being done. It is hoped that this will provide a basis for further sophistication if necessary in practice – if a problem contains unexpected phenomena, then as much advanced knowledge should be used as is necessary, but this should be brought in with a spirit of scepticism.

## Table of Contents

# Useful reading and reference material

| | |
|---|---|
| **Historical works** | |
| Garbrecht, G. (ed.) (1987) *Hydraulics and hydraulic research: a historical review,* Rotterdam ; Boston : A.A. Balkema | An encyclopaedic historical overview |
| Rouse, H. and S. Ince (1957) *History of hydraulics,* Iowa Institute of Hydraulic Research, State University of Iowa | An interesting readable history |
| **Standard fluid mechanics & hydraulics textbooks** | |
| Douglas, J.F., J.M. Gasiorek, and J.A. Swaffield (2001) *Fluid mechanics,* Pearson Education | Standard hydraulics textbook |
| Francis, J.R.D. and P. Minton (1984) *Civil engineering hydraulics*, E. Arnold | A clear and brief presentation |
| Featherstone, R.E., and C. Nalluri (1995) *Civil engineering hydraulics: essential theory with worked examples*, Blackwell Science | Practically-oriented, with examples |
| Rouse, H. (1946) *Elementary mechanics of fluids*, Wiley | Clear and high-level explanation of the basics |
| Street, R. L., G. Z. Watters, and J. K. Vennard (1996) *Elementary fluid mechanics*, Wiley | Standard hydraulics textbook |
| Streeter, V. L., and E. B. Wylie (1998) *Fluid mechanics*, McGraw-Hill | Standard hydraulics textbook |
| White, F. M. (2003) *Fluid Mechanics*, Fifth edn, McGraw-Hill | Standard hydraulics textbook |
| **Worked solutions** | |
| Alexandrou, A. N. (1984) *Solutions to problems in Streeter/Wylie, Fluid mechanics*, McGraw-Hill | |
| Douglas, John F (1962) *Solution of problems in fluid mechanics*,Pitman Paperbacks | |
| **Books which deal more with practical design problems** – of more use in later semesters | |
| Chadwick, A. and J. Morfett (1993) *Hydraulics in civil and environmental engineering*, EFN Spon | Practice-oriented |
| Mays, L. W. (editor-in-chief) (1999) *Hydraulic design handbook*, McGraw-Hill | Encyclopaedic, and outside this course |
| Novak, P. et al. (1996) *Hydraulic structures*, Spon | Practice-oriented |
| Roberson, J. A., J. J. Cassidy, M. H. Chaudhry (1998) *Hydraulic engineering*, Wiley | Practice-oriented |
| Sharp, J.J. (1981) *Hydraulic modelling*, Butterworths | For modelling and dimensional similitude |

# References

Batchelor, G. K. (1967), *An Introduction to Fluid Dynamics*, Cambridge.

Colebrook, C. F. (1939), Turbulent flow in pipes with particular reference to the transition region between the smooth and rough pipe laws, *J. Inst. Civ. Engrs* **11**, 133–156.

Colebrook, C. F. & White, C. M. (1937), Experiments with fluid friction in roughened pipes, *Proc. Roy. Soc. London Ser. A* **161**, 367–381.

Fenton, J. D. (2002), The application of numerical methods and mathematics to hydrography, in *Proc. 11th Australasian Hydrographic Conference, 3 July - 6 July 2002*, Sydney.

Fenton, J. D. (2005), On the energy and momentum principles in hydraulics, in *Proc. 31st Congress IAHR, Seoul*, pp. 625–636.

Haaland, S. E. (1983), Simple and explicit formulas for the friction factor in turbulent pipe flow, *J. Fluids Engng* **105**, 89–90.

Montes, S. (1998), *Hydraulics of Open Channel Flow*, ASCE, New York.

Moody, L. F. (1944), Friction factors for pipe flow, *Trans. ASME* **66**, 671–684 (including discussion).

Rouse, H. (1937), Modern conceptions of the mechanics of fluid turbulence, *Trans. ASCE* **102**(1965 (also published in facsimile form in *Classic Papers in Hydraulics* (1982), by J. S. McNown and others, ASCE)), 52–132.

Sharp, B. B. (1981), *Water Hammer*, Edward Arnold.

Streeter, V. L. & Wylie, E. B. (1981), *Fluid Mechanics*, first SI Metric edn, McGraw-Hill Ryerson, Toronto.

Swamee, P. K. & Jain, A. K. (1976), Explicit equations for pipe-flow problems, *J. Hydraulics Div. ASCE* **102**, 657–664.

White, F. M. (2003), *Fluid Mechanics*, fifth edn, McGraw-Hill, New York.

# 1. The nature and properties of fluids, forces, and flows

## 1.1 Properties of fluids

### 1.1.1 Definition of a fluid

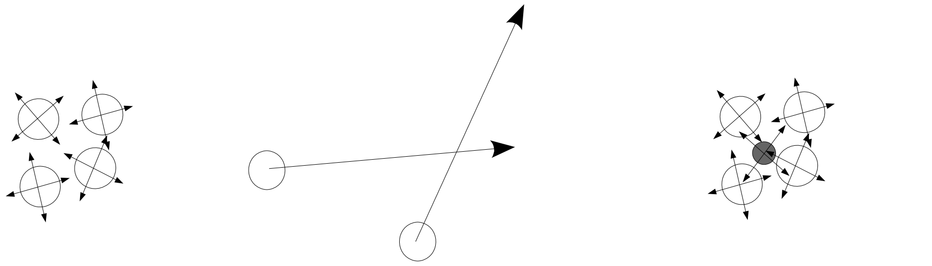

(a) Liquid (b) Gas (c) Liquid with other molecule

Figure 1-1. Behaviour of typical molecules (a) of a liquid, (b) a gas, and (c) a different molecule in a liquid

A fluid is matter which, if subject to an unbalanced external force, suffers a continuous deformation. The forces which may be sustained by a fluid follow from the structure, whereby the molecules are able to move freely. Gas molecules have much larger paths, while liquid molecules tend to be closer to each other and hence are heavier.

Fluids can withstand large compressive forces (pressure), but only negligibly small tensile forces. Fluids at rest cannot sustain shear forces, however fluids in relative motion do give rise to shear forces, resulting from a momentum exchange between the more slowly moving particles and those which are moving faster. The momentum exchange is made possible because the molecules move relatively freely.

Especially in the case of a liquid, we can use the analogy of smooth spheres (ball bearings, billiard balls) to model the motion of molecules. Clearly they withstand compression, but not tension.

| Molecular characteristic | Solids | Fluids | |
|---|---|---|---|
| | | Liquids | Gases |
| Spacing | Small (material is heavy) | | Large (light) |
| Activity | Very little | Vibratory | Great, molecules moving at large velocities and colliding |
| Structure | Rigid, molecules do not move relative to each other. Stress is proportional to strain | If confined, elastic in compression, not in tension or shear. | |
| Response to force | Resisted continuously, static or dynamic | Molecules free to move and slip past one another. If a force is applied it continues to change the alignment of particles. Liquid resistance is dynamic (inertial and viscous). | |

Table 1-1. Characteristics of solids and fluids

### 1.1.2 The continuum hypothesis

In dealing with fluid flows we cannot consider individual molecules. We replace the actual molecular structure by a hypothetical continuous medium, which at a point has the mean properties of the molecules surrounding the point, over a sphere of radius large compared with the mean molecular spacing. The term "fluid particle" is taken to mean a small element of fluid which contains many molecules and which possesses the mean fluid properties at its position in space.

### 1.1.3 Density

The density $\rho$ is the mass per unit volume of the fluid. It may be considered as a point property of the fluid, and is the limit of the ratio of the mass $\delta m$ contained in a small volume $\delta V$ to that volume:

$$\rho = \lim_{\delta V \to 0} \frac{\delta m}{\delta V}.$$

In fact the limit introduced above must be used with caution. As we take the limit $\delta V \to 0$, the density behaves as shown in Figure 1-2. The real limit is $\delta V \to \delta V^*$, which for gases is the cube of the mean free path, and for liquids is the volume of the molecule. For smaller volumes considered the fact that the fluid is actually an assemblage of particles becomes important. In this course we will assume that the fluid is continuous, the *continuum hypothesis*.

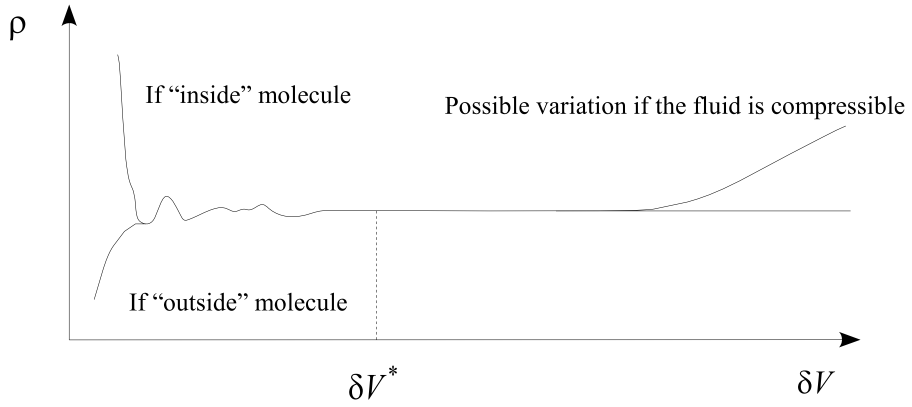


Figure 1-2. Density of a fluid as obtained by considering successively smaller volumes $\delta V$, showing the apparent limit of a constant finite value at a point, but beyond which the continuum hypothesis breaks down.

As the temperature of a fluid increases, the energy of the molecules as shown in Figure 1-1 increases, each molecule requires more space, and the density decreases. This will be quantified below in §1.1.8, where it will be seen that the effect for water is small.

### 1.1.4 Surface tension

This is an important determinant of the exchange processes between the air and water, such as, for example, the purification of water in a reservoir, or the nature of violent flow down a spillway. For the purposes of this course it is not important and will not be considered further.

### 1.1.5 Bulk modulus and compressibility of fluids

The effect of a pressure change $\delta p$ is to bring about a compression or expansion of the fluid by an amount $\delta V$. The two are related by the bulk modulus $K$, constant for a constant temperature, defined:

$$\delta p = -K \frac{\delta V}{V}.$$

The latter term is the "volumetric strain". $K$ is large for liquids, so that density changes due to pressure changes may be neglected in many cases. For water it is $2.070\ \mathrm{G\,N\,m^{-2}}$. If the pressure of water is reduced from 1 atmosphere (101,000 $\mathrm{N\,m^{-2}}$) to zero, the density is reduced by 0.005%. Thus, for many practical purposes water is incompressible with change of pressure.

### 1.1.6 Diffusivity

Fluids may contain molecules of other materials, such as chemical pollutants. The existence of such materials is measured by the mass concentration per unit volume $c$ in a limiting sense as the measuring volume goes to zero. at a point, invoking the continuum hypothesis. The particles will behave rather similarly to individual fluid molecules but where they retain their identity, as suggested in Figure 1-1(c).

Diffusion is the spontaneous spreading of matter (particles or molecules), heat, momentum, or light because of a continuous process of random particle movements. No work is required for diffusion in a closed system. It is one type of transport process, which in many areas of water engineering is not important and can be neglected, yet it is responsible for several important processes as well.

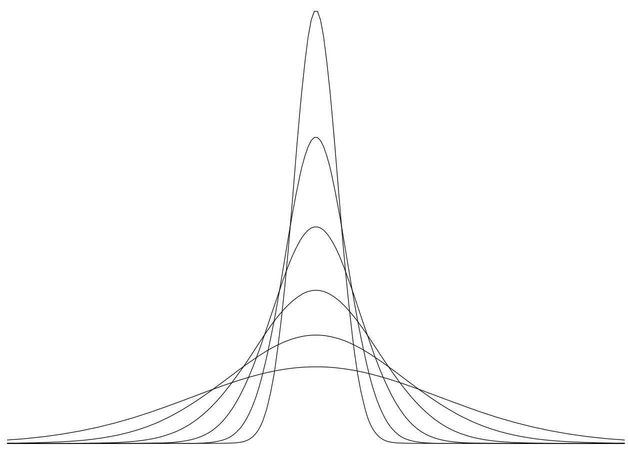

Figure 1-3. Typical behaviour of diffusion of an initial point concentration

We can consider a discrete physical analogy that reveals the nature of diffusion, but instead of a three-dimensional medium, a one-dimensional medium is considered, where a single particle is free to make a series of discrete movements, either to left or right, according to no particular physical law, merely the likelihood that the particle will move and it can move in either direction. If we consider an initial cloud of many particles concentrated near a single point, it can be shown that this process proceeds as shown in Figure 1-3, where the concentration is plotted vertically as a function of horizontal distance $x$. It shows the macroscopic behaviour of diffusion, where irregularities and concentrations spread out as time passes, such that as time becomes infinite the diffusing quantity is everywhere but in vanishingly-small quantities. This is perhaps a surprising result, that in a cloud of particles, if a particle can go in any direction, the net result is for it to spread out. If we consider a region of uniform concentration, say, then if any particle moves, it moves to the same concentration. On the edge of the cloud, however, a particle can move either back into the cloud, not changing the concentration, or it can move out of the cloud, thereby contributing to the spreading out of the cloud. At the next time step, this would be repeated, and so on.

It can be shown that we obtain *Fick's law*[1] for the mass flux (flow) $J_x$ in the $x$ direction due to diffusion:

$$J_x = -\kappa \frac{\partial c}{\partial x}. \tag{1.1}$$

where $\kappa$ is the *coefficient of diffusion*, of dimensions $\mathrm{L}^2\mathrm{T}^{-1}$, expressing the ease with which particles move through the surrounding medium. The negative sign is because particles flow from a region of high concentration to one of low. Note that $J_x$ has units of concentration $\times$ velocity, the rate at which matter is being transported per unit cross-sectional area of flow.

Hence we have seen that the flow of matter is proportional to the gradient of the concentration – but that this does not come from any special physical property of the concentration, such as particles being repelled by similar particles, but merely because where there are many particles there will be more travelling away from that region than are travelling to that region. In all cases of diffusion, the net flux of the transported quantity (atoms, energy, or electrons) is equal to a physical property (diffusivity, thermal conductivity, electrical conductivity) multiplied by a gradient (a concentration, thermal, electric field gradient). Noticeable transport occurs only if there is a gradient - for example in thermal diffusion, if the temperature is constant, heat will move as quickly in one direction as in the other, producing no net heat transport or change in temperature.

In Brownian motion and diffusion the random motion comes from the molecular natures of the constituents. Below it will be shown that in fluids this leads to the physical attribute of viscosity. Subsequently it is shown that in real pipes and waterways the random motion is dominated by the movement in the water of finite masses of water, rather than to individual molecules.

[1] Adolf Fick (born 1829, in Kassel, Germany; died 1901), a medical doctor. He is usually credited with the invention of contact lenses as well.

### 1.1.7 Viscosity

If, instead of the fluid being stationary in a mean sense, if parts of it are moving relative to other parts, then if a fluid particle moves randomly, as shown above, it will in general move into a region of different velocity, there will be some momentum transferred, and an apparent force or stress appears. This gives rise to the phenomenon of *viscosity*, which is a diffusivity associated with the momentum or velocity of the moving fluid, and has the effect of smoothing out velocity gradients throughout the fluid in the same way that we saw that diffusivity of a substance in water leads to smoothing out of irregularities.

**A model of a viscous fluid:** Consider two parallel moving rows of particles, each of mass $m$, with $N$ in each row. The bottom row is initially moving at velocity $u$, the upper at $u+\delta u$, as shown in the figure. At a certain instant, one particle moves, in the random fashion associated with the movement of molecules even in a still fluid, as shown earlier, from the lower to the upper row and another moves in the other direction.

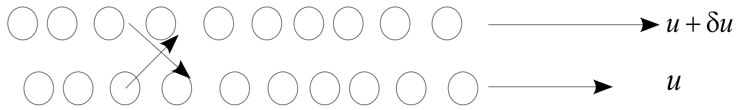


The velocities of the two rows after the exchange are written as $v$ and $v+\delta v$. Now considering the momenta of the two layers, the effect of the exchange of particles has been to increase the momentum of the slow row and decrease that of the fast row. Hence there has been an apparent force across the interface, a *shear stress*.

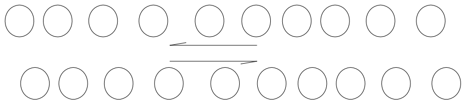

This can be quantified:

| | | |
|---|---|---|
| Initial $x$-momentum of bottom row | = | $(Nm)u$ |
| Initial $x$-momentum of top row | = | $(Nm)(u+\delta u)$ |
| Change of $x$-momentum of bottom row | = | $+m\delta u$ |
| Change of $x$-momentum of top row | = | $-m\delta u$ |
| Final $x$-momentum of bottom row | = | $(Nm)v$ |
| Final $x$-momentum of top row | = | $(Nm)(v+\delta v)$ |

In the absence of other forces, equating the momenta gives

$$\begin{aligned} Nmv &= Nmu + m\,\delta u \\ Nm(v+\delta v) &= Nm(u+\delta u) - m\,\delta u \end{aligned}$$

Thus,

$$\begin{aligned} v &= u + \frac{\delta u}{N}, \quad \text{and} \\ v+\delta v &= u + \delta u - \frac{\delta u}{N}. \end{aligned}$$

Hence the lower slower fluid is moving slightly faster and the faster upper fluid is moving slightly slower than before. Subtracting, the velocity difference between them now gives

$$\delta v = \delta u - 2\frac{\delta u}{N},$$

thus $\delta v < \delta u$, and we can see the effect of viscosity in reducing differences throughout the fluid.

In fact, if we consider the whole shear flow as shown in Figure 1-4, we can obtain an expression for shear stress in the fluid in terms of the velocity gradient, as follows:

$$\text{Impulse of top row on bottom} = m\,\delta u.$$

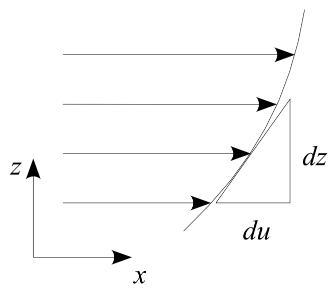


Figure 1-4. Shear flow, where the velocity in one direction $u$ is a function of the transverse velocity co-ordinate $z$

If $T$ is the average time between such momentum exchanges, then

$$\text{mean shear force} = \frac{m\,\delta u}{T}.$$

As the horizontal velocity $u$ is a function of $z$, then if the two rows are $\delta z$ apart, the differential of $u$ is

$$\delta u = \frac{du}{dz}\delta z,$$

and the mean shear stress per unit distance normal to the flow is

$$\text{mean shear stress} = \frac{\text{mean shear force}}{\text{length} \times 1} = \frac{m\,du/dz\,\delta z}{T\,N\,\delta x},$$

where $\delta x$ is the mean particle spacing in $x$. Now, $m$, $N$ $T$, $\delta x$ and $\delta z$ are characteristic of the fluid and not of the flow, and so we have

$$\text{mean shear stress} \propto \frac{du}{dz},$$

the transverse velocity shear gradient. Fluids for which this holds are known as *Newtonian Fluids*, as are most common fluids. The law is written

$$\tau = \mu\frac{du}{dz}, \tag{1.2}$$

where $\mu$ is the *coefficient of dynamic viscosity*, which is defined here. Although we have only considered parallel flows here, the result has been found to apply throughout Newtonian fluid flow.

**Effects of viscosity:** The law (equation 1.2) shows how a transverse shear flow gives rise to shear stresses, which acts, as suggested more immediately by the molecular argument above, so as to redistribute momentum throughout a fluid. (Consider how stirring a bucket of water with a thin rod can bring all the water into rotation - imagine trying to stir a fluid without viscosity!) If the fluid at the boundary of a flow has a certain specified velocity (*i.e.* momentum per unit mass), then viscosity acts so as to distribute that momentum throughout the fluid. This can be shown by considering the entry of flow into a pipe as shown in Figure 1-5. On the pipe wall the fluid velocity must be zero, as the molecules adhere to the wall. Immediately inside the pipe entrance the velocity differences are large, as viscosity has not yet had time to act, but as flow passes down the pipe viscosity acts so as to smooth out the differences, until a balance is reached between the shear stresses set up by the viscosity, the driving pressure gradient, and the momentum of the fluid.

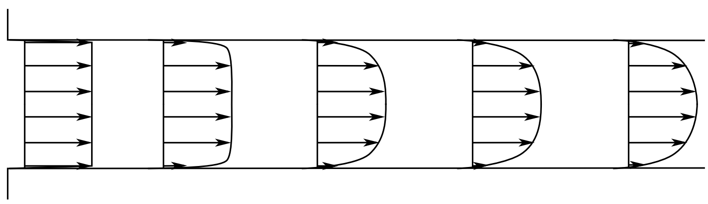

Figure 1-5. Entry of viscous flow into a pipe, showing the effect of viscosity smoothing the initially discontinuous velocity distribution

**Kinematic viscosity:** In the above discussion we gave a physical explanation as to why $\tau = \mu\, du/dz$. In resisting applied forces (such as gravity or pressure) the response of the fluid is proportional to the density $\rho$:

$$\text{Total net force} = \text{ mass} \times \text{ acceleration},$$

so that

$$\begin{aligned}\mu\times & \quad (\text{ terms involving velocity gradients}) + \text{pressure terms} \\ & \propto \quad \rho \times (\text{terms involving fluid accelerations}).\end{aligned}$$

It can be seen that dividing by density $\rho$ shows that in the fundamental equation of motion the viscosity appears in the ratio $\mu/\rho$. This is the *Kinematic viscosity* $\nu$:

$$\nu = \frac{\mu}{\rho}.$$

Typical values for air and water are such that $\mu_{\text{air}}/\mu_{\text{water}} = 1.8 \times 10^{-2}$. However, $\rho_{\text{air}}/\rho_{\text{water}} = 1.2 \times 10^{-3}$, and calculating the ratio of the kinematic viscosities gives:

$$\nu_{\text{air}}/\nu_{\text{water}} = 15.$$

Hence we find that in its effect on the flow patterns, air is 15 times more viscous than water!

However, the viscosities of both air and water are small (compared with honey) and are such that viscous effects are usually confined to thin layers adjacent to boundaries. In the body of the flow viscosity in itself is unimportant, however it is the reason that flows which are large and/or fast enough become unstable and turbulent, so that instead of single molecules transferring momentum, finite masses of water move irregularly through the flow redistributing momentum, and tending to make flows more uniform.. In most flows of water engineering significance, the effects of turbulence are much greater than those of molecular viscosity.

**The relative unimportance of viscous terms in many hydraulic engineering flows**

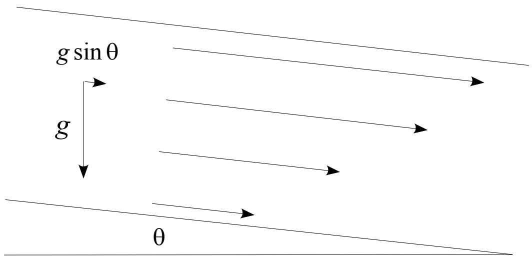


Figure 1-6. Hypothetical laminar flow in a river if molecular viscosity were important

We consider a simple model to give us an idea of the importance of viscosity. In fact, we proceed naively, presuming no knowledge of actual river flows, but supposing – incorrectly as we will see – that the flow is laminar, such that it consists of layers of fluid of different velocity moving smoothly over each other in a macroscopic sense, all irregularities being at a molecular scale.

Consider the hypothetical river as shown in Figure 1-6 with typical characteristics: $2\,\mathrm{m}$ deep, with a slope of $\sin\theta = 10^{-4}$, a surface velocity of $1\,\mathrm{m\,s^{-1}}$, and a velocity on the bottom of 0, as fluid particles on a solid surface do not move. The stress on the bottom can be estimated using Newton's law of viscosity, equation (1.2), assuming a constant velocity gradient as a rough approximation, to calculate the force due to molecular viscosity on the bottom of the stream, giving $du/dz \approx (1-0)/2 = 0.5\,\mathrm{s^{-1}}$:

$$\begin{aligned}\text{Shear stress on bottom} &= \mu\frac{du}{dz} = \rho\nu\frac{du}{dz} \\ &= 1000 \times 10^{-6} \times 0.5 \\ &\approx 5 \times 10^{-4}\,\mathrm{N\,m^{-2}}.\end{aligned}$$

Now we estimate the gravity force on a hypothetical volume in the water extending from the bed to the surface, and from this we obtain the mean stress component parallel to the bed. The vertical gravity force is volume×density×$g$ $= \rho g$×depth×plan area of the volume, so that the pressure due to gravity on the bottom is approximately (assuming $g \approx 10$) given by $1000 \times 10 \times 2 = 20000\,\mathrm{N}$. The component parallel to the bed, multiplying by $\sin\theta$ is $20000 \times 10^{-4} = 2.0\,\mathrm{N}$[2]. Hence the ratio of viscosity/gravity $\approx 5 \times 10^{-4}/2.0 = 0.00025$ Hence, *molecular* viscosity is unimportant in determining the stresses.

However, as we have considered all the forces acting parallel to the bed, and we have obtained a huge imbalance in the forces, our model seems defective. How can a typical river of these dimensions flow without the dominant gravity accelerating the flow hugely? The answer to this question will be presented in §1.4.2.

### 1.1.8 Typical values of physical properties of water

| Temperature ($^\circ$C) | 0 | 4 | 10 | 20 | 30 | ... | 50 | ... | 100 |
|---|---|---|---|---|---|---|---|---|---|
| Density ($\mathrm{kg\,m^{-3}}$) | 999.8 | 1000 | 999.7 | 998.3 | 995.7 | ... | 988 | ... | 958.1 |
| Kinematic viscosity (units of $10^{-6}\ \mathrm{m^2\,s^{-1}}$) | 1.780 | 1.584 | 1.300 | 1.006 | 0.805 | ... | 0.556 | ... | 0.294 |

Table 1-2. Variation with temperature of the properties of pure water with no dissolved substances, from Jirka (2005) for the companion subject to this

The density of water depends on temperature (see Table 1-2), dissolved solid concentration (especially salt), but little with pressure, as we have seen above. Changes in temperature and salinity are responsible for a number of phenomena associated with convection currents and gravity currents, particularly in the ocean and lakes. However in many fluid flows in rivers and pipes, these differences are small and can be ignored.

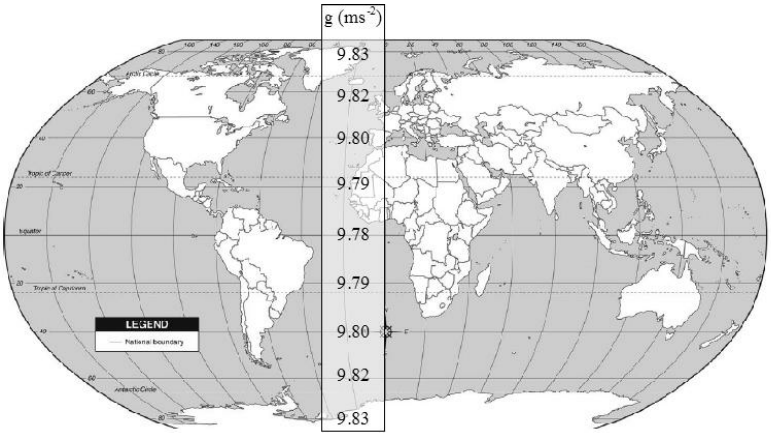


Figure 1-7. Variation of gravitational acceleration $g$ ($\mathrm{m\,s^{-2}}$) with latitude.

Gravitational acceleration varies between $9.78\,\mathrm{m\,s^{-2}}$ at the equator and $9.83\,\mathrm{m\,s^{-2}}$ at the poles, so that students could use an appropriate value, as portrayed in Figure 1-7, however it is clear that a value of $9.8\,\mathrm{m\,s^{-2}}$ is accurate enough, and even a value of $10\ \mathrm{m\,s^{-2}}$ (correct to $2\%$) could be used with an accuracy commensurate with almost all of the theories and methods presented in this course.

| | | |
|---|---|---|
| Density of fresh water $\rho$ | 1000 | $\mathrm{kg\,m^{-3}}$ |
| Density of sea water $\rho$ | 1025 | $\mathrm{kg\,m^{-3}}$ |
| Gravitational acceleration $g$ | $9.8 \approx 10$ | $\mathrm{m\,s^{-2}}$ |
| Kinematic viscosity $\nu$ | $10^{-6}$ | $\mathrm{m^2\,s^{-1}}$ |

Table 1-3. Typical values of physical properties associated with water problems

In view of all the above remarks, in many engineering problems and in this course typical constant values can be assumed, which are set out in Table 1-3. It is a strange fact, and with the exception of the density of fresh water, an accidental one, that all of these quantities are close to an integer power of 10!

[2] To have a feel for what a force specified in Newton is, 1 N is approximately the weight force on an apple!

# 1.2 Forces acting on a fluid

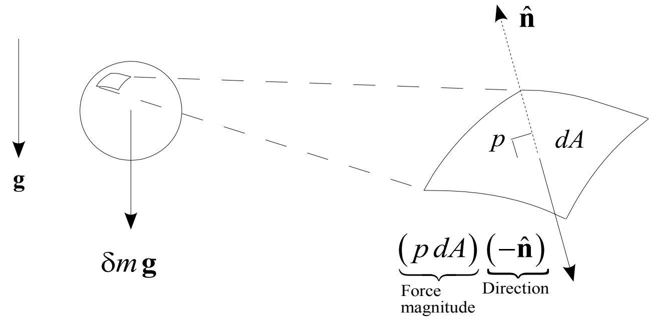


(a) Body force vector acting through centre of mass of fluid particle

(b) Pressure force vector acting normal to local surface of fluid

Figure 1-8. The two types of forces acting on a fluid particle – body force such as gravity acting through the centre of mass, and surface force, in this case pressure acting normally to the local surface.

Consider figure 1-8 showing the two dominant types of forces acting on fluid particles.

1. **Body forces –** this type of force acts at a distance, penetrating deep inside the fluid. - the most common is that due to gravity. It is usually expressed as an acceleration, or, force per unit mass:

$$\delta \mathbf{F}_{\text{body}} = \delta m\, \mathbf{g} = \rho \mathbf{g}\, \delta V,$$

where $\mathbf{g}$ is the acceleration due to gravity, $\mathbf{g} = (0, 0, -g)$, where we have assumed that the $z$ co-ordinate is vertically upwards.

2. **Surface forces**
   a. **Pressure forces** – These are due to molecular motions of particles. Let $\hat{\mathbf{n}}$ be a unit vector normal to the surface, directed into the fluid, then

$$\delta \mathbf{F}_{\text{pressure}} = -p\, dA\, \hat{\mathbf{n}}.$$

   Pressure is a scalar quantity. In a static fluid (one where all particles have the same velocity) there are no other stresses acting, and equilibrium of a finite volume leads to Pascal's Law[3]: *pressure exerted anywhere in a static fluid is transmitted equally in all directions*.

   b. **Shear forces** – the relative motion of real fluids is accompanied by tangential stresses. Those due to viscous effects, whereby momentum exchange due to random movement of molecules occurs, are relatively small in hydraulics problems. Rather more important than that of individual molecules is the momentum exchange by turbulence and large masses of fluid.

# 1.3 Units

Throughout we will use the *Système Internationale*, in terms of metres, kilograms and seconds, the fundamental units of mass (M), length (L) and time (T) respectively. Other quantities are derived from these. All are set out in Table 1-4. Some of the derived quantities will be described further below.

# 1.4 Turbulent flow and the nature of most flows in hydraulics

## 1.4.1 Reynolds' experiments (1883)

Reynolds[4] non-dimensionalised the differential equations which govern the flow of viscous fluid, and found that

[3] Blaise Pascal (1623 – 1662) was a French mathematician, physicist, and religious philosopher, who made important contributions to the construction of mechanical calculators, the study of fluids, and clarified the concepts of pressure and vacuum.

[4] Osborne Reynolds (1842–1912) was a British engineering fluid dynamicist and professor of engineering at Manchester.

| Quantity | Dimensions | Units |
|---|---|---|
| Fundamental quantities | | |
| mass | M | kg |
| length | L | m |
| time | T | s |
| temperature | $\theta$ | $^\circ$C or $^\circ$K = $^\circ$C + 273.15 |
| Derived quantities | | |
| linear velocity | $\mathrm{LT}^{-1}$ | $\mathrm{m\,s^{-1}}$ |
| angular velocity | $\mathrm{T}^{-1}$ | $\mathrm{s^{-1}}$ |
| linear acceleration | $\mathrm{LT}^{-2}$ | $\mathrm{m\,s^{-2}}$ |
| volume flow rate | $\mathrm{L^3T^{-1}}$ | $\mathrm{m^3\,s^{-1}}$ |
| mass flow rate | $\mathrm{MT}^{-1}$ | $\mathrm{kg\,s^{-1}}$ |
| linear momentum | $\mathrm{M\,L\,T^{-1}}$ | $\mathrm{kg\,m\,s^{-1}}$ |
| force | $\mathrm{MLT^{-2}}$ | $1\ \mathrm{kg\,m\,s^{-2}} = 1\ \mathrm{N}$ (Newton) |
| work, energy | $\mathrm{ML^2T^{-2}}$ | $1\,\mathrm{N\,m} = 1\,\mathrm{J}$ (Joule) |
| power | $\mathrm{ML^2T^{-3}}$ | $1\,\mathrm{J\,s^{-1}} = 1\,\mathrm{W}$ (Watt) |
| pressure, stress | $\mathrm{ML^{-1}T^{-2}}$ | $1\,\mathrm{N\,m^{-2}} = 1\,\mathrm{Pa}$ (Pascal) $= 10^{-5}$ bar |
| surface tension | $\mathrm{MT^{-2}}$ | $\mathrm{N\,m^{-1}}$ |
| dynamic viscosity | $\mathrm{ML^{-1}T^{-1}}$ | $1\,\mathrm{kg\,m^{-1}\,s^{-1}} = 10$ Poise |
| kinematic viscosity | $\mathrm{L^2T^{-1}}$ | $1\,\mathrm{m^2\,s^{-1}} = 10^4$ Stokes |

Table 1-4. Quantities, dimensions, and units

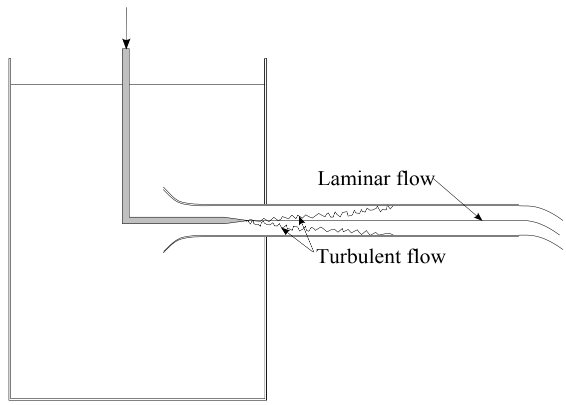


Figure 1-9. Reynolds' apparatus – the diagram showing the dye trace in the pipe for two different flow cases.

for dynamic similarity between two geometrically similar flow situations the dimensionless group Velocity scale $\times$ Length scale $/\nu$ must be the same in the two cases, the quantity which is now called the Reynolds number (for these pipe experiments the mean velocity $U$ and pipe diameter were used). To determine the significance of the dimensionless group Reynolds conducted his experiments on flow of water through glass tubes, as shown in Figure 1-9, with a smooth bellmouth entrance and dye injected into the tube. For small flows the dye stream moved as a straight line through the tube showing that the flow was laminar. With increasing velocity, and hence Reynolds number, the dye stream began to waver and then suddenly broke up and was mixed through the tube. The flow had changed to turbulent flow with its violent interchange of momentum. Starting with turbulent flow in the glass tube, Reynolds found that it always becomes laminar when the velocity is reduced to make $UD/\nu$ less than 2000. Usually flow will change from laminar to turbulent in the range of Reynolds numbers from 2000 to 4000. In laminar flow the losses are proportional to the average velocity, while in turbulent flow, proportional to a power of velocity from 1.7 to 2.

## 1.4.2 The nature of turbulent flows in pipes and channels

Above we considered a simple model of a river in which we assumed the flow was laminar, governed by molecular viscosity, and we found that with typical values of slope and velocity, there was a large imbalance of forces. We could not explain how the momentum could be sufficiently quickly diffused throughout the flow by merely molecular forces. What we did not consider was that a flow of the size and velocity of a river (or, after Reynolds, a pipe or any flow of sufficiently large size and velocity) is unstable, due paradoxically to the presence of viscosity, and becomes turbulent, such that there are large masses of fluid moving irregularly. The resisting force on the bed of the fluid, so as to balance gravity, is much larger, and this is able to be transferred to the fluid by large parcels of fluid moving turbulently. Throughout the rest of this course it is assumed that all flows are turbulent and molecular viscosity will be ignored.

Figure 1-10 shows three ways of visualising the turbulent flow in a channel.

Part (a) shows an instantaneous two-dimensional view that shows the remarkable complexity of the structure, with large regions of fluid moving coherently but also the presence of complicated movements in other regions, and notably with *vortices*, regions of concentrated rotational flow, familiar to anyone who has examined fluid flows in nature by looking at a channel surface. These vortices seem to be a ubiquitous feature of turbulent flow.

Part (b) shows the horizontal velocity $u$ at a point and how it varies with time, showing wild fluctuations, some with a relatively long wavelength, as a large coherently-moving piece of fluid passes the point, some with short wavelengths, as small structures like vortices pass. The figure also shows the mean value $\bar{u}$ of the velocity over time. The analysis of the fluctuations at a point to determine the nature of the flow has had a long history in fluid mechanics, and a great amount of effort has gone into studying how the energy of the flow transfers from large vortices down to smaller and smaller ones.

Part (c) shows the instantaneous and mean fluid velocities across a line from the bottom to the top of the flow. The complexity of the structure is less obvious, but it can be seen that there is spatial variability of both the horizontal and vertical velocities, as is obvious in Part (a). The plot of the mean horizontal fluid velocities, shown by the smooth dashed curve, shows rapid variation near the boundary, such that $d\bar{u}/dz$ is very large, and by analogy with the laminar equation (1.2), the shear stresses are very large. The bed of the channel has been shown in the figure to be composed of stones. It is not necessary for the bed to be rough for the flow to look like this – even for smooth boundaries the instabilities of the flow are such that the flow is similar. Indeed, figure (a) is for a smooth bed.

The energy to create turbulence is typically put into the system at scales the size of the overall geometry. Viscosity is the agent ultimately acting so as to dissipate the turbulent energy in the form of heat. It operates on the smallest possible scales of the flow field – at a molecular level. In between the creation and dissipation turbulent scales there is an orderly *cascade* of turbulent energy by which energy is nonlinearly transmitted from the large to small turbulent fluctuations or scales by a continuously decreasing sequence of turbulent eddies. This has been tersely described by L. F. Richardson, the father of computational fluid mechanics, paraphrasing Jonathan Swift:

*Big whirls have little whirls that feed on their velocity,*
*And little whirls have lesser whirls and so on to viscosity - in the molecular sense.*

### 1.4.3 Boundary layer theory

In the nineteenth century the fields of *hydrodynamics*, the study of fluids with no viscosity, and *hydraulics*, the study of fluids with practical application in real-world situations, had grown far apart from each other. Hydrodynamics could predict the force on an obstacle in a flow – but that prediction was that the force was zero, in contradiction of all experience. Already in that century the partial differential equation that governs the motion of a fluid with viscosity – the Navier-Stokes equation – had been developed, but it was too complicated for practical problems in that era.

In 1904, at a mathematics conference in Heidelberg, Ludwig Prandtl[5] presented the idea that provided the basis for the modern science of fluid mechanics, reconciling some of the differences and difficulties of traditional hydraulics and nineteenth-century hydrodynamics. This idea, of *boundary layer theory* was subsequently developed and extended, mainly through Prandtl and the people who went to work with him in Göttingen. The initial problem tackled was the flow past a flat plate aligned with the flow, again a problem that was trivial in inviscid hydrodynamics. Prandtl's method was to divide the flow into different regions in which the dynamics are different – an outer flow where viscosity is unimportant, and a thin inner viscous ("boundary") layer next to the surface. The equations for each region were separately solved, but their boundary conditions were selected so that the solutions blended into each other to yield a unified approximation. In the same paper, Prandtl also showed how the partial differential equations that governed the boundary layer could be reduced to one ordinary differential equation using a combination of the independent variables.Figure 1-11 shows how a boundary layer develops over a flat smooth plate, initially laminar and then becoming turbulent. The effects of viscosity can still be considered as being confined to

5 Ludwig Prandtl (1875-1953), German engineer and fluid dynamicist; the father of modern fluid mechanics.

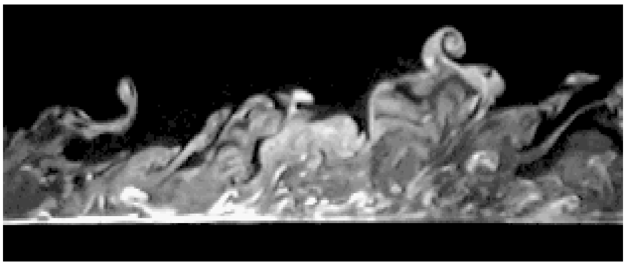

(a) Instantaneous image of a turbulent flow - from "Volumetric visualization of coherent structure in a low Reynolds number turbulent boundary layer" published in the *International Journal of Fluid Dynamics* (1997), Vol.1, Article 3, by C. Delo and A.J. Smits.

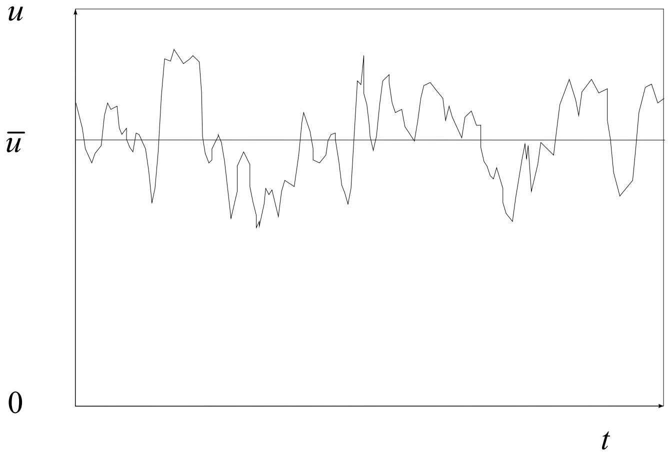


(b) The variation with time of the horizontal velocity at a point in a turbulent flow, showing its fluctuations around a mean value

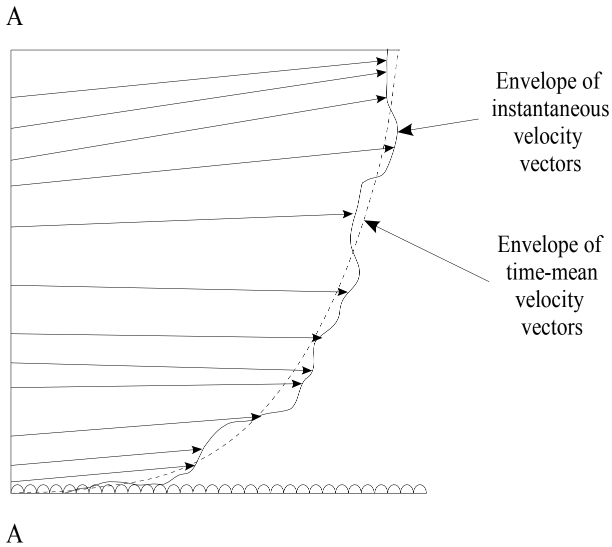


(c) The instantaneous and time-mean velocities over a section of a channel

Figure 1-10. Three ways of depicting a turbulent shear flow in a channel

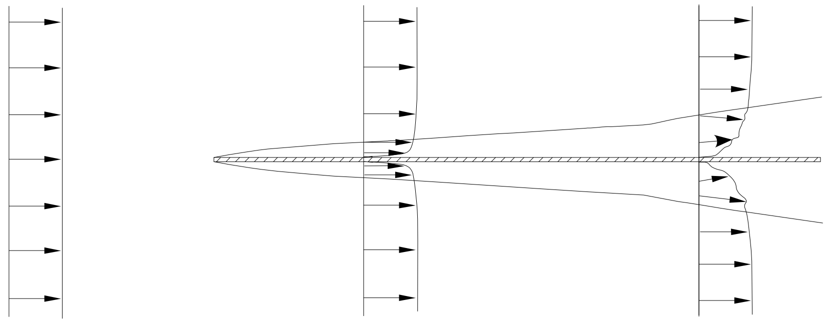


Figure 1-11. Growth of boundary layer (BL) over a flat plate, showing how viscous effects are confined to the boundary layer

the boundary layer itself.

In this hydromechanics course, we are concerned with very long conduits of water, relative to their width, and in these the boundary layer is always turbulent and grows so as to occupy all the flow. We will be able to assume that the flow does not vary down the stream.

### 1.4.4 Prandtl - von Kármán universal turbulent velocity distribution

The apparent shear stress in turbulent flow can be represented by

$$\tau = (\mu + \eta)\frac{du}{dz}, \tag{1.3}$$

where $\eta$ is the *eddy viscosity* due to the turbulent motions, and where in this section we will use the simpler symbol $u$ for the mean horizontal velocity, for which we should ideally use $\bar{u}$. In §1.1.7 of these notes it was shown that the laminar viscosity can be explained by a simple ball model. Here a similar concept is used, but for finite masses of fluid. Prandtl showed that the eddy viscosity can be given by an expression

$$\eta = \rho l^2 \frac{du}{dz}, \tag{1.4}$$

where $l$ is the so-called *mixing length*, expressing the mean distance that a fluid parcel travels before having its momentum changed by its new environment. In turbulent flow there is a violent interchange of parcels of fluid except at a boundary, so that $l$ must go to zero at boundaries. Measurements have shown that the shear stress in a turbulent flow is close to being constant, and so, substituting $\tau = \tau_0$, the *wall shear stress*, and equation (1.4) in equation (1.3), and neglecting molecular viscosity $\mu$,

$$\tau_0 = \rho l^2 \left(\frac{du}{dz}\right)^2. \tag{1.5}$$

After similarity considerations, von Kármán[6] suggested that $l = \kappa z$,where $\kappa$ is a universal constant in turbulent flow. Introducing the symbol of the *shear velocity* $u_*$:

$$u_* = \sqrt{\frac{\tau_0}{\rho}}, \tag{1.6}$$

equation (1.5) can be written

$$\frac{du}{dz} = \frac{u_*}{\kappa z},$$

which can be integrated to give

$$\frac{u}{u_*} = \frac{1}{\kappa}\ln z + \text{constant}. \tag{1.7}$$

This Prandtl-von Kármán universal velocity law agrees very well with experiment in both pipes and channels. For

[6] Theodore von Kármán (1881-1963), Hungarian mathematician and aerodynamicist with numerous important contributions.

smooth-walled pipes as $z \to 0$ it is replaced by a laminar law. In this case it is written

$$\frac{u}{u_*} = \frac{1}{\kappa} \ln \frac{z u_*}{\nu} + A,$$

where $\kappa = 0.40$ and $A \approx 5$ from measurements by Nikuradse. At the centre of a pipe, where $du/dz = 0$ this fails, but this is unimportant in practice.

Prandtl also developed a convenient power-law velocity distribution formula for turbulent pipe flow

$$\frac{u}{u_m} = \left(\frac{r}{a}\right)^n,$$

where $u_m$ is the velocity at the centreline, $r$ is the distance from the pipe centre, $a$ is the pipe radius, and $n \approx 1/7$ for slower flows and less for faster ones. This is not related to the fundamental mechanics of the flow, but is sometimes convenient, especially as it satisfies the condition that $du/dr = 0$ at the centre of the pipe, such that the velocity is a maximum there.

What we have ignored in this section is the fact that very close to the bed viscosity controls the vertical transport of momentum, and the region closest to the boundary is called the *laminar sub-layer*, because within the region turbulence is suppressed by viscosity. In this region the velocity profile is linear, as we expect from the earlier discussion of viscosity. This layer exists even for rough beds, if the individual roughness elements do not project too far into the flow.

Above the laminar sub-layer the velocity profile is logarithmic, as predicted by equation (1.7). For rough boundaries equation (1.7) can be written

$$\frac{u}{u_*} = \frac{1}{\kappa} \ln \frac{z}{z_0}, \tag{1.8}$$

where $z_0$ is the elevation at which the velocity is zero. In practice this has been found to be about $k_s/30$, where $k_s$ is a measure of the size of the boundary roughnesses, and is the equivalent sand grain roughness. This gives the velocity distribution law for turbulent flow over rough boundaries

$$\frac{u}{u_*} = \frac{1}{\kappa} \ln \frac{z}{k_s/30} = \frac{1}{\kappa} \ln \frac{30\, z}{k_s}, \tag{1.9}$$

The profile shape depends on the bed texture, as described by the boundary roughness $k_s$ and the magnitude is directly proportional to the shear velocity $u_*$, which is related to the shear stress on the bed by $\tau_0 = \rho u_*^2$. The *logarithmic velocity distribution* has been found to be widely applicable throughout hydraulics, meteorology, and oceanography, including pipe flows, channel flow, the flow of the atmosphere over the sea and land, and in the oceans where there is a current in water of finite depth.

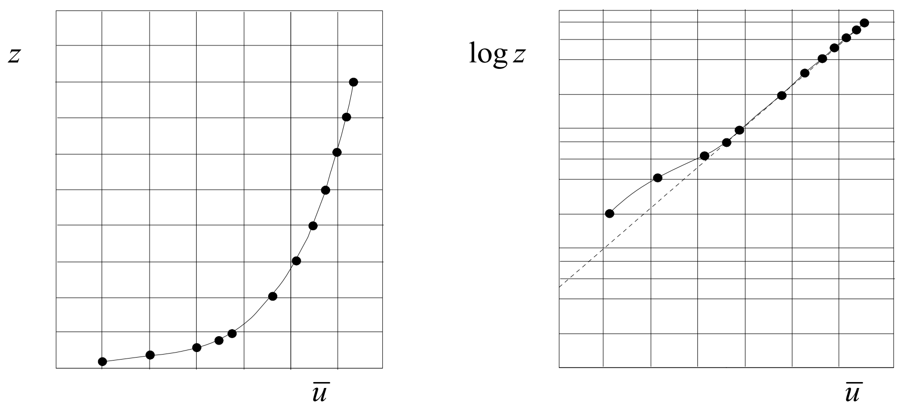


(a) Natural co-ordinates (b) Semi-logarithmic plot

Figure 1-12. Measurements of time mean horizontal velocity in a channel

An example of a time-mean velocity profile is plotted in two forms in Figure 1-12, using linear and semi-logarithmic plots. The linear axes reveal the physical nature of the boundary layer profile, which is typical of velocity distributions in rivers. Near the bed, however, the profile seems rather more linear than logarithmic. On the semi-logarithmic axes the logarithmic portion of the profile appears as a straight line, and it is clear that the two points closest to the bed do not follow the same log-linear trend as the rest of the profile. The dashed straight line on the figure is the log-linear fit to the velocity profile, ignoring those two points. This plot shows that they lie within the laminar sub-layer. By fitting equation (1.9) to the points which appear on a straight line we can estimate the characteristic roughness size $k_s$, and the friction velocity $u_*$.

### 1.4.5 The dynamic equation governing fluid motion and the Reynolds number

In this section we consider briefly the fundamental partial differential equation that governs the motion at each point throughout the fluid. As we have already seen, the solutions to this equation actually show unsteady chaotic or turbulent behaviour, and the equation is far too difficult to solve for many practical problems. However we examine it here to obtain insights into the nature of viscosity and what approximations can be made. Having done that we will move on to the traditional approximations of hydraulics, where solutions to practical problems can be obtained, not by solving the partial differential equation throughout the fluid, but by considering the conservation equations of mass, momentum, and energy.

**The Navier-Stokes equation:** If we consider the momentum of a fluid particle in three dimensions, and equate the rate of change of momentum of the fluid particle, the following vector equation is obtained:

$$\underbrace{\frac{d\mathbf{u}}{dt}}_{\substack{\text{1. Acceleration}\\\text{of particle}}} = \underbrace{\mathbf{g}}_{\substack{\text{2. Acceleration}\\\text{of gravity}}} - \underbrace{\frac{1}{\rho}\nabla p}_{\substack{\text{3. Pressure}\\\text{gradient term}}} + \underbrace{\frac{\mu}{\rho}\nabla^2\mathbf{u}}_{\substack{\text{4. Viscous}\\\text{diffusion term}}} . \qquad \text{(Navier-Stokes equation)}$$

It is perhaps surprising that the motion of all air and water and other Newtonian fluids are governed by such a simple equation. Considering each of the four contributions:

1. The particle acceleration term is actually more complicated than it appears, if is written, not as the acceleration of a particle, but in terms of the time and space derivatives at a fixed point in space. For present purposes this does not matter, and it will be left in this form.
2. The gravitational acceleration term $\mathbf{g} = (0, 0, -g) = -g\mathbf{k}$, where $g$ is the scalar value of the acceleration. We consider inertial cartesian co-ordinates such that $z$ is vertically upwards, with unit vector $\mathbf{k}$, in which case there is only the one component shown.
3. The pressure gradient term occurs in a simple manner, such that its contribution to the acceleration of a particle is simply $\nabla p = (\partial p/\partial x, \partial p/\partial y, \partial p/\partial z)$ divided by the density, with a negative sign in front, such that if fluid pressure increases in the $x$ direction, say, then $\partial p/\partial x$ is positive and the whole term for that component, $-(\partial p/\partial x)/\rho$ is negative, and the fluid will decelerate by an amount proportional to $1/\rho$ such that the acceleration will be greater for lighter fluids. All of that physical interpretation is obvious; it is not so obvious that it be capable of such simple mathematical expression.

   In the special case of no fluid movement at all, $\mathbf{u} = \mathbf{0}$ throughout, and the Navier-Stokes equation becomes simply $\nabla p = \rho\mathbf{g}$. Considering each of the components in that case:

   $$\frac{\partial p}{\partial x} = 0, \quad \frac{\partial p}{\partial y} = 0, \quad \text{and} \quad \frac{\partial p}{\partial z} = -\rho g, \qquad (1.10)$$

   stating that in a stationary fluid the pressure is constant on a horizontal plane (no variation with $x$ and $y$) and has a constant vertical gradient throughout the fluid if it is incompressible ($\rho$ constant).
4. The remaining component of the Navier-Stokes equation is the $\nu\nabla^2\mathbf{u}$, where we have substituted $\nu = \mu/\rho$, the kinematic viscosity (see §1.1.7). The Laplacian operator $\nabla^2$ is a diffusion or smoothing operator that occurs throughout physics. It has the form

   $$\nabla^2 = \frac{\partial^2}{\partial x^2} + \frac{\partial^2}{\partial y^2} + \frac{\partial^2}{\partial z^2},$$

   the sum of the second derivatives in the three co-ordinate directions. As an example of the nature of solutions to that equation, we can consider the heat equation governing the distribution of temperature $\theta$ in a body, $\partial\theta/\partial t = \kappa\nabla^2\theta$, where $\kappa$ is a diffusion coefficient for heat transfer. If temperature $\theta$ has a local maximum such that all the second derivatives are negative, then $\partial\theta/\partial t$ is negative, and the temperature there will diminish. In this way, all uneven gradients throughout the field tend to diffuse out until the temperature field is as smooth as possible, compatible with the boundary conditions.

In the Navier-Stokes equation the whole last term 4 is a viscous diffusion term for velocity, such that there is a tendency for the velocity field to diffuse such that rapid changes are diminished. This fits with some of our earlier descriptions of viscosity as a diffusion phenomenon. Like the pressure gradient term, it is noteworthy that this term is capable of such simple expression.

**Magnitude of terms:** Now an estimate is made of the size of the terms in the Navier-Stokes equation. We consider a flow, whether along a conduit (pipe or channel) or past a body, such that a typical length scale of the flow is $L$, and a typical velocity scale is $U$. We non-dimensionalise co-ordinates with respect to the length scale $L$ such that we introduce dimensionless co-ordinates $x_* = x/L$, $y_* = y/L$, and $z_* = z/L$ such that in our field of flow, $x_*$, $y_*$, and $z_*$ all have maximum magnitudes of about 1. As the flow is sweeping through our field of interest at a speed of $U$, this means that the time taken for the flow to cross the region is given by $t = L/U$, which suggest the introduction of a time scale $t_* = tU/L$, such that a typical time of transit of a fluid particle is about $t_* \approx 1$.

Having non-dimensionalised the independent variables $x$, $y$, $z$, and $t$, we now consider the dependent variables. It is obvious that we choose $\mathbf{u}_* = \mathbf{u}/U$ so that all velocity components are scaled with respect to the overall velocity scale and have a typical maximum magnitude of 1. It is not so obvious, but the final results show it to be so, that we introduce a dimensionless pressure $p_*$ modified so as to express it relative to hydrostatic pressure and non-dimensionalised with respect to $\rho U^2$. This factor will be seen to recur throughout the rather simpler momentum and force considerations later in these notes – in fact we will see that a typical dynamic pressure due to fluid impact is $\rho U^2$. Hence we write

$$p_* = \frac{p + \rho g z}{\rho U^2}.$$

Now, recognising that if $x_* = x/L$ *etc*, then $x = Lx_*$, $\partial/\partial x = (1/L)\,\partial/\partial x_*$ *etc*, $\nabla = (1/L)\,\nabla_*$, $\nabla^2 = (1/L^2)\,\nabla_*^2$, $d/dt = (U/L)\,(d/dt_*)$, and substituting into the Navier-Stokes equation:

$$\frac{U}{L}\frac{d}{dt_*}\left(U\mathbf{u}_*\right) = (0,0,-g) - \frac{1}{\rho}\frac{1}{L}\nabla_*\left(\rho U^2 p_* - \rho g L z_*\right) + \frac{\nu}{L^2}\nabla_*^2\left(U\mathbf{u}_*\right).$$

Now, observing that $\nabla_* z_* = (0,0,1)$, and $\mathbf{g} = (0,0,-g)$, using the fact that $U$ and $L$ are constant, and finally multiplying each term in the equation by $L/U^2$:

$$\frac{d\mathbf{u}_*}{dt_*} = -\nabla_* p_* + \frac{\nu}{UL}\nabla_*^2\mathbf{u}_*. \tag{1.11}$$

where all the starred (*) quantities have a maximum magnitude of the order of 1. We have found that there is only one dimensionless parameter in the equation governing the flow, and this is the dimensionless viscosity

$$\nu_* = \frac{\nu}{UL}. \tag{1.12}$$

For a given fluid and flow, the viscosity is unimportant if the quantity $\nu_* \ll 1$, that is, if the product of a typical velocity and typical length of our flow are much larger than the kinematic viscosity.

**The Reynolds number:** It is an historical accident that in his 1883 paper, Osborne Reynolds introduced the quantity that has since been called the *Reynolds Number* and given the symbol $R$, which is the *inverse* of the dimensionless viscosity, defined as

$$R = \frac{UL}{\nu} = \frac{1}{\nu_*}, \tag{1.13}$$

which has been almost universally used as the measure of the relative importance of viscosity. It would have been more satisfying if that number had been defined upside down as dimensionless viscosity! With the traditional definition, high Reynolds number flows are those which are large and/or fast such that the effects of viscosity are small. In environmental hydraulics problems, with, say, a typical length scale of $1\,\mathrm{m}$, a velocity scale of $1\,\mathrm{m\,s^{-1}}$, and a typical value for water at 20°C of $\nu = 1 \times 10^{-6}\,\mathrm{m^2\,s^{-1}}$, a value of $R = 10^6$ ($\nu_* = 10^{-6}$) is obtained, showing how viscosity is unimportant in many outdoor problems. Flows in pipes, however, because they can be smaller and have slower flow, may have Reynolds numbers of the order of $10^3$, when viscous effects may be present.

**An interpretation – the ratio of inertia to viscous forces** Above we used a highly mathematical treatment, considering the dynamic equation of flow, and found that the Reynolds number was the inverse of dimensionless viscosity. A simpler statement is often made concerning the Reynolds number, that it is the ratio of inertial forces to viscous forces in a flow. To obtain an idea of this, and to give us an idea of the integrated approach we will later use, let us consider the *steady* (unchanging in time) flow of a viscous fluid in a region of flow of length scale $L_x$ in the direction of flow, and $L$ in both transverse directions. If $U$ is the scale of the main velocity, then the rate of volume transport through the flow is the velocity times the cross-sectional area through which it flows, $U \times L^2$. Hence the rate of *mass* transport through the flow is of a scale $\rho U \times L^2$, in units of mass per unit time. The scale of rate of *momentum* transport is then obtained by multiplying this by $U$ to give $\rho U^2 L^2$.

To estimate the viscous forces, the scale of the velocity gradient is estimated by considering the magnitude of the $x$-velocity $U$ divided by the length scale $L$ over which the velocity goes from 0 on a boundary to the main magnitude, giving the scale of $du/dz$ to be $U/L$, although a precise value might be closer to $U/(L/2)$, and hence the viscous stress on the wall is of a magnitude $\mu U/L$. Multiplying by the area over which that acts, of the length of the flow times a transverse length, giving $L_x L$, the viscous force on the boundaries has a scale $\mu U/L \times L_x L = \mu U L_x$.

Now calculating the ratio of the two terms we have obtained,

$$\frac{\text{Viscous force on wall}}{\text{Rate of momentum transport}} = \frac{\mu U L_x}{\rho U^2 L^2} = \frac{\mu}{\rho} \frac{L_x}{U L^2}. \tag{1.14}$$

It is possible to make two deductions from this:

1. To solve our original problem, to estimate the overall ratio of viscous force to inertia, we could say that all length scales in the problem are the same, such that $L_x \approx L$, we obtain the ratio to be $\nu/UL = \nu_* = 1/R$, and so it is legitimate to say that the Reynolds number is the ratio of inertial to viscous stresses.
2. In a boundary layer, in a region close to a wall, however, the transverse scale is that of the rather smaller boundary layer thickness, such that $L \ll L_x$ and the ratio as estimated in equation will be very much greater, which is effectively what Prandtl discovered, that viscous effects are most important in the boundary layer.

### 1.4.6 The drag force on bodies in the flow

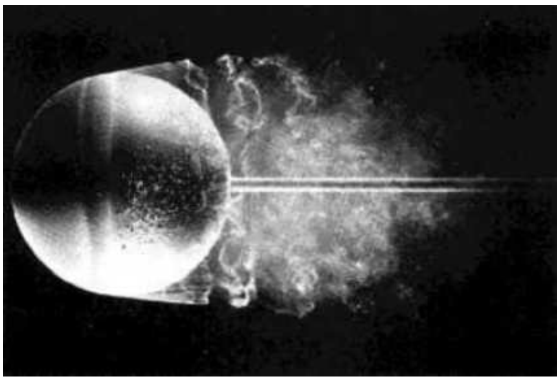

Figure 1-13. Flow past a sphere showing separation and turbulence in the separation zone

"The theory of drag is weak and inadequate", wrote White (2003, p478), in talking about a body immersed in a flow. In fact, except for a idealised objects such as spheres, cylinders, and flat plates, there is almost no theory, as the flow is changed abruptly by the body, and is very complicated one. Usually *flow separation* occurs, such as shown in Figure 1-13, where the boundary layer flow on the upstream part of the sphere separates at about the equator of the sphere. The pressure in the separation zone is much less than the upstream pressure, and so there is a large force on the body in the direction of flow. Most reliable results for the drag force on immersed bodies are experimental.

In laminar flows, at small Reynolds numbers, where viscosity is important, the forces on the body are primarily viscous ones, proportional to the velocity, or more properly to the velocity gradients. For large Reynolds numbers, where the viscous influence is limited to boundary layers on the upstream side of the body, and most force is due to the effects of separation of the boundary layer and the difference between pressures upstream and downstream of the body. In this case, it has been experimentally observed, and an approximate momentum theory shows, that the drag force is proportional to the square of the velocity. Hence, as this is the more important case, the way that force on a body is calculated is to express it using an empirical *dimensionless drag coefficient* $C_{\mathrm{D}}$, such that the magnitude of the drag force $F$ is written

$$F = \tfrac{1}{2}\rho C_{\mathrm{D}} A U^2, \tag{1.15}$$

where $U$ is the velocity of the upstream flow, and $A$ is area, which for aircraft wings might be the plan area, but for most non-streamlined objects is the projected or frontal area, that as seen by the stream as it approaches. The other terms come from a simple inviscid theory for the maximum possible pressure on the upstream face of a bluff body that we will study later, such that $p_{\max} = \frac{1}{2}\rho U^2$. From this it is clear that equation (1.15) is the rather empirical expression that the total force on a body is the maximum pressure on the upstream face multiplied by the projected area of the body, the whole corrected by $C_{\mathrm{D}}$, $F = p_{\max} A C_{\mathrm{D}}$.

If, such as is the case for wave forces on oil platforms, or bridge piers subject to tides, the direction of the incident velocity $\mathbf{U}$ can reverse, ideally equation (1.15) should be written in the vector sense $\mathbf{F} = F\hat{\mathbf{F}}$, where $\hat{\mathbf{F}}$ is a unit vector specifying the direction of the force, which is always in the direction of the flow velocity, such that $\hat{\mathbf{F}} = \mathbf{U}/U$, giving

$$\mathbf{F} = \tfrac{1}{2}\rho C_{\mathrm{D}} A U \mathbf{U}, \tag{1.16}$$

or in a further generalisation, if the body is subject to an oblique velocity vector $\mathbf{U} = (U, V, W)$, the drag force on the body is

$$\mathbf{F} = \tfrac{1}{2}\rho C_{\mathrm{D}} A \left|\mathbf{U}\right| \mathbf{U}, \tag{1.17}$$

where the magnitude of the velocity vector $|\mathbf{U}| = \sqrt{U^2 + V^2 + W^2}$.

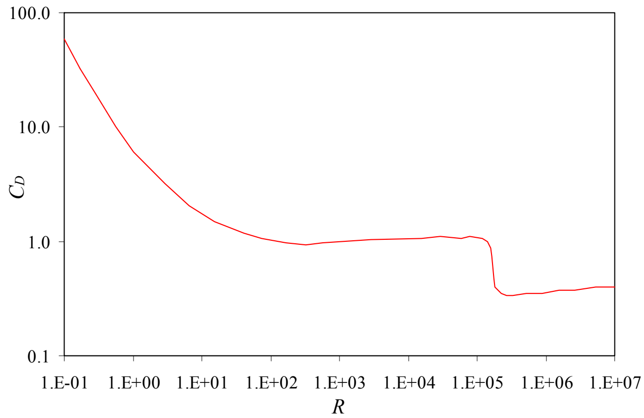


Figure 1-14. Cylinder – variation of drag coefficient $C_{\mathrm{D}}$ with Reynolds number $R$

For smooth bodies such as spheres or circular cylinders there is a finite variation of $C_{\mathrm{D}}$ with Reynolds number, as shown in Figure 1-14. In the small Reynolds number limit the flow is dominated by viscosity and this limit we expect $F \sim U^1$, and to do this it is necessary for $C_{\mathrm{D}} \sim 1/R$. The sudden dip in the curve between $R = 10^5$ and 10ˆ is a result of the boundary layer becoming turbulent, when the transport of momentum is very effective at replenishing the near-wall momentum and the boundary layer can persist for a longer distance without separating, and the drag is less.

For bodies which are not smooth, however, the points of separation of the boundary layer are well-defined, at the corners, and the variation of $C_{\mathrm{D}}$ with $R$ is very small. Typical drag coefficients are shown in the table:

| Shape | $C_{\mathrm{D}}$ |
|---|---|
| 2-D | |
| Square cylinder | 2.1 |
| Ditto, at 45° | 1.6 |
| Flat plate | 2.0 |
| 3-D | |
| Cube | 1.07 |
| Circular disk | 1.17 |
| Rectangular plate | 1.18 – 2 |

# 2. Hydrostatics

An understanding of fluid statics is essential for the design of hydraulic structures, tanks, ships, pressure measurement and meteorology. We will consider the equilibrium of a mass of fluid which is at rest, or in uniform motion, when no element of fluid moves relative to any other element. As there are no velocity gradients, there are no shear stresses. The pressure forces balance applied body forces, in accordance with Newton's second law.

## 2.1 Fundamentals

### 2.1.1 Pressure at a point

The pressure in a fluid in static equilibrium is the same in all directions. Pressure is a scalar quantity that arises from the non-directional nature of the oscillations of fluid particles, nominally at rest here. This was considered in §1.2.

### 2.1.2 The pressure in a fluid under static equilibrium

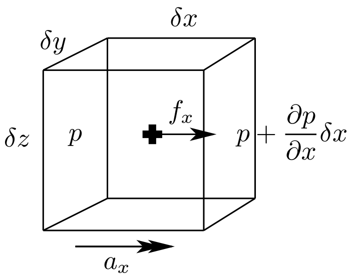


Figure 2-1.

Consider an element of fluid in static equilibrium with components of body forces $f_x$, $f_y$ and $f_z$ per unit mass. The fluid has accelerations $a_x$, $a_y$ and $a_z$. Considering motion in the $x$ direction only at this stage, as shown in Figure 2-1, the acceleration in the $x$ direction is caused by the net force in the $x$ direction on the faces which are normal to that direction. The net force in the $x$ direction due to pressure forces is

$$-\left(p + \frac{\partial p}{\partial x}\,\delta x\right)\,\delta y\,\delta z + p\,\delta y\,\delta z = -\frac{\partial p}{\partial x}\,\delta x\,\delta y\,\delta z. \qquad (2.1)$$

Considering Newton's second law in the $x$ direction: mass$\times$acceleration in $x$ direction=net force in $x$, this gives

$$\begin{aligned}(\rho\,\delta x\,\delta y\,\delta z)\,a_x &= \text{body force} + \text{net pressure force}\\ &= (\rho\,\delta x\,\delta y\,\delta z)\,f_x - \frac{\partial p}{\partial x}\,\delta x\,\delta y\,\delta z,\end{aligned}$$

and cancelling the common factors of the volume of the body $\delta x\,\delta y\,\delta z$, gives

$$\frac{\partial p}{\partial x} = \rho\,(f_x - a_x) \qquad (2.2)$$

and we obtain expressions for the $y$ and $z$ components which are the same, with $x$ replaced throughout by $y$ and $z$ respectively. Thus we have:

The pressure gradient at a point $=$ fluid density $\times$ (body force per unit mass - fluid acceleration),

or in vector terms

$$\nabla p = \rho\,(\mathbf{f} - \mathbf{a})\,, \qquad (2.3)$$

where $\mathbf{f} = (f_x, f_y, f_z)$ is the body force per unit mass, and $\mathbf{a} = (a_x, a_y, a_z)$ is the fluid acceleration.

### 2.1.3 Fluid at rest in a gravity field

In the usual case of a body of fluid at rest in a field of constant gravity, where $x$ and $y$ are in a horizontal plane and $z$ is vertically upwards,

$$a_x = a_y = a_z = 0 \quad \text{and} \quad f_x = f_y = 0,\ f_z = -g \approx -9.8\,\mathrm{m\,s^{-2}},$$

and substituting into equation (2.2) with similar equations for the other co-ordinates, we obtain

$$\frac{\partial p}{\partial x} = \frac{\partial p}{\partial y} = 0, \qquad (2.4a)$$

$$\frac{\partial p}{\partial z} = -\rho g. \qquad (2.4b)$$

That is, the pressure does not vary with $x$ or $y$, such that on any horizontal plane the pressure is constant, such as anywhere on the plane XX or the plane YY *within the fluid* in Figure 2-2. This is also known as Pascal's law.

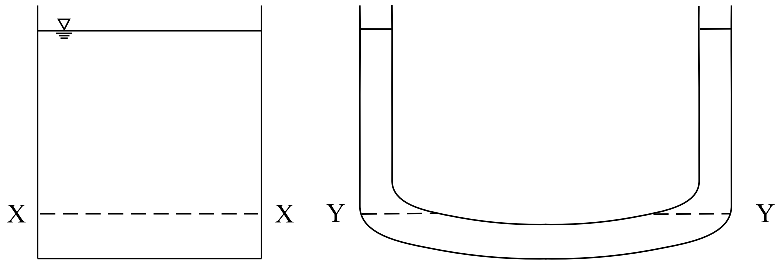


Figure 2-2. Two vessels and two typical horizontal planes, such that within the fluid the pressure on each plane is constant

Equation (2.4b) can be integrated in common cases where the density $\rho$ is a known function of pressure $p$. For most problems in hydraulics the fluid can be considered incompressible, such that $\rho$ is constant, and the integration is simple:

$$\begin{aligned} \int \frac{\partial p}{\partial z} dz &= \int (-\rho g) dz, \quad \text{giving} \\ \int \mathrm{d}p &= -\rho g \int dz, \quad \text{and integrating,} \\ p &= -\rho g z + C(x, y), \end{aligned}$$

where because we integrated a partial derivative the quantity $C$ is in general a function of the other two variables $x$ and $y$. However, the other differential equations (2.4a) show that $C$ cannot be a function of $x$ or $y$ so that it is a constant throughout the fluid. Thus we have the equation governing the pressure in an incompressible fluid in a constant gravity field, the

**Hydrostatic Pressure Equation:**

$$p + \rho g z = \text{Constant throughout the fluid} \tag{2.5}$$

It is simpler to solve many problems in the form of equation (2.5), as we will see below while considering some pressure measurement devices. However, many other problems are most easily solved by expressing the pressure as a function of depth below the surface rather than elevation above a point. To do this the constant is evaluated by considering a special point in the fluid, usually on the surface.

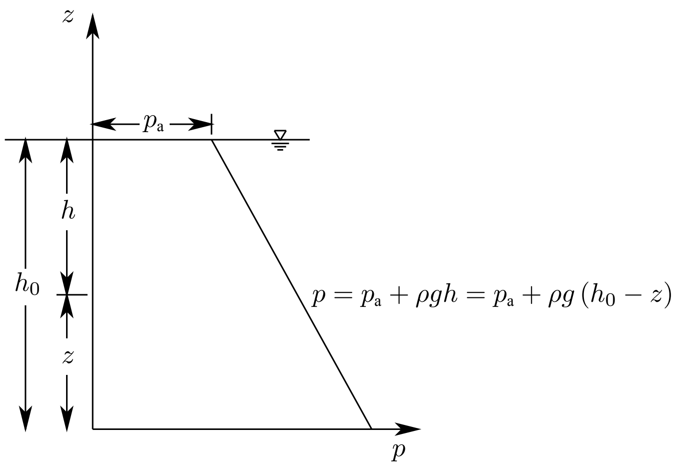


Figure 2-3. Hydrostatic pressure variation with depth

Consider the general situation shown in Figure 2-3 that shows a graph of pressure plotted horizontally against elevation using a datum (reference level) that is a vertical distance $h_0$ below the surface. When $z = h_0$ the pressure is atmospheric, denoted by $p_{\mathrm{a}}$, and so

$$p + \rho g z = \text{Constant} = p_{\mathrm{a}} + \rho g h_0,$$

thereby evaluating the constant and enabling us to write the equation for pressure $p$ at an arbitrary point with elevation $z$ as

$$p - p_{\mathrm{a}} = \rho g (h_0 - z) \quad \text{or} \quad p = p_{\mathrm{a}} + \rho g (h_0 - z).$$

Since $h_0 - z = h$, the height of the free surface above the point, this becomes

$$p - p_{\mathrm{a}} = \rho g h$$

and almost always we measure pressure as *gauge pressure*, relative to the atmosphere, as shown in Figure 2-4, so that we usually just write

$$p = \rho g h, \tag{2.6}$$

so that the pressure at a point is given by the density $\rho$ multiplied by gravitational acceleration $g$ multiplied by the depth of water above the point.

**Gauge, absolute, and vacuum pressures** Figure 2-4 shows, on an absolute pressure scale, how the gauge pressure, widely used for engineering purposes, is measured relative to the (variable) atmospheric pressure; and vacuum pressure, used in engineering applications such as brakes for vehicles, is measured from the same datum but in the other direction. An absolute vacuum corresponds to a vacuum pressure of one atmosphere.

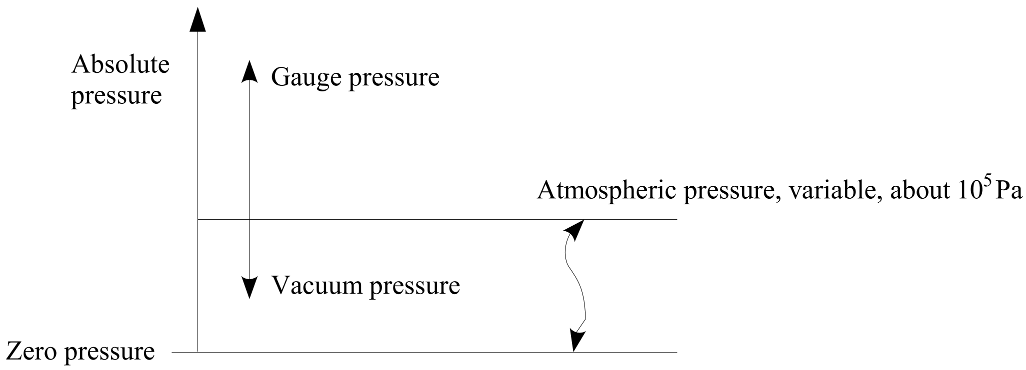


Figure 2-4. Definitions of gauge, absolute, and vacuum pressures.

**Equivalent static head:** Throughout engineering, pressures are often expressed as the equivalent height of liquid which can be supported by that pressure, called the *head*, here denoted by $h$:

$$h = \frac{p}{\rho g}.$$

### 2.1.4 Units

Pressure is a force per unit area, so in fundamental *SI* units it is $\mathrm{N\,m^{-2}}$, for which a special name is used, a Pascal, or Pa. We will see that this is an appropriate name, and that it has a value of about $10^5\,\mathrm{Pa}$. Atmospheric pressure used to be specified in terms of 1/1000 of that, or millibar, however they are not *SI* units. Instead of a millibar, the exactly numerical equivalent value of "hectoPascal" or "hPa" is used, which is a 1/100 of a Pascal. Atmospheric pressure varies usually in the range $980-1030\,\mathrm{hPa}$. Hurricane Wilma was the most intense hurricane ever recorded in the Atlantic basin, in the 2005 season; the eye pressure was $882\,\mathrm{hPa}$.

**Example 2.1** (a) Find the gauge pressure when you swim to a depth of $3\,\mathrm{m}$; (b) estimate the pressure force on an eyeball there.

(a) Assuming that the water is fresh such that the density is approximately $1000\,\mathrm{kg\,m^{-3}}$, and take $g \approx 10\ \mathrm{ms^{-2}}$:

$$p = \rho g h = 1000 \times 10 \times 3 = 30\,000\,\mathrm{N\,m^{-2}} = 30\,000\,\mathrm{Pa}.$$

(b) To estimate the force, assume that an eyeball is $2\,\mathrm{cm}$ in diameter, and that the force is that on a circle of the same diameter, thus

$$\text{Force} = \text{ pressure} \times \text{area} = 30\,000 \times \frac{\pi}{4} \times 0.02^2 \approx 9\,\mathrm{N},$$

which, remembering that 1 Newton is approximately the gravitational force on a small apple, is about the weight of 9 apples!

### 2.1.5 The mercury barometer and atmospheric pressure

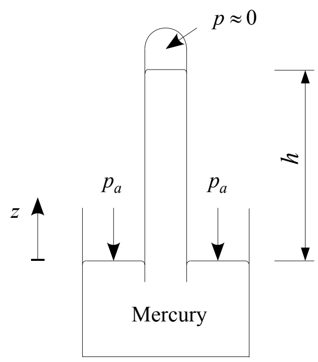


Figure 2-5. Mercury barometer.

Consider the hydrostatic pressure equation (2.5) for all points within the mercury of the barometer shown in Figure 2-5:

$$p + \rho g z = \text{Constant}.$$

We apply this at two points: at the surface open to the air and secondly at the surface in the tube, at which the pressure is the vapour pressure of mercury, close to zero

$$\begin{aligned} p_{\mathrm{a}} + 0 &= 0 + \rho g h, \quad \text{thus} \\ p_{\mathrm{a}} &= \rho g h. \end{aligned}$$

The density of mercury is about $13\,600\,\mathrm{kg\,m^{-3}}$, and typically $h$ is about $0.76\,\mathrm{m}$, hence

$$p_{\mathrm{a}} \approx 13\,600 \times 9.8 \times 0.76 \approx 1 \times 10^5 \ \mathrm{N\,m^{-2}}.$$

In terms of the equivalent height of water, which it is sometimes convenient to use, $h = p/\rho g \approx 10^5/1000/10 \approx 10\,\mathrm{m}$.

### 2.1.6 Pressure measurement by manometer

**(a) The simple manometer**

Consider the U-tube in Figure 2-6 filled with manometric fluid of density $\rho_{\mathrm{m}}$ with one end attached to a point X where the pressure of the fluid, of density $\rho_{\mathrm{f}}$, is to be measured. The other end is open to the atmosphere.

In the fluid, using the hydrostatic pressure equation (2.5) at both X and B:

$$p_{\mathrm{X}} + \rho_{\mathrm{f}} g h_1 = p_{\mathrm{B}} + 0.$$

In the manometric fluid, also using the hydrostatic pressure equation at B and at the surface open to the air:

$$p_{\mathrm{B}} + 0 = p_{\mathrm{a}} + \rho_{\mathrm{m}} g h_2.$$

Eliminating the unknown intermediate pressure $p_{\mathrm{B}}$:

$$p_{\mathrm{X}} - p_{\mathrm{a}} = \rho_{\mathrm{m}} g h_2 - \rho_{\mathrm{f}} g h_1,$$

thus by measuring the height difference of the fluid in the manometer we can calculate the gauge pressure at X. In

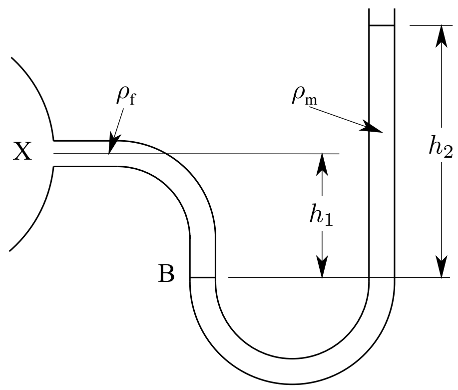


Figure 2-6. Simple manometer, measuring the pressure in a vessel relative to the atmosphere

the special case where the same fluid is used throughout,

$$p_X - p_a = \rho_f\, g (h_2 - h_1).$$

**(b) The U-tube manometer**

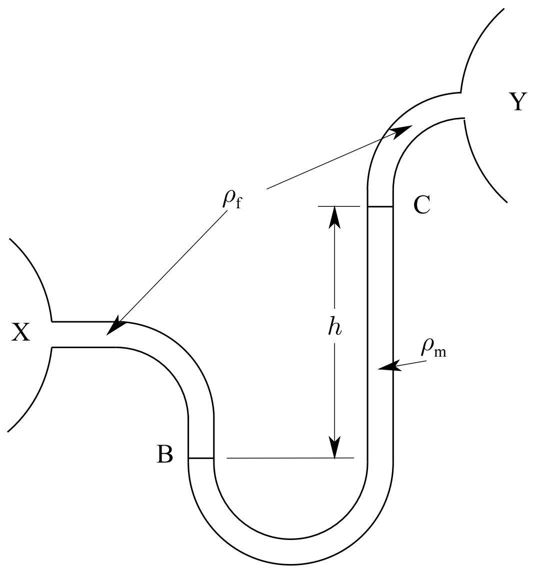


Figure 2-7. U-tube manometer, used to measure the pressure difference between two points

In experimental fluid mechanics we often wish to measure pressure *differences*. Consider the manometer shown in Figure 2-7. Fluid of density $\rho_f$ occupies points X and Y, between which the pressure difference is to be measured. They could be two points on the same pipe. The manometric fluid has density $\rho_m$ and has a difference between its ends of $h$. Applying the hydrostatic pressure equation between X and B, within the working fluid:

$$p_X + \rho_f g z_X = p_B + \rho_f\, g z_B, \tag{2.7}$$

between B and C in the manometric fluid,

$$p_B + \rho_m\, g z_B = p_C + \rho_m\, g z_C, \tag{2.8}$$

and in the other working fluid, between C and Y:

$$p_C + \rho_f\, g z_C = p_Y + \rho_f\, g z_Y. \tag{2.9}$$

We can eliminate $p_{\mathrm{B}}$ between equations (2.7) and (2.8) to give

$$p_{\mathrm{X}}+\rho_{\mathrm{f}}\, g z_{\mathrm{X}}=p_{\mathrm{C}}+\rho_{\mathrm{m}}\, g(z_{\mathrm{C}}-z_{\mathrm{B}})+\rho_{\mathrm{f}}\, g z_{\mathrm{B}},$$

and eliminating $p_{\mathrm{C}}$ by using this equation and equation (2.9):

$$p_{\mathrm{X}}-p_{\mathrm{Y}}=\rho_{\mathrm{f}}\, g(z_{\mathrm{B}}-z_{\mathrm{X}}+z_{\mathrm{Y}}-z_{\mathrm{C}})+\rho_{\mathrm{m}}\, g(z_{\mathrm{C}}-z_{\mathrm{B}}).$$

However, $z_{\mathrm{C}}-z_{\mathrm{B}}=h$, the measured manometric height, and the individual elevations of B and C disappear, giving the relatively simple result

$$p_{\mathrm{X}}-p_{\mathrm{Y}}=(\rho_{\mathrm{m}}-\rho_{\mathrm{f}})gh+\rho_{\mathrm{f}}\, g(z_{\mathrm{Y}}-z_{\mathrm{X}}).$$

Notice that the contribution of the manometric height depends on the *difference* between the densities of the two fluids.

### 2.1.7 An application – industrial hydraulics

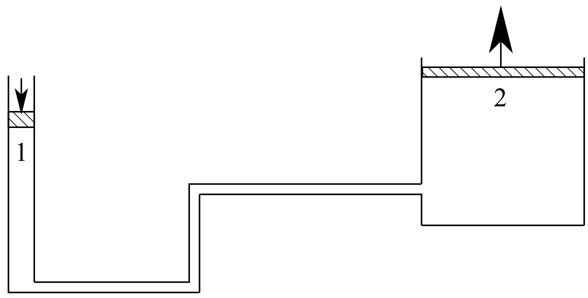


Figure 2-8. Operation of an hydraulic lift or jack

Consider the problem shown in Figure 2-8 in which an actuator (a small cylinder with a piston in it, but probably a pump in more modern applications) can apply a force to a fluid, and the pressure so generated is then transmitted throughout the fluid to the other end of the fluid line where a larger cylinder and piston are placed. Use of the hydrostatic pressure equation in the fluid between points 1 and 2 gives

$$p_1=p_2+\rho g\left(z_2-z_1\right).$$

Now, $p_1=F_1/A_1$, with a similar result for piston 2, giving

$$\frac{F_1}{A_1}=\frac{F_2}{A_2}+\rho g\left(z_2-z_1\right).$$

In practical cases the term involving the difference in elevation is negligible, so that the force which can be lifted by the hydraulic jack is

$$F_2\approx F_1\left(\frac{A_2}{A_1}\right).$$

For large values of $A_2/A_1$ large forces can be exerted, such as the control surfaces on a large aircraft.

### 2.1.8 Pressures in accelerating fluids

Consider equation (2.2) for the pressure gradient:

$$\frac{\partial p}{\partial x}=\rho(f_x-a_x), \tag{2.2}$$

with similar equations for $y$ and $z$.

1. **Fluid accelerating vertically**

Let the vertical acceleration be $a_z$, upwards, the other components being zero. Equation (2.3) gives

$$\frac{\partial p}{\partial x} = \frac{\partial p}{\partial y} = 0, \frac{\partial p}{\partial z} = \rho(-g - a_z) = -\rho(a_z + g),$$

which are the same equations as obtained before, but with $g$ replaced by $a+g$, so that the vertical acceleration and gravity simply combine algebraically.

2. **Fluid accelerating horizontally**

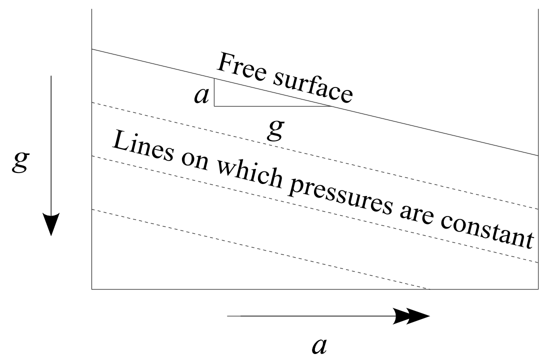


Figure 2-9. Vessel accelerating to the right, showing tilted water surface and pressure contours.

Consider the container in Figure 2-9 which is accelerating in the positive $x$ direction with acceleration $a$. Equation (2.2) gives

$$\frac{\partial p}{\partial x} = \rho(0 - a), \quad \frac{\partial p}{\partial y} = 0, \quad \text{and} \quad \frac{\partial p}{\partial z} = \rho(-g - 0).$$

These equations may be integrated to give

$$\begin{aligned} p &= -\rho a x - \rho g z + C \\ &= -\rho(ax + gz) + C, \end{aligned}$$

where $C$ is a constant of integration. From this we can find the equation of surfaces on which the pressure is constant, $p_1$ say:

$$\frac{p_1 - C}{-\rho} = ax + gz,$$

hence

$$z = D - \frac{a}{g}x,$$

where $D$ is a constant. Clearly, surfaces on which pressure is constant are planes, with a gradient in the $x$-direction of $-a/g$. The free surface, on which $p = p_{\mathrm{a}}$ is a special case.

## 2.2 Forces on submerged planar objects

Consider the submerged plate of arbitrary shape shown in Figure 2-10, inclined at an angle $\theta$ to the horizontal. We introduce the co-ordinate $s$ with origin at the axis OO where the plane of the plate intersects the plane of the free surface. The shape of the plate is defined by a specified breadth as a function of $s$, $b(s)$. At any horizontal line on the plate which is $h$ below the surface the hydrostatic pressure equation gives,

$$p = p_{\mathrm{a}} + \rho g h$$

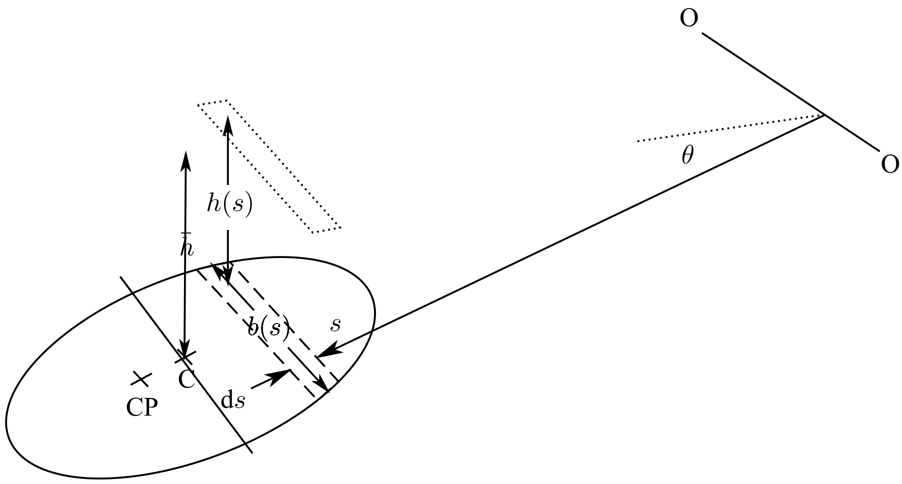


Figure 2-10. Inclined underwater plane surface and axis OO where it intersects the plane of the surface

and the force on an element which is $ds$ wide and $b(s)$ long is

$$\begin{aligned} dF &= p\,dA, \text{ where } dA \text{ is the area of the element,} \\ &= p\,b(s)\,ds \\ &= (p_\text{a} + \rho g h)\,b(s)\,ds. \end{aligned}$$

Now, $h = s\,\sin\theta$, therefore

$$dF = p_\text{a} b(s)\,ds + \rho g \sin\theta\,s\,b(s)\;ds. \tag{2.10}$$

Integrating over the whole plate to find the total force on one side gives

$$F = \int dF = p_\text{a} \int b(s)\,ds + \rho g \sin\theta \int b(s)\,s\,ds,$$

where the first integral is simply the *area* of the plate, $A$, while the second is its *first moment of area* $M_\text{OO}$ *about the intersection line* OO *of the plane of the plate and the free surface*, which has be written as $M_\text{OO} = A\bar{s}$, where $\bar{s}$ is the co-ordinate of the centroid C, giving

$$F = p_\text{a} A + \rho g \sin\theta\,A\,\bar{s}. \tag{2.11}$$

However the depth of the centroid $\bar{h} = \bar{s}\sin\theta$, so force can be written quite simply as

$$F = p_\text{a} A + \rho g A \bar{h}, \tag{2.12}$$

which is often able to be simply calculated without taking moments, if the plate is a simple shape. As the pressure at the centroid is $p_\text{C} = p_\text{a} + \rho g \bar{h}$, the result can be simply stated

Force on plate = Area × Pressure at centroid.

In design calculations it is often necessary to know the position of *Centre of Pressure* (CP), the point at which the total force can be considered to act. Taking moments about OO, substituting equation (2.10), and integrating:

$$\begin{aligned} \text{Moment of force about O} &= \int s\,dF = p_\text{a} \int b(s)\,s\,ds + \rho g \sin\theta \int b(s)\,s^2\,ds \\ &= p_\text{a} A\,\bar{s} + \rho g \sin\theta\,I_\text{OO}, \end{aligned} \tag{2.13}$$

where $I_\text{OO}$ is the *Second Moment of Area* of the plate about the axis OO. If $s_\text{CP}$ is , By definition, $s_\text{CP}$, the $s$ co-ordinate of the centre of pressure is such that the moment of the force is equal to $F\,s_\text{CP}$, and so, substituting equation (2.11) into that and setting equal to the result of equation (2.13), we have

$$s_\text{CP} = \frac{p_\text{a} A\,\bar{s} + \rho g \sin\theta\,I_\text{OO}}{p_\text{a} A + \rho g A \bar{h}}. \tag{2.14}$$

Almost always the atmospheric pressure is ignored, as calculating the force on one side of a plate usually means that the other side of the plate also is subject to atmospheric pressure, *e.g.* the side of a ship shown in Figure 2-11, or the interior of a submarine.

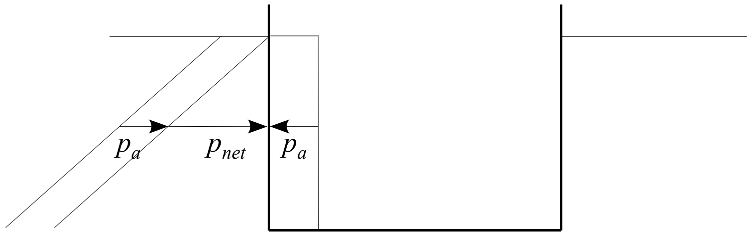


Figure 2-11. Situation, such as the side of a ship, where the atmospheric pressure contributes equally on both sides such that it can be ignored.

Substituting $p_{\mathrm{a}} = 0$ into equation (2.14) and using $\bar{h} = \bar{s}\sin\theta$ gives the expressions

$$s_{\mathrm{CP}} = \frac{\sin\theta\, I_{\mathrm{OO}}}{A\bar{h}} = \frac{I_{\mathrm{OO}}}{A\bar{s}}. \tag{2.15}$$

**Note:** although the force can be calculated by using the depth of the centroid of the plate, *it does not act through the centroid*, *i.e.* $s_{\mathrm{CP}} \neq \bar{s}$.

In some cases, for simple shapes such as rectangles and circles, the second moment of area $I_{\mathrm{CC}}$ of the plane about an axis through its centroid is already known and does not have to be determined by integration. It is convenient to use the *Parallel Axis Theorem*, which in this case is

$$I_{\mathrm{OO}} = I_{\mathrm{CC}} + A\,\bar{s}^2, \tag{2.16}$$

to calculate the distance of the centre of pressure from the centroid. Substituting this into equation (2.15)

$$s_{\mathrm{CP}} = \frac{I_{\mathrm{CC}} + A\,\bar{s}^2}{A\bar{s}} = \frac{I_{\mathrm{CC}}}{A\bar{s}} + \bar{s}. \tag{2.17}$$

This formula can be re-written to give the expression for the *distance of the centre of pressure from the centroid in the plane of the plate*:

$$s_{\mathrm{CP}} - \bar{s} = \frac{I_{\mathrm{CC}}}{A\bar{s}} = \frac{\text{2nd Moment of area about axis at the centroid}}{\text{1st Moment of area about axis at the surface}}. \tag{2.18}$$

In the limit where the plate is much smaller than the distance from the axis, this will tend to zero, where the relative variation of pressure over the plate is small.

**Example 2.2** A circular cover 125 cm in diameter is immersed in water so that the deepest part is 150 cm below the surface, and the shallowest part 60 cm below the surface. Find the total force due to water acting on one side of the cover, and the distance of the centre of pressure from the centroid. You may assume that the second moment of area of a circle of diameter $D$ about a diameter is $I_{\mathrm{CC}} = \pi D^4/64$.

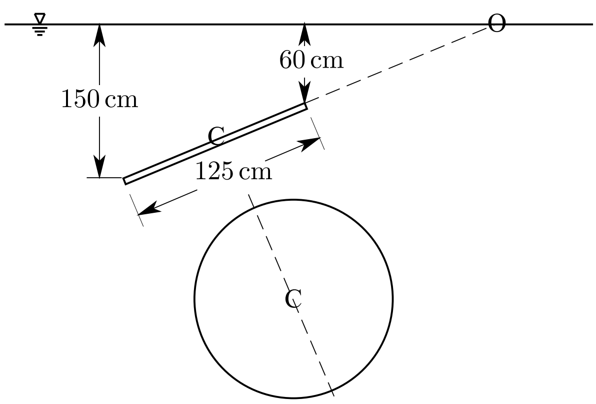

| | |
|---|---|
| Circle: | Area $A = \frac{\pi}{4} \times 1.25^2 = 1.228\,\mathrm{m}^2$, |
| Depth to centroid $\bar{h}$: | By symmetry: $\bar{h} = 0.5(0.6 + 1.5) = 1.05\,\mathrm{m}$, |
| Force: equation (2.12): | $F = \rho g A \bar{h} = 1000 \times 9.8 \times 1.228 \times 1.05 = 12.6\,\mathrm{kN}$ (*Ans.*) |
| Simple trigonometry: | $\sin\theta = (150 - 60)/125 = 0.72$, |
| Simple trigonometry: | $\bar{s} = \bar{h}/\sin\theta = 1.05/0.72 = 1.458\ \mathrm{m}$, |
| Formula given: | $I_{\mathrm{CC}} = \pi D^4/64 = 0.120\,\mathrm{m}^4$, |
| Position of Centre of Pressure (equation 2.18): | $s_{\mathrm{CP}} - \bar{s} = I_{\mathrm{CC}}/A\bar{s} = 0.120/\left(1.228 \times 1.458\right) = 0.067\ \mathrm{m}$, |
| | Centre of pressure is $6.7\,\mathrm{cm}$ from centroid |

## 2.3 Forces on submerged boundaries of general shape

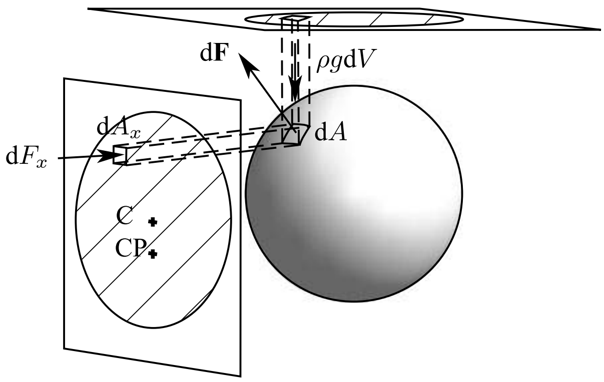


Figure 2-12. Projection of boundary element onto two planes: (a) the free surface, to calculate the vertical force, and (b) a vertical plane perpendicular to the desired horizontal force direction

Forces on submerged boundaries of general shape can be calculated surprisingly simply. Consider the underwater boundary in figure 2-12, with an element of area $\mathrm{d}A$. Consider also the two elemental prisms constructed from $\mathrm{d}A$, one to the free surface, which has a volume $\mathrm{d}V$, and one in a horizontal direction, denoted by $x$, in which direction we require the force, with elemental cross-sectional area $\mathrm{d}A_x$ when projected onto a plane perpendicular to that direction. The results we obtain for this prism will be valid for all horizontal directions, so it will not be necessary to consider separately here another direction perpendicular to this.

### 2.3.1 Horizontal

The horizontal element has a vertical force on it due to the weight force of the fluid in it, but for it we are only concerned with horizontal forces in the direction along the element, and so, as there are no other horizontal forces on the prism, this means that the $x$-component of the force of the fluid on the curved surface is equal to $\mathrm{d}F_x$, the force of fluid on the projection $\mathrm{d}A_x$ onto a vertical plane. This holds for all elements of the surface, and so we can write for the whole surface:

*Any horizontal component of force on a submerged surface is equal to the force on a projection of that surface onto a vertical plane perpendicular to the component.*

For such a calculation, we can use all the results of §2.2 for the forces on a planar surface, for the special case of a vertical plane $\theta = \pi/2$. Equations (2.12) and (2.18) give,

$$F_x = \rho g A_x \bar{h}_x \quad \text{and} \quad h_{\mathrm{CP}} - \bar{h}_x = \frac{I_{\mathrm{CC}}}{A_x \bar{h}_x}, \tag{2.19}$$

where we have used the notation $\bar{h}_x$ for the depth of the centroid of the projected area $A_x$.

**Example 2.3** A tank attached to the side wall of an underwater structure is of the shape of half a sphere, a hemisphere. It has a diameter $D$ and its centre is $d$ below the surface. Calculate the horizontal force and its position.

By symmetry, the net force will be normal to the side wall, and there is no force to left or right in the plane of the wall. To calculate the force we have simply to use equation (2.19), where the projected area of the hemisphere is a circle, with centroid at its centre, $d$ below the surface:

$$F_x = \rho g A_x \bar{h}_x = \rho g \frac{\pi D^2}{4} d.$$

To obtain the position of its resultant point of application, we use the fact that for a circle, $I_{\mathrm{CC}} = \pi D^4/64$,

$$h_{\mathrm{CP}} - d = \frac{I_{\mathrm{CC}}}{Ad} = \frac{\pi D^4}{64} \frac{4}{\pi D^2 d} = \frac{D^2}{16d}.$$

Note that if we re-express this to calculate the distance between centre of pressure and centroid relative to the *radius* (half the diameter) we find

$$\frac{h_{\mathrm{CP}} - d}{D/2} = \frac{D}{8d},$$

showing that for large submergence, $D/d \to 0$, and the centre of pressure will approach the centroid, which holds for all submerged surfaces. in the deep water limit

**Example 2.4** A mixing tank is a vertical cylinder of height $H$ and diameter $D$ filled with fluid of density $\rho$.

(a) Calculate the total horizontal force $F$ on one half of the tank? (this would be used to design the tank walls, which must carry forces of $F/2$ as shown).

(b) How far above the base of the tank does it act?

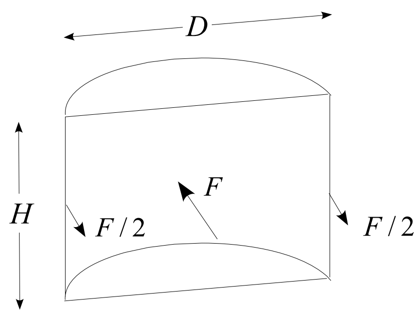


**Answer:** (a) The force on the semi-circular cylinder is equal to that on its projected area, which is the rectangle across its centre, with dimensions $H \times D$. The centroid of the area is at its geometric centre, such that $\bar{h} = H/2$.

$$\begin{aligned} F &= \rho g A_x \bar{h}_x \\ &= \rho g H D \times H/2 \\ &= \tfrac{1}{2} \rho g H^2 D. \end{aligned}$$

(b) The distance between centre of pressure and centroid:

$$h_{\mathrm{CP}} - \bar{h}_x = \frac{I_{\mathrm{CC}}}{A\bar{h}_x}.$$

For the rectangle, the second moment of area $I_{\mathrm{CC}}$ about a horizontal axis through the centroid is, $I_{\mathrm{CC}} = DH^3/12$, hence

$$h_{\mathrm{CP}} - \bar{h}_x = \frac{DH^3}{12} \frac{1}{HD \times H/2} = \frac{H}{6},$$

below the centroid, so the distance of the centre of pressure above the base is $H/2 - H/6 = H/3$.

## 2.3.2 Vertical

Considering the vertical element of fluid, there are only two vertical forces acting on it: one is the weight force of the fluid $\rho g\, \mathrm{d}V$, and the other is the vertical component of the element on the fluid. For equilibrium of the element, the two must be equal. This holds for all elements of the boundary, and so we can write that the vertical force on the whole boundary is equal to $\rho g V$, the weight force on the fluid between the boundary and the plane of the free surface.

Now, however, there is an important generalisation, and that is if any or all of the region between the boundary and the surface is not occupied by fluid, for example if there were another body in the fluid, breaking up the prismatic volume. In fact, this has no effect on the results, for the pressure on the boundary is the same, whether or not part of the volume is unoccupied by fluid, and the force on the boundary is the same as if all the region between boundary and surface were occupied by fluid. Hence we can write the relatively simple and powerful result:

> *The force component in the direction of gravity on a submerged boundary is equal to the weight force on the fluid in the volume bounded by:*
> 1. *the boundary itself, and*
> 2. *its projection onto a plane at the level of the free surface.*
>
> *Contributions are (downwards/upwards) if the surface is (below/above) the local fluid.*

To locate the position of the resultant vertical force, the body force of the vertical prismatic element is at the centre of the prism, and integrating over all such prisms to form the body, the resultant acts through the centre of volume of the body, giving

> *The vertical force component acts through the centre of gravity of the volume between the submerged boundary and the water surface.*

**Example 2.5** The corner of a tank is bevelled by equal dimensions $d$ as shown in the figure. It is filled to $h$ above the top of the bevel. What is the force on the triangular corner?

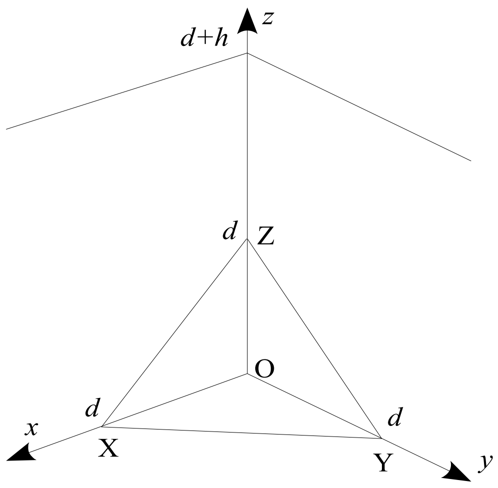


$$\begin{aligned}
\text{Force in } x \text{ direction} &= \text{Force on projection OYZ} \\
&= \rho g A_{OYZ}\, \bar{h}_{OYZ} \\
&= \rho g \times \tfrac{1}{2} d^2 \times \left(h + \tfrac{2}{3} d\right) = \frac{\rho g d^2}{6}(3h + 2d) \\
&= \text{Force in } y \text{ direction by symmetry}
\end{aligned}$$

$$\begin{aligned}
\text{Force in } z \text{ direction} &= \text{Weight force on prism above XYZ} \\
&= \rho g \times \text{ Volume} \\
&= \rho g \times \frac{d^2}{2} \times \tfrac{1}{3}(h + d + h + d + h) \\
&= \frac{\rho g d^2}{6}(3h + 2d).
\end{aligned}$$

Thus, each of the force components is the same. This is what we would expect for such a surface whose direction cosines are the same for all 3 directions.

### 2.3.3 Horizontal force on a vertical wall with the water level at the top

The force on a straight vertical wall with water level at the top is a very common problem, such as sea walls, tanks, and retaining walls. The answer has been provided in Example 2.4 above, originally for the force on a curved wall, which we saw was the same as for a rectangular wall. We replace the diameter of the tank by the length $L$ of the wall and the results immediately follow:

$$F = \tfrac{1}{2}\rho g H^2 L, \quad \text{or,force per unit length } \frac{F}{L} = \tfrac{1}{2}\rho g H^2.$$
$$\text{Height of resultant force above the base} = \frac{H}{3} \text{ or, } \frac{2H}{3} \text{ from the surface.}$$

### 2.3.4 More complicated situations

**Why have we written "at the level of the free surface" in determining vertical forces?:**

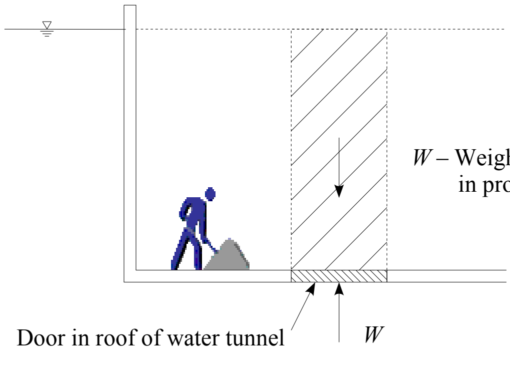


Figure 2-13. Calculation of force in a situation where water does not occupy all the projected volume

In the above derivation we used the expression $p = \rho g h$, where $h$ was the height of the free surface above a general point on the solid surface. It is not necessary for all of the volume between the free and solid surfaces to be occupied by fluid – the result still holds, that the force is that on the volume between the solid surface and its projection on the free surface. Consider the situation in Figure 2-13 where it is required to calculate the force on a door in the roof of a tunnel which is full of water, but above the door is air. The calculation of the volume proceeds, whether or not there is water actually there. Note that in this case the force is upwards. In the above derivation we suppressed the vector and algebraic notation for the sign of the force to make the results simpler. We must interpret the sign of the force, based on the physical nature of the problem. *The force is always in the direction from the water on to the solid surface*, whether the surface is to the left, right, above or below the water.

**What if the surface is multivalued in a co-ordinate direction?:**

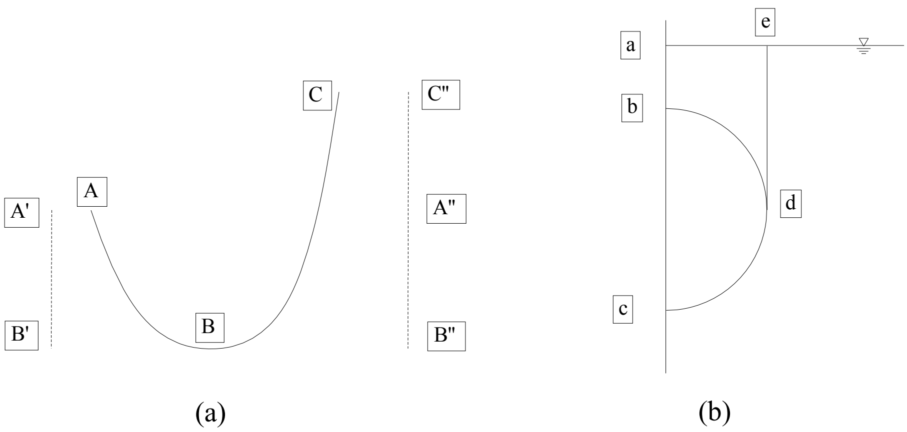


Figure 2-14. Geometric constructions for calculating forces on multivalued objects

If a solid surface bends such that there might be water to left *and* right of parts of it, or above *and* below parts, then we combine the forces in an algebraic sense such that we have to pay attention to the sign of the force over each element of the surface. This has the effect that we usually just have the *net* projected surface area for horizontal forces and the *net* projected volume for vertical forces – often just the body volume itself.

We consider two simple examples. Figure 2-14(a) shows a surface that dips down into water. The location of the free surface is not important and has not been shown. The problem is to calculate the net force on the surface ABC. The fluid on the section AB exerts a force to the right the same as that on the projection A′B′. The fluid on the section BC exerts a force the same as that on the projection B″C″ to the left. However, the force on the section B″A″ is the same as that on the section A′B′ but in the opposite direction so that the two cancel. hence, the net force on the surface is that given by that on the *net projection* A″C″.

Similar considerations for vertical forces are exemplified by Figure 2-14(b), showing the cross-section of a hemisphere, for example. The net vertical force on the hemisphere is composed of two parts, (i) that of the upwards force on the surface cd, which is equal to the gravity force on the liquid in the volume $V_{\text{abcdea}}$, and (ii) that of the downwards force on the surface bd, equal to the gravity force on the liquid in the volume $V_{\text{abdea}}$. The net upwards force is the algebraic sum of the forces on the two volumes, so the required volume is $V_{\text{abcdea}} - V_{\text{abdea}} = V_{\text{bcdb}}$, which is simply the *volume of the body*, in this case.

For any body which is completely immersed in the fluid, with a closed surface as this one, the net force on the body is the weight force that would be exerted if fluid were to occupy the volume of the body. In this way, we have proved *Archimedes' Theorem*!

**Example 2.6** A radial gate on a spillway is in the form of a circular arc of radius $R = 6\,\text{m}$, and retains a depth of $H = 6\,\text{m}$ of water. What is the magnitude, direction, and location of the force per unit length of gate?

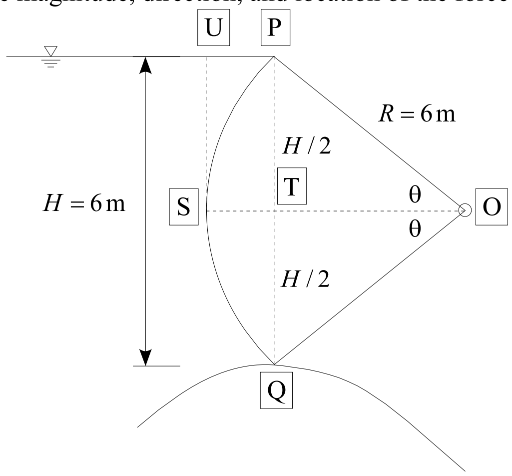


From above, the magnitude of the horizontal force is equal to the force that would be exerted on the horizontal projection of the gate, *i.e.* on the rectangle formed by the line PQ and extending $1\,\text{m}$ normal to the plane of the drawing:

$$\begin{aligned} R_H &= \rho g \underbrace{A\bar{h}}_{\text{PQ}} \\ &= \rho g \times H \times 1 \times \tfrac{H}{2} \\ &= \tfrac{1}{2}\rho g H^2 = \tfrac{1}{2} \times 1000 \times 9.8 \times 6^2 \\ &= 176\,\text{kN}. \end{aligned}$$

The vertical force is a combination of the negative downwards force on PS (fluid above the surface) plus the upwards force on SQ such that, from above, the net upwards force is the weight force on the volume between SQ and the surface, namely UPQS, minus the weight force on the volume between PS and the surface, namely UPS.

The net volume is the "displaced volume" PQS, that is

$$\begin{aligned} R_V &= +\text{Weight force on the volume PQS} \\ &= +\rho g \times 2 \times \text{Volume of PST} \\ &= 2\rho g \times 1 \times \left( \underbrace{\tfrac{1}{2}R^2\theta}_{\text{Sector OPSO}} - \underbrace{\tfrac{1}{2}\tfrac{H}{2}R\cos\theta}_{\text{Triangle OPTO}} \right) \\ &= \rho g \left( R^2\theta - \tfrac{1}{2}HR\cos\theta \right) \end{aligned}$$

but $\sin\theta = (H/2)/R = 1/2$ and $\theta = \pi/6$, giving $R_V = 1000 \times 9.8 \times (36 \times \pi/6 - 18 \times \cos\pi/6) = 32\,\mathrm{kN}$,which is positive, hence upwards, as we might expect because the pressures on the underside of the gate are greater than on the upper side. The water tends to lift the gate off the spillway, and for stability it will have to be sufficiently heavy.

The angle of elevation of the force is $\tan^{-1}(32/176) = 0.18 = 0.18 \times 180/\pi \approx 10°$.

The position of the force: we can do this easily here, for a basic feature of radial gates is that the pressure everywhere on the gate acts normally to the circular surface of the gate, hence goes through the pivot O and so does the resultant, so that there is no net moment on the gate.

## 2.4 The buoyancy and stability of submerged and floating bodies

The methods used above to calculate the force on a surface can be used to calculate the buoyancy forces on totally or partially submerged bodies, that is, surfaces which are closed within the fluid or closed by a plane surface at the level of the free surface.

### 2.4.1 Totally-submerged body

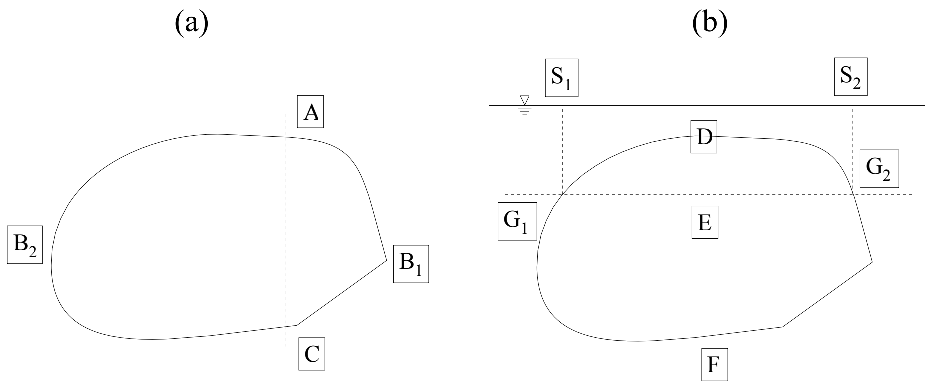


Figure 2-15. Submerged body showing arbitrary points for force calculations

Consider the submerged body in Figure 2-15(a) intersected by an arbitrary vertical plane AC, which is the projected area of each of the two surfaces closed by the plane, $\mathrm{AB_1C}$ and $\mathrm{AB_2C}$, so that the forces on each of the two surfaces are equal (and opposite), hence there is no resultant force on the body. Consider how human development might have progressed had it been possible for an irregularly-shaped object to propel itself!

Now consider the body intersected by an arbitrary horizontal plane $\mathrm{G_1G_2}$ as in Figure 2-15(b), where $\mathrm{S_1}$ and $\mathrm{S_2}$ are points in the free surface where the intersection of the plane and the body are projected to the surface. The vertical (downwards as sketched) force on $\mathrm{G_1DG_2}$ is equal to the weight of fluid in $\mathrm{G_1DG_2S_2S_1G_1}$ while the vertical force (almost all of it upwards here) on $\mathrm{G_1FG_2}$ is equal to the weight of fluid which would occupy the volume $\mathrm{G_1FG_2S_2S_1G_1}$. Hence, the *net buoyancy force*, the net upwards force, is the weight of fluid which would occupy *the difference* between the two volumes, namely the volume of the body.

That is, the buoyancy force is upwards and is equal to the gravity force on the volume of fluid displaced. This is *Archimedes' Principle*, and is easily extended to the case where the body is floating. In this case the body floats at such a level in the water that the weight of the whole body equals that of the weight of fluid displaced by that part of the body beneath the waterline.

**Example 2.7** A rectangular pontoon has a width $B = 6\,\mathrm{m}$, length $L = 12\,\mathrm{m}$, and a draught of $D = 1.5\,\mathrm{m}$ in fresh water. Calculate
(a) the weight of the pontoon,
(b) its draught in sea water of relative density 1.025, and
(c) the load which can be supported by the pontoon in fresh water if the maximum draught is $2\,\mathrm{m}$.

(a)

$$\begin{aligned}\text{Weight of pontoon} &= \text{weight of water displaced}\\ &= \rho g B L D\\ &= 1000 \times 9.8 \times 6 \times 12 \times 1.5\\ &= 1060\,\mathrm{kN}.\end{aligned}$$

(b) In sea water

$$\begin{aligned}1060 &= 1025 \times 9.8 \times 6 \times 12 \times D\\ D &= 1.47\,\mathrm{m}\end{aligned}$$

(c) For $2\,\mathrm{m}$ draught in fresh water,

$$\text{Total buoyancy force} = 1000 \times 9.8 \times 6 \times 12 \times 2 = 1410\,\mathrm{kN}.$$

Therefore the load which can be supported is $1410 - 1060 = 350\,\mathrm{kN}$.

## 2.4.2 Centre of buoyancy

The *centre of buoyancy* is the position in space where the buoyant force may be considered to act for the purposes of taking moments. It is at the centre of mass of the fluid displaced by the body, whether submerged or floating.

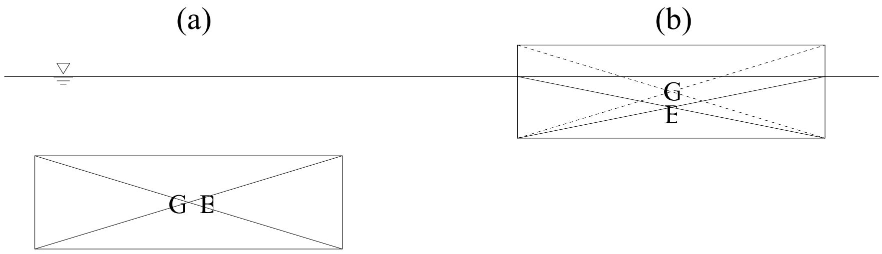


Figure 2-16. Illustration of the centre of buoyancy of a regular body which is (a) submerged, or (b) floating.

Consider two solid rectangular blocks of the same size, but different densities. The one in (a) is heavier than the liquid, it does not float, and if it is homogeneous the centres of buoyancy B and gravity G will coincide. In case (b) the block is lighter than the fluid, it floats, and the displaced volume is less than its total volume, and G is above B as shown.

## 2.4.3 Stability of submerged bodies

Consider the balloon in the illustration. Its centre of buoyancy is close to the centre of the envelope, while its centre of gravity is near the gondola. It has been given a small positive (anti-clockwise) displacement by a gust of wind. Consider the lines of action of the equal and opposite weight and buoyancy forces – it is clear that the moment set up by the displacement is negative and acts so as to reduce the displacement. In this case, and for any submerged body, as long as B is above G, the configuration is stable.

Now consider Figure 2-16(b) for the floating block, where G is *above* B. Do we expect that configuration to be unstable? If not, why not? The explanation and limits for stability will be given in the following section.

## 2.4.4 Stability of floating bodies

For most floating bodies, the centre of gravity is above the centre of buoyancy, and from the above we might expect

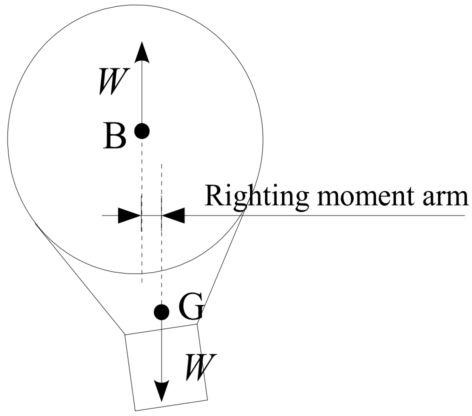


Figure 2-17. Forces acting on a submerged body

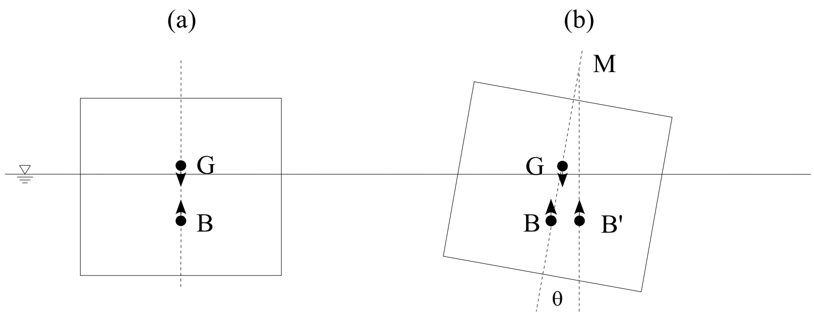


Figure 2-18. (a) Floating body with the common potentially-unstable situation where the centre of gravity is above the centre of buoyancy, and (b) showing how for an angle of rotation the displaced fluid is now a trapezoidal shape and the centre of buoyancy has moved sideways, enough in this case for there to be a restoring force on the body.

the system to be unstable. However, if the body rotates, the shape of the displaced volume changes, such that the centre of buoyancy moves laterally. Hence we have to calculate how much movement there is for a particular body or ship to determine whether it is stable or otherwise. Figure 2-18 shows a stable situation where the centre of buoyancy for an angle of roll $\theta$ has moved from B to B$^{\prime}$, enough that a restoring force has been set up. The amount of movement depends on $\theta$, so that a more fundamental quantity is the distance BM, where M is as shown in the figure, such that for a small angle of rotation $\theta$ the distance that the centre of buoyancy moves is

$$\mathrm{BB}' = \mathrm{BM}\,\theta. \tag{2.20}$$

The condition that the body be stable is that M be above G, such that the *Metacentric Height* GM is positive.

We can calculate the distance BB$'$ by taking moments of volume about the axis of rotation of the body at the waterline, as the centre of buoyancy is at the centre of the mass of fluid displaced. After a rotation $\theta$, the change of first moment of volume is due to the change of first moment of volume just of the wedge-shaped regions shown in Figure 2-19, as the displaced volume below them is unchanged. Hence,

$$\text{Displaced volume} \times \mathrm{BB}' = \text{Change of first moment of volume in the region between the unperturbed and rotated states.}$$

Let the displaced volume is $V$, and if at any point over the waterline plane the *increase* in displacement is $h$, then if $y$ is the distance of that point from the axis parallel to the axis of rotation, at the waterline, then

$$h = y \tan\theta \approx y\theta,$$

for small $\theta$. On the left side of Figure 2-19, $y$ is negative and hence $h$ will be negative, as the displacement has

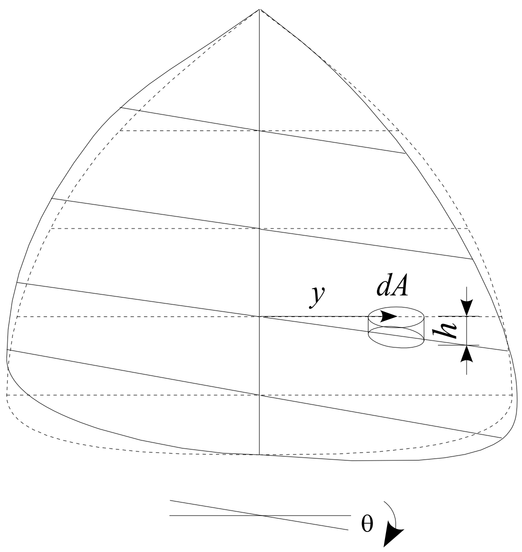


Figure 2-19. View of vessel from stern, showing original waterline cross-section (dashed) and the new position of that section after rolling a small angle $\theta$.

decreased there. Let $dA$ be the element of area of the waterline cross-section, then

$$\begin{aligned} V \times \mathrm{BB}' &= \int_A y\, h\, dA \\ &= \int_A y^2\, \theta\, dA \\ &= \theta \int_A y^2\, dA \\ &= \theta I, \end{aligned}$$

where $I$ is the second moment of area of the waterline cross-section about an axis parallel to the axis of rotation, and so, from this and equation (2.20) we have

$$\mathrm{BM} = \frac{I}{V}. \tag{2.21}$$

That is, the distance of the metacentre above the centre of buoyancy is a purely geometrical quantity, equal to the ratio of the second moment of area of the waterline cross-section to the displaced volume. To determine whether the body is stable, we must calculate (see Figure 2-18)

$$\mathrm{GM} = \mathrm{BM} - \mathrm{BG}, \tag{2.22}$$

and if GM is positive the body will be stable for rotation about an axis parallel to that considered. The position of the centre of gravity, giving BG, is difficult to calculate for ships. To summarise, the procedure is:

**Determination of the stability of a floating body:**

1. Calculate the vertical distance BM= $I/V$.
2. Determine the undisturbed position of the centre of buoyancy B from the geometry of the displaced volume.
3. Determine the position of the centre of mass of the body by measurement (see below) or by knowledge of its shape and mass distribution.
4. Determine the metacentric height GM = BM − BG.

**Measuring metacentric height**

For ships, especially narrow vessels (small $I$!) such as navy ships, the determination of metacentric height is important but difficult, and it is often done experimentally by measuring the angle of tilt caused by moving a load a known distance across the deck of the ship.

**Effect of free water on the stability of a vessel**

If water comes on board a vessel and is free to move as the vessel moves, this can be catastrophic, such as has been experienced with some Roll-on-roll-off vehicular ferries, when water has covered the vehicle deck. As the vessel rolls, and the centre of buoyancy moves, so does the water move, and the centre of gravity of the vessel also moves in this case, possibly endangering stability, as shown on Figure 2-20(a).

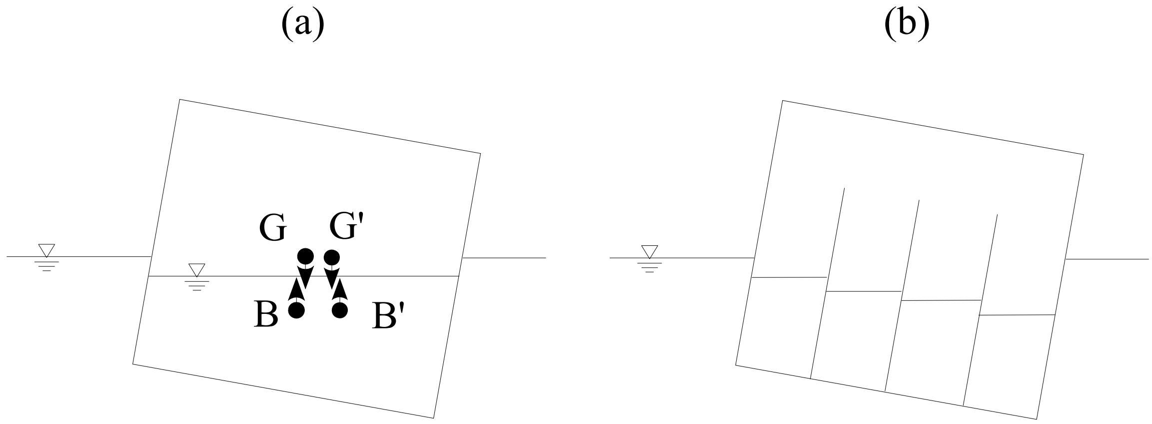


Figure 2-20. (a) The effect of free water on the stability of a vessel, and (b) how bulkheads restrict the lateral movement of water and the centre of gravity of the vessel

**Bulkheads**

Figure 2-20(b) shows how the installation of bulkheads restricts the lateral movement of water and that of the centre of gravity of the vessel. Lesson: if you are on a vehicular ferry and there are no bulkheads between lanes, be ready to leap overboard if anything goes wrong ...

**Example 2.8** A block of wood has sides $L \times L \times D$ and has relative density $\sigma$. Examine the conditions for stability if it floats with side $D$ vertical.

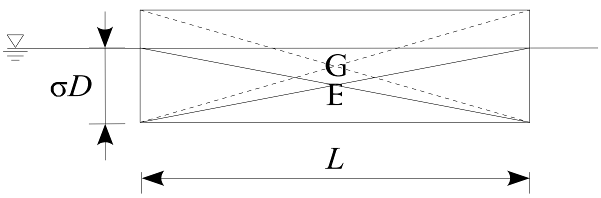


Find the draught $d$:

$$\begin{aligned} \text{Weight of block} &= \text{Weight of water displaced} \\ \rho G \times L^2 D &= \rho L^2 d \\ \therefore d &= GD \end{aligned}$$

Find an expression for the metacentric height GM. Firstly, using the well-known expression for the second moment of area of a rectangle about a transverse axis:

$$\text{BM} = \frac{I}{V} = \frac{\frac{1}{12} \times L \times L^3}{L^2 \times \sigma D} = \frac{L^2}{12\sigma D},$$

and from the figure

$$\begin{aligned} \text{BG} &= \frac{D}{2} - \tfrac{1}{2}\sigma D = \frac{D}{2}(1-\sigma) \\ \therefore \quad & \text{GM} = \text{BM} - \text{BG} = \frac{L^2}{12\sigma D} - \frac{D}{2}(1-\sigma). \end{aligned}$$

The limiting condition for stability is when GM $= 0$, so solving the equation for $D$ gives the solution

$$\frac{D}{L} = \frac{1}{\sqrt{6\sigma(1-\sigma)}},$$

with the condition for stability that

$$\frac{D}{L} \leqslant \frac{1}{\sqrt{6\sigma(1-\sigma)}}.$$

We examine this in a couple of special cases: (1) in the limit as $\sigma \to 1$, as the density of the block approaches that of water, the limiting $D/L \to \infty$, which seems right, that the block is sitting very low in the water, which would be a stable configuration; (2) in the limit as $\sigma \to 0$,also the limiting $D/L \to \infty$, which also seems right, if one imagines a polystyrene block sitting almost on top of the water. Another case (3), $\sigma > 1$, of course, leads to the block falling to the bottom, a most unstable situation!

# 3. Fluid kinematics and flux of quantities

## 3.1 Kinematic definitions

Fluids in motion are rather more complicated: the motion varies from place to place and from time to time. In this section we are concerned with common terminology and descriptions of the flow, and the specification of fluid motion.

**Steady/unsteady flow:** where the flow at each place (does not change / does change) with *time*.

**Uniform/nonuniform flow:** where the flow (does not vary / does vary) with *position*.

**Laminar flow:** where fluid particles move along smooth paths in laminas or layers. This occurs where velocities are small or viscosity is large or if the size of the flow is small, *e.g.* the flow of honey, the motion around a dust particle in air. In civil and environmental engineering flows flow is almost never laminar, but is *turbulent*.

**Turbulent flow:** where the fluid flow fluctuates in time, apparently randomly, about some mean condition, *e.g.* the flow of wind, water in pipes, water in a river. In practice we tend to work with mean flow properties, however in this course we will adopt empirical means of incorporating some of the effects of turbulence. Consider the $x$ component of velocity at $u$ a point written as a sum of steady ($\bar{u}$) and fluctuating ($u'$) components:

$$u = \bar{u} + u'.$$

Let us compute the time mean value of $u$ at a point by integrating over a long period of time $T$:

$$\bar{u} = \frac{1}{T}\int_0^T u\, dt = \frac{1}{T}\int_0^T (\bar{u} + u')\ dt = \bar{u} + \frac{1}{T}\int_0^T u'\, dt,$$

and we see that by definition, the mean of the fluctuations, which we write as $\overline{u'}$, is

$$\overline{u'} = \frac{1}{T}\int_0^T u'\, dt = 0. \tag{3.1}$$

Now let us compute the mean value of the square of the velocity, such as we might find in computing the mean pressure on an object in the flow:

$$\begin{aligned}
\overline{u^2} &= \overline{(\bar{u} + u')^2} = \overline{\bar{u}^2 + 2\bar{u}u' + u'^2},\ \text{expanding,} \\
&= \overline{\bar{u}^2} + \overline{2\bar{u}\,u'} + \overline{u'^2},\ \text{considering each term in turn,} \\
&= \bar{u}^2 + 2\bar{u}\,\overline{u'} + \overline{u'^2},\ \text{but, as }\ \overline{u'} = 0\ \text{from(3.1),} \\
&= \bar{u}^2 + \overline{u'^2}.
\end{aligned} \tag{3.2}$$

hence we see that the mean of the square of the fluctuating velocity is not equal to the square of the mean of the fluctuating velocity, but that there is also a component $\overline{u'^2}$, the mean of the fluctuating components.

**Eulerian and Lagrangian descriptions:** Lagrangian descriptions use the motion of fluid particles. Eulerian descriptions study the motion at points in space, each point being occupied by different fluid particles at different times.

The fluid properties we usually need to specify a flow at all points and times are:

1. Fluid velocity $\mathbf{u} = (u, v, w)$ a vector quantity, in terms of components in $(x, y, z)$ co-ordinates,
2. Pressure $p$, a scalar, which in compressible flow will determine the density at a point, and
3. For flow with a free surface the height of that surface is also important.

### Flow lines

**Streamlines:** a streamline is a line in space such that everywhere the local velocity vector is tangential to it, whether unsteady or not, whether in three dimensions or not.

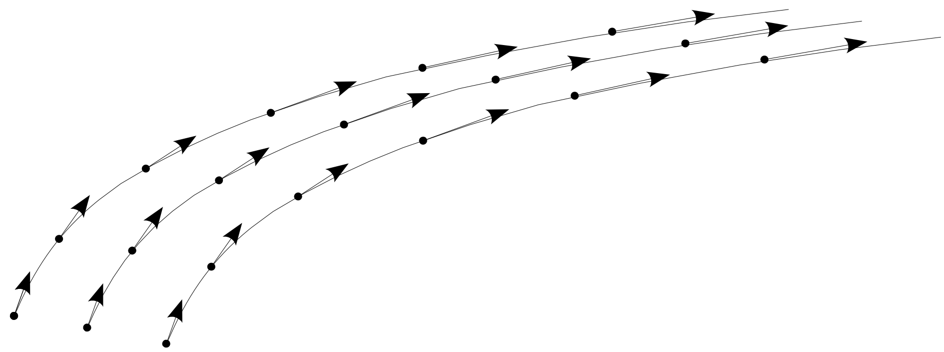

Figure 3-1. Typical streamlines showing how the velocity vectors are tangential

Figure 3-1 shows typical streamlines and velocity vectors. As the velocity vector is tangential at all points of a streamline, there is no flow across a streamline, and in steady 2-D flow, the mass rate of flow between any two streamlines is constant. Where streamlines converge, as shown in the figure, the velocity must increase as shown to maintain that flow. Hence, a plot of streamlines implicitly shows us the direction and magnitude of the velocities.

**Streamtubes:** In 3-D flows the equivalent is a streamtube, which is a closed surface made up of streamlines, as shown in Figure 3-2. There is no flow through a streamtube surface, hence the mass rate of flow through the streamtube is constant at all sections.

**Pathlines:** a pathline is the path followed by an individual particle, which is a more Lagrangian concept. For steady flow streamlines and pathlines coincide.

**Streaklines:** a streakline is a line joining the positions of all particles which have passed through a certain point. They also coincide with streamlines and pathlines for steady flow.

## 3.2 Flux of volume, mass, momentum and energy across a surface

It is necessary for us to be able to calculate the total quantity of fluid and integral quantities such as mass, momentum, and energy flowing across an arbitrary surface in space, which we will then apply to the rather more simple case of control surfaces. Consider an element of an arbitrary surface shown in Figure 3-3 through which fluid flows at velocity $\mathbf{u}$. The velocity component perpendicular to the surface is $|\mathbf{u}|\cos\theta = \mathbf{u}\cdot\hat{\mathbf{n}}$. In a time $dt$ the volume of fluid which passes across the surface is $\mathbf{u}\cdot\hat{\mathbf{n}}\,dt\,dA$, or, the *rate* of volume transport is $\mathbf{u}\cdot\hat{\mathbf{n}}\,dA$. Other quantities easily follow from this: multiplying by density $\rho$ gives the rate of *mass* transport, multiplying by velocity $\mathbf{u}$ gives the rate of transport of *momentum* due to fluid inertia (there is another contribution due to pressure

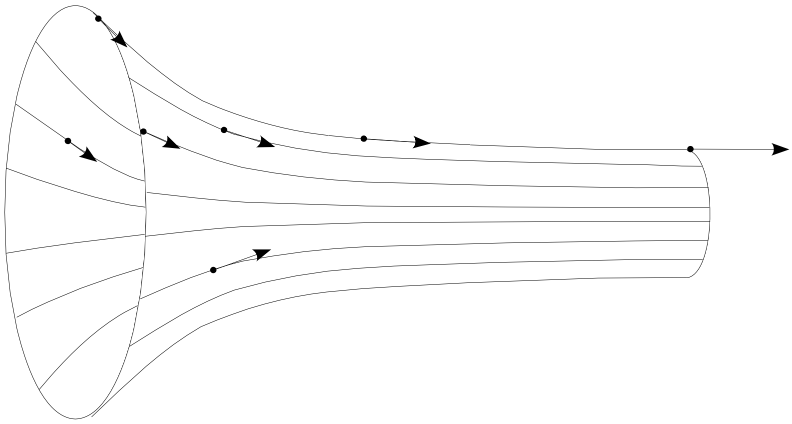

Figure 3-2. Streamtube with velocity vectors tangential to the component streamlines and greater where velocity is greatest.

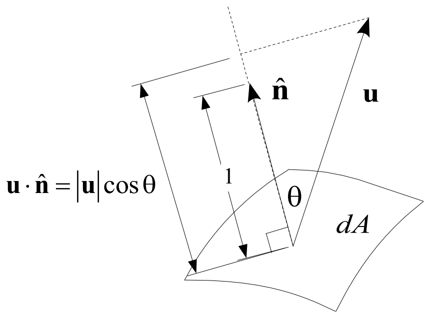


Figure 3-3. Element of surface $dA$ with local velocity vector $\mathbf{u}$ showing how the velocity component normal to the surface is $\mathbf{u}\cdot\hat{\mathbf{n}}$.

for total momentum), and if $e$ is the energy per unit mass, multiplying by $e$ gives the rate of energy transport across the element. By integrating over the whole surface $A$, not necessarily closed, gives the transport of each of the quantities, so that we can write

$$\text{Rate of}\left\{\begin{array}{c}\text{volume}\\ \text{mass}\\ \text{inertial momentum}\\ \text{energy}\end{array}\right.\ \text{transport across surface } A = \int_A \left[\begin{array}{c}1\\ \rho\\ \rho\mathbf{u}\\ \rho e\end{array}\right]\mathbf{u}\cdot\hat{\mathbf{n}}\,dA. \tag{3.3}$$

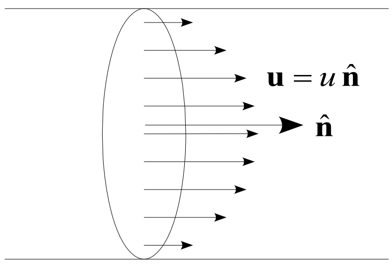


Figure 3-4. Pipe flow, showing a transverse section such that $\mathbf{u}$ and $\hat{\mathbf{n}}$ are parallel. Note that the magnitude of the velocity varies over the section.

Note that as $\mathbf{u}\cdot\hat{\mathbf{n}}$ is a scalar there is no problem in multiplying this simply by either a vector or a scalar. In hydraulic practice such integrals are usually evaluated more easily. For example, across a pipe or channel which is locally straight, to calculate the rates of transport we choose a surface perpendicular to the flow, as in Figure 3-4, as is described below.

**Flux across solid boundaries:** There can be no velocity component normal to a solid boundary, such that every solid boundary satisfies the boundary condition

$$\mathbf{u} \cdot \hat{\mathbf{n}} = 0 \tag{3.4}$$

and so from equation (3.3) there can be no volume, mass, momentum, or energy transfer across solid boundaries.

## 3.3 Control volume, control surface

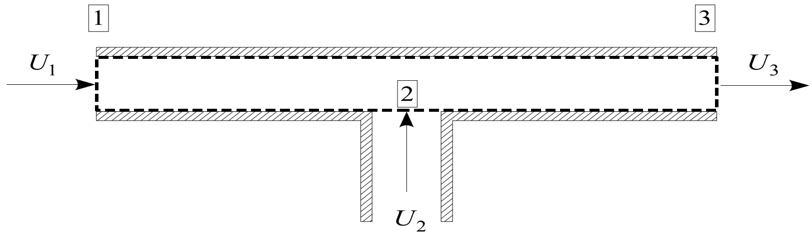


Figure 3-5. Typical control volume for a problem where one pipe joins another.

A *control volume* refers to a fixed region in space through which fluid flows, forming an open system. The boundary of this system is its *control surface*. A typical control surface is shown in Figure 3-5. The control volume for a particular problem is chosen for reasons of convenience. The control surface will usually follow solid boundaries where these are present and will not cut through solid boundaries, as sometimes we have to calculate all the forces on a control surface, which is difficult to do with solid boundaries. Where the control surface cuts the flow direction it will usually be chosen so as to do so at right angles. Problems where control surfaces are most useful are those where the fluid enters or leaves via pipes or channels whose cross-sectional area is relatively small, which fortunately, is usually the case. The reasons for this will be made obvious below.

# 4. Conservation of mass – the continuity equation

Now we consider successively conservation of mass, momentum, and energy, for *steady* flows, although the effects of turbulence will be incorporated. Each conservation principle helps us to solve a variety of problems in hydromechanics.

For *steady* flow, the mass conservation equation for a fluid within a control surface (CS) can be written

$$\int_{\mathrm{CS}} \rho\, \mathbf{u} \cdot \hat{\mathbf{n}}\, dA = 0, \tag{4.1}$$

such that the integral over the control surface of the mass rate of flow is zero, so that matter does not accumulate within the control volume. This is the mass conservation equation. Equation (3.4) states that $\mathbf{u} \cdot \hat{\mathbf{n}} = 0$ on solid boundaries, and so for practical problems we have

$$\int_{\text{Flow boundaries}} \rho\, \mathbf{u} \cdot \hat{\mathbf{n}}\, dA = 0, \tag{4.2}$$

where we only have to consider those parts of the control surface through which fluid flows. In most hydraulics the density of water varies very little and so $\rho$ can be assumed to be a constant, so that it can be taken outside the integral sign, and as it is a common factor, it can be neglected altogether.

If the flow through each flow boundary cuts the boundary at right angles, we can write the velocity as $\mathbf{u} = \pm u\, \hat{\mathbf{n}}$, such that $\mathbf{u} \cdot \hat{\mathbf{n}} = \pm u$, where the plus/minus sign is taken when the flow leaves/enters the control volume. Then across any section of area $A$ we have the contribution $\int_A \mathbf{u} \cdot \hat{\mathbf{n}}\, dA = \pm \int_A u\, dA$, which is $\pm Q$, the *volume flow rate* or *discharge* across the section. Sometimes it is convenient to express this in terms of $U$, the mean velocity, such that

$$\text{Rate of volume transport across surface } = \int_A u\, dA = Q = UA.$$

The mass conservation equation now becomes, for a control surface through which an incompressible fluid crosses each boundary at right angles,

$$\pm Q_1 \pm Q_2 \pm \ldots = \pm U_1 A_1 \pm U_2 A_2 \pm \ldots = 0, \tag{4.3}$$

which is the *continuity equation*, where the sign in each case is chosen according as to whether the velocity or discharge is assumed to be leaving or entering the control volume. For the velocities as shown in Figure 3-5, this would become

$$Q_3 - Q_1 - Q_2 = U_3 A_3 - U_1 A_1 - U_2 A_2 = 0.$$

**Example 4.1** Fluid flows down a circular pipe of diameter $D_1$ at speed $U_1$. It passes through a contraction to a smaller diameter $D_2$, as shown in Figure 4-1. What is the mean velocity in the second pipe?

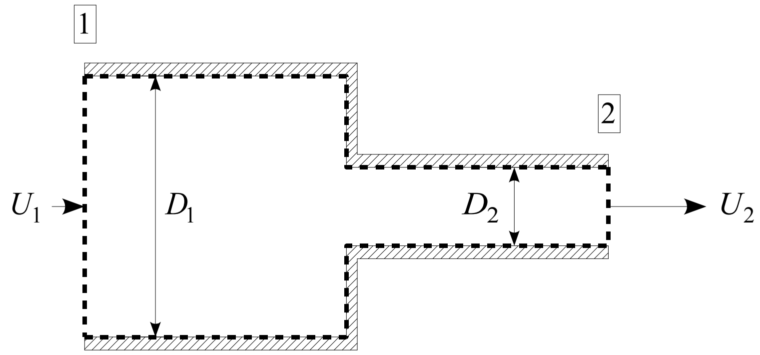


Figure 4-1. Control volume for example

Note that the control surface follows the solid boundaries or crosses the flow direction at right-angles. We have the convention that flows out of the control volume are positive and those in are negative, hence

$$\begin{aligned} -U_1 A_1 + U_2 A_2 &= 0, \\ -U_1 \frac{\pi}{4} D_1^2 + U_2 \frac{\pi}{4} D_2^2 &= 0, \\ \text{Hence} \quad U_2 &= U_1 \left(\frac{D_1}{D_2}\right)^2. \end{aligned}$$

# 5. Conservation of momentum and forces on bodies

**Formulation:** Newton's second law states that the net rate of change of momentum is equal to the force applied. In equation (3.3) we obtained

$$\text{Momentum transport across a surface} = \int_A \rho \mathbf{u}\, \mathbf{u} \cdot \hat{\mathbf{n}}\, dA, \tag{5.1}$$

hence for a closed control surface CS we have to add all such contributions, so that

$$\text{Net rate of change of momentum transport across control surface} = \int_{\text{CS}} \rho \mathbf{u}\, \mathbf{u} \cdot \hat{\mathbf{n}}\, dA.$$

There are two main contributions to the force applied. One is due to surface forces, the pressure $p$ over the surface. On an element of the control surface with area $dA$ and outwardly-directed normal $\hat{\mathbf{n}}$ the pressure force on the fluid in the control surface has a magnitude of $p\, dA$ (simply pressure multiplied by area) and a direction $-\hat{\mathbf{n}}$, because the pressure acts normal to the surface and the direction of the force on the fluid is directed inwards to the control volume.

The other contribution is the sum of all the body forces, which will be usually due to gravity. We let these be denoted by $\mathbf{F}_{\text{body}}$. In many problems the body force is relatively unimportant. Equating the rate of change of momentum to the applied forces and taking the pressure force over to the other side we obtain the *integral* *momentum theorem* for steady flow

$$\int_{\mathrm{CS}} \rho\mathbf{u}\,\mathbf{u}\cdot\hat{\mathbf{n}}\,dA + \int_{\mathrm{CS}} p\,\hat{\mathbf{n}}\,dA = \mathbf{F}_{\text{body}}. \tag{5.2}$$

This form enables us to solve a number of problems yielding the force of fluid on objects and structures .Now the integrals in equation (5.2) will be separated into those over surfaces through which fluid flows and solid surfaces:

$$\sum_{\substack{\text{Fluid}\\ \text{surfaces}}} \left( \int_A (\rho\mathbf{u}\,\mathbf{u}\cdot\hat{\mathbf{n}} + p\,\hat{\mathbf{n}})\; dA \right) + \sum_{\substack{\text{Solid}\\ \text{surfaces}}} \left( \int_A \rho\mathbf{u}\,\mathbf{u}\cdot\hat{\mathbf{n}}\,dA + \int_A p\,\hat{\mathbf{n}}\,dA \right) = \mathbf{F}_{\text{body}}.$$

However, as $\mathbf{u}\cdot\hat{\mathbf{n}} = 0$ on all solid surfaces, there are no contributions. Also on the solid surfaces, unless we know all details of the flow field, we do not know the pressure $p$. However the sum of all those contributions is the total force $\mathbf{P}$ of the fluid on the surrounding structure. Hence we have the theorem in a more practical form for calculating the force on objects:

$$\text{Total force on solid surfaces} = \mathbf{P} = -\sum_{\substack{\text{Fluid}\\ \text{surfaces}}} \left( \underbrace{\int_A (\rho\mathbf{u}\,\mathbf{u}\cdot\hat{\mathbf{n}} + p\,\hat{\mathbf{n}})\; dA}_{\text{Momentum flux}} \right) + \mathbf{F}_{\text{body}}. \tag{5.3}$$

Note the use of the term *momentum flux* for the integral shown – it includes contributions from the inertial momentum flux and from pressure.

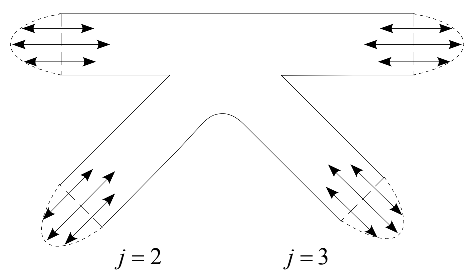


Figure 5-1. Control surface with fluid which is entering or leaving everywhere crossing the control surface (long dashes) at right angles, but where velocity may vary across the element, as shown with short dashes.

**Inertial momentum flux:** Here we evaluate the integral describing the transport of momentum by fluid velocity. In many situations *we can choose the control surface such that on each part where the fluid crosses it, the local surface element is planar, and the velocity crosses it at right angles*, as shown in Figure 5-1. We write for one control surface element, denoted by $j$, $\mathbf{u}_j = \pm u_j \hat{\mathbf{n}}_j$,where $u_j$ is the fluid speed, whose magnitude might vary over that part of the control surface through which it passes, but whose direction is perpendicular either in the direction of the unit normal or opposite to it. Hence, for a particular element $j$,

$$\int_{A_j} \rho\mathbf{u}_j\,\mathbf{u}_j\cdot\hat{\mathbf{n}}_j\,dA = \int_{A_j} \rho\,(\pm u_j\hat{\mathbf{n}}_j)\;(\pm u_j)\;dA = +\hat{\mathbf{n}}_j\,\rho \int_{A_j} u_j^2\,dA, \tag{5.4}$$

where, as $(\pm)\times(\pm)$ is always positive, the surprising result has been obtained that the contribution to momentum flux is always in the direction of the outwardly-directed normal, whether the fluid is entering or leaving the control volume. Also we have assumed that the area $A_j$ is planar such that $\hat{\mathbf{n}}_j$ is constant, so that we have been able to take the $\hat{\mathbf{n}}_j$ outside the integral sign.

**Approximation of the integral allowing for turbulence and boundary layers:** Although it has not been written explicitly, it is understood that equation (5.4) is evaluated in a time mean sense. In equation (3.2) we saw that if a flow is turbulent, then $\overline{u^2} = \bar{u}^2 + \overline{u'^2}$, such that the time mean of the square of the velocity is greater than the square of the mean velocity. In this way, we should include the effects of turbulence in the inertial momentum flux by writing the integral on the right of equation (5.4) as

$$\int_{A_j} u_j^2\, dA = \int_{A_j} \left(\bar{u}_j^2 + \overline{u_j'^2}\right)\, dA. \tag{5.5}$$

Usually we do not know the nature of the turbulence structure, or even the actual velocity distribution across the flow, so that we approximate this in a simple sense by recognising that the time mean velocity at any point and the magnitude of the turbulent fluctuations are all of the scale of the mean velocity in the flow in a time and spatial mean sense, $\bar{U}_j = Q_j/A_j$, such that we write for the integral in space of the time mean of the squared velocities:

$$\int_{A_j} u_j^2\, dA = \int_{A_j} \left(\bar{u}_j^2 + \overline{u_j'^2}\right)\, dA \approx \beta_j \bar{U}_j^2 A_j = \beta_j \left(\frac{Q_j}{A_j}\right)^2 A_j = \beta_j \frac{Q_j^2}{A_j}. \tag{e23}$$

The coefficient $\beta_j$ is called a Boussinesq[7] coefficient, who introduced it to allow for the spatial variation of velocity. Allowing for the effects of time variation, turbulence, has been noted recently (Fenton 2005).

The coefficients $\beta_j$ have typical values of 1.2. Almost all, if not all, textbooks introduce this quantity for open channel flow (without turbulence) but then assume it is equal to 1. Surprisingly, for pipe flow it seems not to have been used at all. In this course we consider it important and will include it.

We are left with the result that over the surface $A_j$ the contribution to momentum flux due to fluid velocity is $\rho\beta_j \bar{U}_j^2 A_j \hat{\mathbf{n}}_j$, where $\beta_j$ is the Boussinesq coefficient.

**Momentum flux due to pressure:** The contribution due to pressure at each element in equation (5.3) is $\int_{A_j} p\, \hat{\mathbf{n}}\, dA$. In most problems where simple momentum considerations are used, the pressure variation across a section is not complicated. To evaluate the term a hydrostatic pressure distribution could be assumed so that we can replace the integral by $\bar{p}_j\, A_j\, \hat{\mathbf{n}}_j$,where $\bar{p}_j$ is the mean pressure at that section, obtained by assuming a hydrostatic pressure distribution, or as the relative size of the section is usually not large, effects of gravity are ignored altogether and we just assume the pressure is constant.

**Combining:** Collecting terms due to velocity and pressure and summing over all such surfaces we have a simple approximation to equation (5.3) above:

$$\mathbf{P} = \sum_j \left(\rho\beta_j \bar{U}_j^2 + \bar{p}_j\right) A_j\ (-\hat{\mathbf{n}}_j) + \mathbf{F}_{\text{body}}, \text{ in terms of velocity,} \tag{5.6a}$$

$$\mathbf{P} = \sum_j \left(\rho\beta_j \frac{Q_j^2}{A_j} + \bar{p}_j A_j\right) (-\hat{\mathbf{n}}_j) + \mathbf{F}_{\text{body}}, \text{ in terms of discharge.} \tag{5.6b}$$

It is a simple and surprising result that all contributions to $\mathbf{P}$ from the fluid are in the opposite direction to the unit normal vector. That is, all contributions are in the direction given by $-\hat{\mathbf{n}}_j$, whether the flow is entering or leaving the control volume, and that is also the direction of pressure contributions. Students should remember this when reading other textbooks, where this simplifying result has not been used.

**Example 5.1** Consider a jet of water of area $A_1$ and mean velocity $U_1$ directed horizontally at a vertical plate. It is assumed that the velocities are so great that the effects of gravity are small and can be neglected. Draw a control surface and calculate the force on the plate, assuming that the fluid after impact travels parallel to the plate.

7 J. J. Boussinesq (1842-1929) was a French academic engineer who studied many problems of flows and waves allowing for variations of physical quantities across the section.

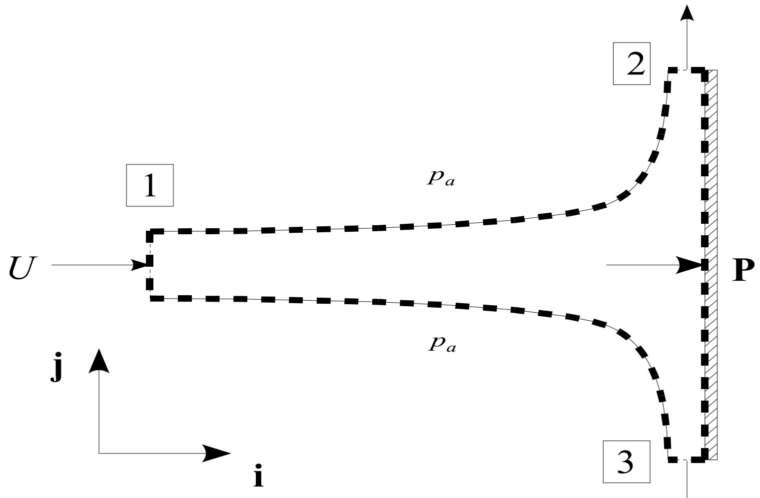


Jet of water striking a plate and being diverted along the plate

After impact water travels parallel to the plate. Consider the figure. On section 1, $\hat{\mathbf{n}} = -\mathbf{i}$, on surface 2, $\hat{\mathbf{n}} = \mathbf{j}$, surface 3, $\hat{\mathbf{n}} = -\mathbf{j}$, and so those sections play no role in horizontal momentum and force. The force on the plate is $\mathbf{P} = P\mathbf{i}$. There are no contributions to the horizontal ($\mathbf{i}$) momentum flux on the surfaces 2 and 3, and as the whole system can be assumed to be at constant pressure $p_a$ (except on the plate itself), substituting into the momentum equation (5.6a) gives

$$P\mathbf{i} = \rho\beta_1 U_1^2 A_1\ (-(-\mathbf{i})) + 0\mathbf{i}, \text{ giving } P = +\rho\beta_1 U_1^2 A_1.$$

**Example 5.2** Repeat, but where after impact, water is diverted back in the other directionNow consider Figure

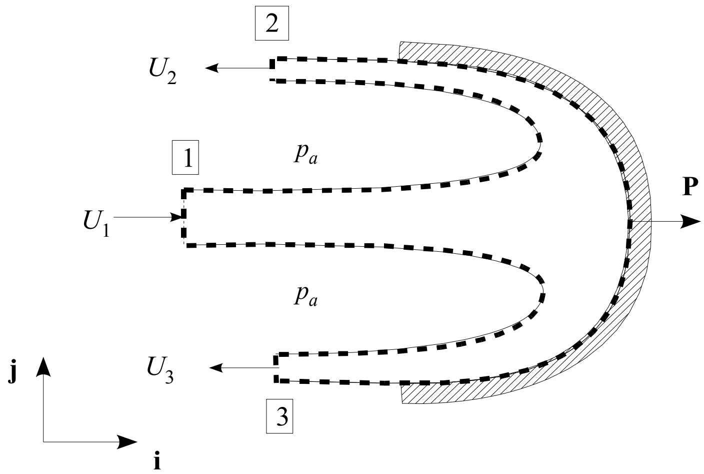


Figure 5-2. Case of jet being diverted back from whence it came

5-2. The crucial point is that while at 1 $\hat{\mathbf{n}}_1 = -\mathbf{i}$ as before, but at 2 and 3, now we have also $\hat{\mathbf{n}}_2 = \hat{\mathbf{n}}_3 = -\mathbf{i}$. Substituting into the momentum equation (5.6a) gives

$$P\mathbf{i} = \rho\beta_1 U_1^2 A_1\ (-(-\mathbf{i})) + \rho\beta_2 U_2^2 A_2\ (-(-\mathbf{i})) + \rho\beta_3 U_3^2 A_3\ (-(-\mathbf{i})) + 0\mathbf{i}.$$

There is no energy loss in this example, and so by conservation of energy the fluid at 2 and 3 will also have a speed of $U_1$, $U_2 = U_3 = U_1$. By mass conservation

$$-U_1 A_1 + U_2 A_2 + U_3 A_3 = 0, \qquad \text{and} \qquad A_2 + A_3 = A_1.$$

As the problem is symmetrical we can assume $A_2 = A_3 = A_1/2$. We assume $\beta_2 = \beta_3 = \beta_1$, and so we obtain

$$P\mathbf{i} = \rho\beta_1 U_1^2 A_1\, \mathbf{i} + \tfrac{1}{2}\rho\beta_1 U_1^2 A_1\, \mathbf{i} + \tfrac{1}{2}\rho\beta_1 U_1^2 A_1\, \mathbf{i},$$

giving

$$P = 2\rho\beta_1 U_1^2 A_1,$$

twice the force in the first example (a), because the change of momentum has been twice that case. Not only was the jet stilled in the **i** direction, but its momentum was completely reversed.

Now a rather more difficult example is presented.

### Example 5.3 Calculation of force on a pipe bend

This is an important example, for it shows us the principles in a general sense. Fluid of density $\rho$ and speed $U$ flows along a pipe of constant area $A$ which has a bend such that the flow is deviated by an angle $\theta$. Calculate the force of the fluid on the bend. It can be assumed that there is little pressure loss in the bend, such that $p$ is constant throughout, and body forces can be ignored. The arrangement is shown on Figure 5-3.It is helpful to use

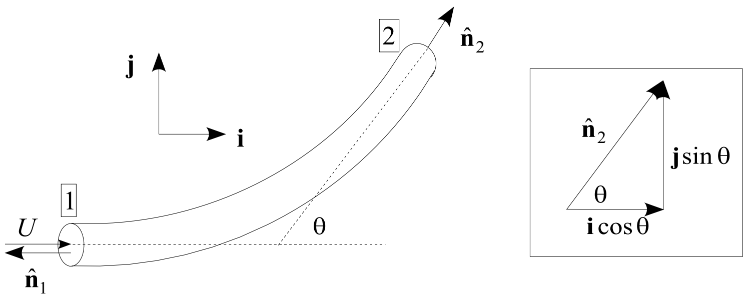


Figure 5-3. Pipe bend

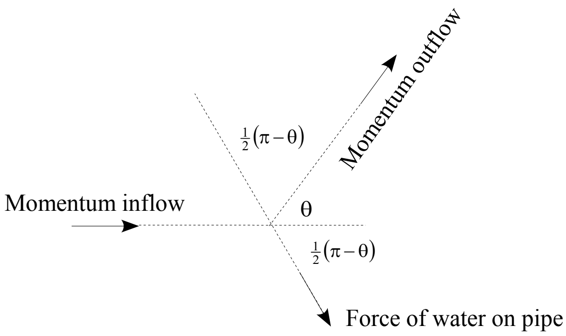


Figure 5-4. Direction of momentum fluxes and force for pipe bend.

unit vectors **i** and **j** as shown. At 1, $\hat{\mathbf{n}}_1 = -\mathbf{i}$, and $\mathbf{u}_1 = U\,\mathbf{i}$, and the contribution to momentum flux in equation (5.6a) is

$$\left(\rho\beta U^2 + p\right) A(-\mathbf{i}).$$

From the construction in the subsidiary diagram, $\hat{\mathbf{n}}_2 = \mathbf{i}\cos\boldsymbol{\theta} + \mathbf{j}\sin\theta$. Hence, at 2 $\mathbf{u}_2 = U\,\hat{\mathbf{n}}_2$ , and the momentum flux is

$$\left(\rho\beta U^2 + p\right) A\,\hat{\mathbf{n}}_2 = \left(\rho\beta U^2 + p\right) A\left(\mathbf{i}\cos\theta + \mathbf{j}\sin\theta\right).$$

Using equation (5.3) we have

$$\mathbf{P} = -\left(-\mathbf{i}A\left(\rho\beta U^2 + p\right) + A\left(\rho\beta U^2 + p\right)\left(\mathbf{i}\cos\theta + \mathbf{j}\sin\theta\right)\right) + \underbrace{\mathbf{0}}_{\text{Body force}},$$

from which we obtain

$$\mathbf{P} = A\left(p + \rho\beta U^2\right)\left(\mathbf{i}\left(1-\cos\theta\right) - \mathbf{j}\sin\theta\right).$$

This answer is adequate, however further insight can be obtained from the trigonometric formulae $1 - \cos\boldsymbol{\theta} = 2\sin^2(\theta/2)$ and $\sin\theta = 2\sin(\theta/2)\cos(\theta/2)$, giving the solution

$$\mathbf{P} = 2A\left(p + \rho\beta U^2\right)\sin\tfrac{\theta}{2}\left(\mathbf{i}\sin\tfrac{\theta}{2} - \mathbf{j}\cos\tfrac{\theta}{2}\right)$$

The magnitude of the force is

$$P = |\mathbf{P}| = 2A\left(p + \rho\beta U^2\right)\sin\tfrac{\theta}{2},$$

and the direction can be obtained a little more simply by considering the unit vector in the direction of the force: $\mathbf{i}\sin(\theta/2) - \mathbf{j}\cos(\theta/2)$. This can be written as

$$\mathbf{i}\cos\left(\tfrac{\theta-\pi}{2}\right) + \mathbf{j}\sin\left(\tfrac{\theta-\pi}{2}\right),$$

in the classical form $\mathbf{i}\cos\phi + \mathbf{j}\sin\phi$, showing that the phase angle of the force is $\theta/2 - \pi/2$. Consideration of the angles involved in Figure 5-4 shows that this seems correct, that the direction of the force of the water is outwards, and symmetric with respect to the inflow and outflow. Other noteworthy features of the solution are that forces on the pipe bend exist even if there is no flow, because the direction of the force due to pressure at inlet is not the same as at outlet. For design purposes the relative contributions of pressure and "inertia" may be quite different. Also in an unsteady state, when there might be pressure surges on the line (waterhammer) there might be large forces. Considering the solution for different values of $\theta$ (a) for $\theta = 0$, no deviation, there is no force, (b) the maximum force is when $\theta = \pi$,when the water is turned around completely, and (c) if the water does a complete loop, $\theta = 2\pi$, the net force is zero.

# 6. Conservation of energy

## 6.1 The energy equation in integral form

The energy equation in integral form can be written for a control volume CV bounded by a control surface CS, where there is no heat added or work done on the fluid inside the control volume:

$$\underbrace{\frac{\partial}{\partial t}\int_{\mathrm{CV}} \rho e\, dV}_{\text{Rate of change of energy inside CV}} + \underbrace{\int_{\mathrm{CS}} \rho e\, \mathbf{u}.\hat{\mathbf{n}}\, dA}_{\text{Flux of energy across CS}} + \underbrace{\int_{\mathrm{CS}} p\, \mathbf{u}.\hat{\mathbf{n}}\, dA}_{\text{Rate of work done by pressure}} = 0, \tag{6.1}$$

where $t$ is time, $\rho$ is density, $dV$ is an element of volume, $\rho e$ is the internal energy per unit volume of fluid, ignoring nuclear, electrical, magnetic, surface tension, and intrinsic energy due to molecular spacing, leaving the sum of the potential and kinetic energies such that the internal energy *per unit mass* is

$$e = gz + \tfrac{1}{2}\left(u^2 + v^2 + w^2\right), \tag{6.2}$$

where the velocity vector $\mathbf{u} = (u, v, w)$ in a cartesian coordinate system, the co-ordinate $z$ is vertically upwards, $p$ is pressure, $\hat{\mathbf{n}}$ is a unit vector with direction normal to and directed outwards from the control surface such that $\mathbf{u}.\hat{\mathbf{n}}$ is the component of velocity normal to the surface at any point, and $dS$ is the elemental area of the control surface.

Here *steady* flow is considered, at least in a time-mean sense, so that the first term in equation (6.1) is zero. The equation becomes, after dividing by density $\rho$:

$$\int_{\mathrm{CS}} \left(\frac{p}{\rho} + gz + \frac{1}{2}\left(u^2 + v^2 + w^2\right)\right) \mathbf{u}.\hat{\mathbf{n}}\, dA = 0. \tag{6.3}$$

It is intended to consider problems such as flows in pipes and open channels where there are negligible *distributed* energy contributions from lateral flows. It is only necessary to consider flow entering or leaving across finite parts of the control surface, such as a section across a pipe or channel or in the side of the pipe or channel. To do this there is the problem of integrating the contribution over a finite plane denoted by $A_j$ which is also used as the symbol for the cross-sectional area. As energy (a scalar) is being considered and not momentum (a vector), it is *not* necessary to take particular orientations of parts of the control surface to be vertical, especially in the case of pipes. To this end, when the integral is evaluated over a finite plane $u$ will be taken to be the velocity along the pipe or channel, and $v$ and $w$ to be perpendicular to that.

The contribution over a section of area $A_j$ is then $\pm\dot{E}_j$, depending on whether the flow is leaving/entering the control volume, where

$$\dot{E}_j = \int\limits_{A_j} \left( \frac{p}{\rho} + gz + \frac{1}{2}\left(u^2+v^2+w^2\right)\right) u\, dA,$$

Now we consider the individual contributions to this integral.

The pressure distribution in a pipe or open channel (river, canal, drain, *etc.*) is usually very close to hydrostatic (streamlines are very close to all being parallel), so that $p/\rho + gz$ is constant over a section through which flow passes, and we try to ensure that at all points at which flow crosses the control surface that this is true. Hence we can take the first two terms of the integral outside the integral sign and use the result that $\int_A \mathbf{u}\cdot\hat{\mathbf{n}}\, dA = Q$ to give

$$\dot{E}_j = (p+\rho g z)\, Q + \frac{\rho}{2}\int\limits_{A_j} \left(u^2+v^2+w^2\right)\, u\, dA, \qquad (6.4)$$

where $p$ and $z$ are the pressure and elevation at any point on a particular section.

Now, in the same spirit as for momentum, when we introduced a coefficient $\beta$ to allow for a non-constant velocity distribution, we introduce a coefficient $\alpha$ such that it allows for the variation of the kinetic energy term across the section

$$\int\limits_{A} \left(u^2+v^2+w^2\right)\, u\, dA = \alpha U^3 A = \alpha \frac{Q^3}{A^2}. \qquad (6.5)$$

Textbooks, strangely, take just the first component under the integral sign and write

$$\int\limits_A u^3 dA = \alpha U^3 A,$$

where $\alpha$ is the *Coriolis*[8] coefficient, for which a typical value is $\alpha \approx 1.25$. We think that the more general coefficient defined in equation (6.5) should be used, and it will be in this course. With equation (6.4) and this definition of $\alpha$:

$$\text{Rate of energy transport across } j\text{th part of the control surface} = \dot{E}_j = (p_j + \rho g z_j)\, Q_j + \alpha_j \frac{\rho}{2}\frac{Q_j^3}{A_j^2}.$$

This can be written in a factorised form

$$\dot{E}_j = \underbrace{\rho Q_j}_{\text{Mass rate of flow}} \times \left( \underbrace{\frac{p_j}{\rho} + g z_j + \frac{\alpha_j}{2}\frac{Q_j^2}{A_j^2}}_{\text{Energy per unit mass}} \right).$$

The energy per unit mass has units of $\mathrm{J\,kg^{-1}}$. It is common in civil and environmental engineering problems to factor out gravitational acceleration and to write

$$\dot{E} = \rho g Q_j \times \left( \underbrace{\frac{p_j}{\rho g} + z_j + \frac{\alpha_j}{2g}\frac{Q_j^2}{A_j^2}}_{\text{Mean total head of the flow}} \right), \qquad (6.6)$$

where the quantity in the brackets has units of length, corresponding to elevation, and is termed the *Mean total head of the flow* $H$, the mean energy per unit mass divided by $g$. The three components are:

$\frac{p}{\rho g}$ = pressure head, the height of fluid corresponding to the pressure $p$,

$z$ = elevation, and

$\frac{\alpha}{2g}\frac{Q^2}{A^2}$ = kinetic energy head, the height which a flow of mean speed $Q/A$ could reach.

[8] G. G. de Coriolis (1792-1843) was a French military and academic engineer, most famous for his contribution to accelerations in rotating frames.

This form is more convenient, because often in hydraulics elevations are more important and useful than actual energies. For example, the height of a reservoir surface, or the height of a levee bank on a river might be known and govern design calculations.

Now, evaluating the integral energy equation (6.3) using these approximations over each of the parts of the control surface through which fluid flows, numbered 1, 2, 3, ... gives an energy equation similar to equation (4.3) for the mass conservation equation

$$\pm\dot{E}_1 \pm \dot{E}_2 \pm \dot{E}_3 \pm \ldots = \pm\rho_1 g Q_1 H_1 \pm \rho_2 g Q_2 H_2 \pm \rho_3 g Q_3 H_3 \pm \ldots = 0, \qquad (6.7)$$

where the positive/negative sign is taken for fluid leaving/entering the control volume. In almost all hydraulics problems the density can be assumed to be constant, and so dividing through by the common density and gravity, we have the

**Energy conservation equation for a control surface**

$$\pm Q_1 H_1 \pm Q_2 H_2 \pm Q_3 H_3 \pm \ldots = 0. \qquad (6.8)$$

We will be considering this more later when we consider systems of pipes. For the moment, however, we will consider a length of pipe or channel in which water enters at only one point and leaves at another.

## 6.2 Application to simple systems

For a length of pipe or channel where there are no other entry or exit points for fluid, using equation (6.8) and the definition of head in equation (6.6):

$$-Q_{\text{in}}\left(\frac{p}{\rho g}+z+\frac{\alpha}{2g}\frac{Q^2}{A^2}\right)_{\text{in}} + Q_{\text{out}}\left(\frac{p}{\rho g}+z+\frac{\alpha}{2g}\frac{Q^2}{A^2}\right)_{\text{out}} = 0, \qquad (6.9)$$

and the continuity equation (4.3) gives $-Q_{\text{in}} + Q_{\text{out}} = 0$, so $Q_{\text{in}} = Q_{\text{out}} = Q$, so that the discharge is a common factor in equation (6.9), and we can divide through by $Q$:

$$\left(\frac{p}{\rho g}+z+\frac{\alpha}{2g}\frac{Q^2}{A^2}\right)_{\text{in}} = \left(\frac{p}{\rho g}+z+\frac{\alpha}{2g}\frac{Q^2}{A^2}\right)_{\text{out}}. \qquad (6.10)$$

In this form the equation is very useful and we can solve a number of useful hydraulic problems. However, to give more accurate practical results, an empirical allowance can be made for friction, and in many applications the equation is used in the form

$$H_{\text{in}} = H_{\text{out}} + \Delta H,$$

where $\Delta H$ is a head loss. In many situations it is given as an empirical coefficient times the kinetic head, as will be seen below.

### 6.2.1 Hydrostatic case

Notice that if there is no flow, $Q = 0$, the energy equation becomes

$$\left(\frac{p}{\rho g}+z\right)_1 = \left(\frac{p}{\rho g}+z\right)_2,$$

which is the Hydrostatic Pressure Equation.

### 6.2.2 A physical deduction

Note that as the quantity $p/\rho g + z + U^2/2g$, where $U = Q/A$, is conserved, then for the same elevation, a region of high/low velocity actually has a low/high pressure. This may come as a surprise, as we associate fast-flowing air with larger pressures. In fact, what we feel in a strong wind as high pressure is actually caused by our body bringing the wind to a low velocity locally. We will use this principle later to describe the Venturi meter for measuring flow in pipes.

**Example 6.1 A Siphon**

Consider the tank shown. On the left side is a pipe with one end under the water and the other end below the level of the water surface. However the pipe is not full of water, and no flow can occur. The pipe on the right has been filled with water (possibly by submerging it, closing an end, and quickly bringing that end out of the tank and below the surface level). Flow is possible, even though part of the pipe is above the water surface. This is a siphon.

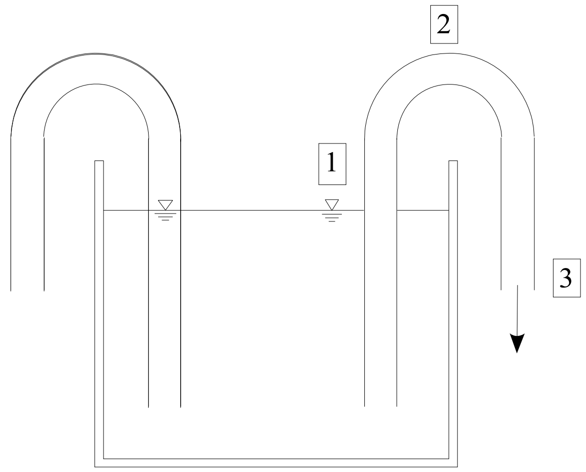


(a) Calculate the velocity of flow at 3 in terms of the elevations of points 1 and 3. Ignore friction losses.

(b) calculate the pressure at 2 in terms also of its elevation.

(a) We consider a control volume made up of the solid surfaces through which no flow can pass, an open face that of the free surface in the tank, and the other open face that at 3. As the velocity with which the surface at 1 drops we will ignore it. Equation (6.10) gives:

$$\begin{aligned}\left(\frac{p}{\rho g}+z+\frac{\alpha}{2g}\frac{Q^2}{A^2}\right)_1 &= \left(\frac{p}{\rho g}+z+\frac{\alpha}{2g}\frac{Q^2}{A^2}\right)_3\\ \frac{0}{\rho g}+z_1+0 &= \frac{0}{\rho g}+z_3+\frac{\alpha}{2g}U_3^2,\end{aligned}$$

which gives

$$U_3=\sqrt{\frac{2g}{\alpha}\left(z_1-z_3\right)}.$$

Note that the factor $\alpha$ does play a role. The velocity of flow is reduced by a factor $1/\sqrt{\alpha}$, which if $\alpha \approx 1.3$ is $0.88$.

(b) Now consider the control volume with the entry face across the pipe at 2. Equation (6.10) gives:

$$\begin{aligned}\left(\frac{p}{\rho g}+z+\frac{\alpha}{2g}\frac{Q^2}{A^2}\right)_2 &= \left(\frac{p}{\rho g}+z+\frac{\alpha}{2g}\frac{Q^2}{A^2}\right)_3\\ \frac{p_2}{\rho g}+z_2+\frac{\alpha}{2g}U_2^2 &= \frac{0}{\rho g}+z_3+\frac{\alpha}{2g}U_3^2,\end{aligned}$$

now solving the equation and using the fact that if the pipe has the same cross-sectional area, then mass conservation gives us $U_2=U_3$,

$$p_2=\rho g\left(z_3-z_2\right).$$

As $z_3-z_2$ is negative, so is this pressure, relative to atmospheric. Flow is possible provided that point 2 is not too high. If $p_2$ drops to the vapour pressure of the water, then the water boils, vapour pockets develop in it, and the flow will stop. At 20°C the vapour pressure of water is $2.5\,\mathrm{kPa}$, *i.e.* a gauge pressure of roughly $-100+2.5=-97.5\,\mathrm{kPa}$, corresponding to $z_3-z_2=p_2/\rho g=-97.5\times 10^3/1000/9.8\approx -10\,\mathrm{m}$, or point 2 being about $10\,\mathrm{m}$ above point 3. Of course, near 100°C the vapour pressure of water is close to atmospheric pressure, so that practically no elevation difference is possible without the water boiling.

**Example 6.2** Application of the integral form of the energy equation – The Venturi[9] meter

[9] Giovanni Battista Venturi (1746-1822), Italian physicist.

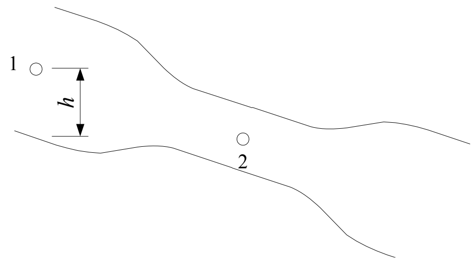


Consider the gradual constriction in the pipe shown, where there are pressure tapping points in the horizontal side of the pipe at point 1 before the constriction and point 2 in the constriction. Generally (unless $h$ were large) the pressure at 2 is always less than that at 1 (higher velocities/lower pressures). Using a control volume crossing the pipe at 1 and 2 and applying equation (6.10), the integral energy theorem for a single inlet and outlet,

$$\frac{p_1}{\rho g} + z_1 + \frac{\alpha}{2g}\frac{Q^2}{A_1^2} = \frac{p_2}{\rho g} + z_2 + \frac{\alpha}{2g}\frac{Q^2}{A_2^2}.$$

Solving for $Q$ and using $z_1 = z_2 + h$ gives

$$Q = \sqrt{\frac{2}{\alpha}\frac{\frac{p_1 - p_2}{\rho} + gh}{\frac{1}{A_2^2} - \frac{1}{A_1^2}}}.$$

Hence we see that by measuring the pressure change between 1 and 2 we can obtain an approximation to the discharge. It is interesting that other presentations introduce a coefficient $C\ (< 1)$ in front to agree with experiment. In our presentation, by including the parameter $\alpha\ (> 1)$ we may have gone some way to quantifying that.

## 6.3 Bernoulli's equation along a streamline

Most presentations of the energy principle in hydraulics actually use Bernoulli's[10] equation, which is an energy-like result obtained from non-trivial momentum considerations for flow through an infinitesimal streamtube (see, for example, §3.7 ofWhite 2003). The result that $H$ is constant along a streamline. This is not as useful as widely believed, as in general this Bernoulli "constant" varies across streamlines, a point that is not always emphasised. Nevertheless, it is in the Bernoulli form that many tutorial and practical problems involving pipes and channels are analysed, and almost all of them ignore the fact that the kinetic energy density varies across a flow. In this course we consider primarily the energy equation in integral form, which allows for cross-stream variation.

There are, however, certain local problems where using *Bernoulli's equation* is easier than the energy conservation equation. It can be stated:

*In steady, frictionless, incompressible flow, the head* $H = \frac{p}{\rho g} + z + \frac{V^2}{2g}$ *is constant along a streamline,*

where $V$ is the fluid speed such that $V^2 = u^2 + v^2 + w^2$. As it is written for frictionless flow along a streamline only, Bernoulli's equation is often not particularly useful for hydraulic engineering, as in both pipes and open channel flows we have to consider the situation where the energy per unit mass varies across the section. It does, however, give simple answers to some simple problems. Nevertheless in many textbooks the application of energy conservation is often described as being application of Bernoulli's equation.

**Example 6.3** The surface of a tank is $h$ above a hole in the side. Calculate the velocity of flow through the hole.

[10] Daniel Bernoulli (1700-1782) was a Swiss mathematician and hydraulician who came from a remarkable family of mathematicians. He is given most credit for this theorem, but his father Johann was also involved.

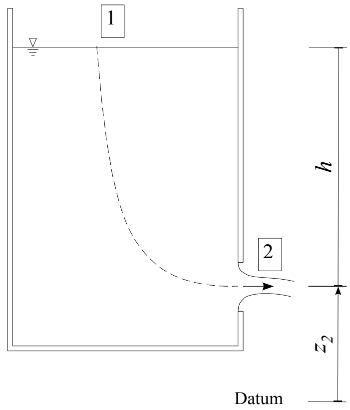


The situation is substantially friction-free. We apply Bernoulli's theorem between two points on any streamline:

Point 1 which is on the surface, where the elevation relative to an arbitrary datum is $z_2 + h$, the pressure is atmospheric, and where we ignore the small velocity at which the surface drops as water flows out, and

Point 2 just outside the hole, where the elevation is $z_2$, the streamlines are parallel and the pressure is atmospheric,

$$\begin{aligned} \left(\frac{p}{\rho g}+z+\frac{V^2}{2g}\right)_1 &= \left(\frac{p}{\rho g}+z+\frac{V^2}{2g}\right)_2 \\ \frac{p_a}{\rho g}+z_2+h+\frac{0^2}{2g} &= \frac{p_a}{\rho g}+z_2+\frac{V_2^2}{2g}, \end{aligned}$$

from which $V_2 = \sqrt{2gh}$ is quickly obtained. Note that this is the same velocity that a particle dropped from that height would achieve. Also notice that the atmospheric pressure cancelled, so we may as well take it to be zero, and the $z_2$ cancelled, so that we may as well take the datum at one of the points considered.

**Example 6.4** The Do-It-Yourself Velocity Meter

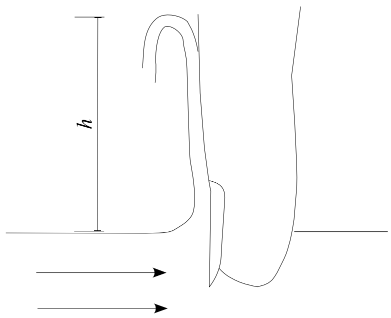


One simple way of measuring the flow velocity in a stream – or from a boat – is to put your finger in the water, and estimate the height $h$ to which the diverted water rises until it has a velocity close to zero. Applying Bernoulli's theorem along the streamline between a point on the surface of the water where the velocity to be measured is $U$, and the highest point to which the water rises, both of which are at atmospheric pressure, gives

$$\frac{0}{\rho g}+0+\frac{U^2}{2g}=\frac{0}{\rho g}+h+\frac{0^2}{2g},$$

giving $U = \sqrt{2gh}$.

**Example 6.5** – the simple Pitot[11] tube: application of Bernoulli's equation along a streamline

Consider an L-shaped tube open at both ends inserted into a flowing stream as shown, with one end level with a point A at which we want to measure the velocity, which is at depth $d$ below the free surface.

[11] Henri de Pitot (1695-1771), French scientist, mathematician, and engineer.

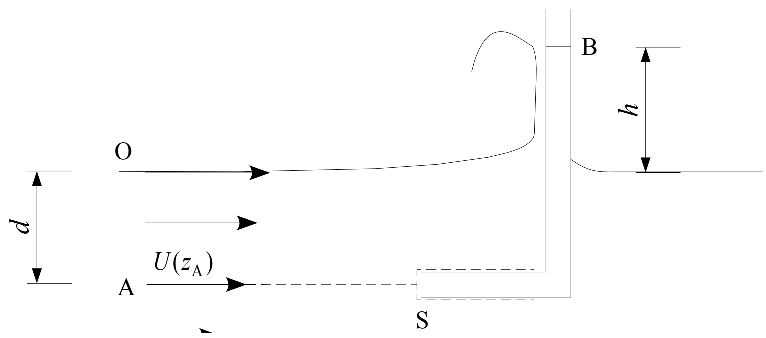


Note that the velocity in the stream varies with depth such that the flow is rotational, and we cannot apply Bernoulli's equation across the streamlines, however we can still apply it along any streamline, and here we apply it along that which passes through A until it strikes the centre of the open tube, inside which the fluid is stationary. The point S, where the fluid locally is brought to a stop, is called a stagnation point, and here the streamline divides around the tube as shown, or more properly, the infinitesimal streamtube separates out into a wider one which passes down the side of the tube.

The surface inside the tube rises to a height $h$ above the free surface. Initially we need the pressure at A. Between a point O on the surface above and A all streamlines are parallel, and hence the pressure distribution is hydrostatic:

$$p_A = \rho g d.$$

Writing Bernoulli's equation between A and the stagnation point S where the velocity is zero, and using the result for $p_A$:

$$\begin{aligned} \frac{p_A}{\rho g} + z_A + \frac{V_A^2}{2g} &= \frac{p_S}{\rho g} + z_S + \frac{V_S^2}{2g} \\ \frac{\rho g d}{\rho g} + z_A + \frac{U_A^2}{2g} &= \frac{p_S}{\rho g} + z_A + \frac{0^2}{2g} \end{aligned} \tag{6.11}$$

Now, inside the tube, the hydrostatic pressure equation gives

$$p_S = \rho g \left(h + d\right),$$

and substituting into equation (6.11) gives

$$U_A = \sqrt{2gh},$$

expressed only in terms of the height of water above the free surface. For different points in the flow, $U_A$ varies, and of course so does $h$. In practice, due to losses a coefficient $C$ might be placed in front of the expression for $U_A$, with $C < 1$. In aeronautics there are rather more sophisticated versions of this.

Note that the fluid at the surface striking the vertical part of the tube, will in general rise to a height corresponding to the velocity at the surface. In general, as the velocity at O is greater than that at A, it will rise higher than the level in the tube.

## 6.4 Crocco's law – a generalisation of Bernoulli's law

It is surprising that this law is not more widely known in hydraulic engineering, as it is a generalisation of Bernoulli's law which describes variation of head across streamlines. Firstly we have to introduce the concept of the *vorticity* of a fluid at a point, which is the curl of the velocity:

$$\boldsymbol{\omega} = \nabla \times \mathbf{u}. \qquad \text{(Definition of vorticity)}$$

It is a very important quantity in fluid mechanics, which is proportional to the angular velocity (and angular momentum) of the fluid at a point, as

$$\boldsymbol{\omega} = 2 \times \text{angular velocity of fluid}.$$

In terms of velocity components $(u, v, w)$ in an $(x, y, z)$ co-ordinate system it is

$$\boldsymbol{\omega} = \begin{vmatrix} \mathbf{i} & \mathbf{j} & \mathbf{k} \\ \partial/\partial x & \partial/\partial y & \partial/\partial z \\ u & v & w \end{vmatrix} = \mathbf{i}\left(\frac{\partial w}{\partial y} - \frac{\partial v}{\partial z}\right) + \mathbf{j}\left(\frac{\partial u}{\partial z} - \frac{\partial w}{\partial x}\right) + \mathbf{k}\left(\frac{\partial v}{\partial x} - \frac{\partial u}{\partial y}\right). \tag{6.12}$$

For the case of a planar flow, $\mathbf{u} = u\,\mathbf{i} + w\,\mathbf{k}$, such that $v = 0$ and with no variation in the $y$ direction, $\partial/\partial y \equiv 0$, equation (6.12) gives

$$\boldsymbol{\omega} = \mathbf{j}\left(\frac{\partial u}{\partial z} - \frac{\partial w}{\partial x}\right), \tag{6.13}$$

and is directed normal to the plane of flow. The right-hand-law applies, as with angular velocity, such that with a clenched fist, the fingers give the sense of motion of fluid particles, the thumb gives the direction of the vector.

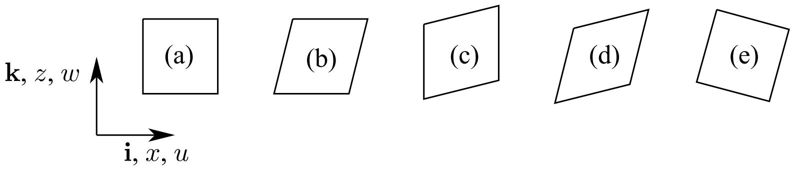


Figure 6-1. Effects of different combinations of velocity gradients on a fluid particle

We can obtain a physical feel for this quantity by considering an initially rectangular particle of fluid as shown in Figure 6-1(a). If the horizontal velocity $u$ increases with the vertical co-ordinate $z$ then due to that effect alone, after a short time the fluid element will be like in (b), where the left and right sides have rotated *clockwise*. However, if the vertical velocity $w$ increases with $x$ then due to this effect alone, after a short time the fluid element will be as in (c) where top and bottom have rotated *anticlockwise*. The combination of these two effects will be to give the shape shown in (d), such that a fluid element deforms but its net or average rotation could be quite small or even zero. This is borne out by equation (6.13), such that if $\partial u/\partial z$ is positive and $\partial w/\partial x$ is also positive, the combined effect is to tend to cancel each other. If, on the other hand, the fluid element is rotating clockwise as if it were a solid body, then $\partial u/\partial z$ is positive but $\partial w/\partial x$ is negative, such that the two combined as in (6.13) reinforce each other, giving a result as in (e), and the vorticity will indeed be about twice the angular velocity of each component. The clockwise rotation in this case is consistent with the direction of vorticity being into the plane.

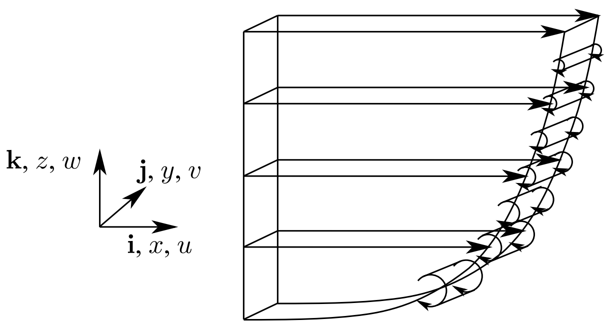


Figure 6-2. Uniform channel shear flow showing co-ordinates and effect of shear in causing rotation of fluid elements

**Example 6.6** Examine the vorticity of a planar uniform channel flow where the velocity is $u = U(z)\,\mathbf{i}$, as shown in the figure, showing how the velocity is zero on the bed, and increases away from the bed. The vorticity is given by equation (6.13): $\boldsymbol{\omega} = \mathbf{j}\,dU/dz = \mathbf{j}\,U'(z)$, so that the magnitude of the vorticity is given by the velocity gradient and its direction is perpendicular to the flow. In the figure, the sliding of layers of fluid over lower slower layers, causing fluid elements to rotate clockwise from our viewpoint, is represented on the figure by cylinders of fluid where the radius of the cylinder increases with increasing vorticity. This has no physical meaning, but is just a graphical device to give an idea of the fact that as $U'(z)$ is greatest near the bed, the vorticity is greatest there.

**Crocco's Law[12]:** tells us how the head actually varies throughout a flow. For the same conditions as Bernoulli's law, steady, frictionless, incompressible but possibly rotational flow, the law is (see p160 of Batchelor

[12] Luigi Crocco (1909-1986), Italian applied mathematician and aeronautical engineer. The law was discovered in 1936.

1967)[13]:

$$\nabla (gH) = \mathbf{u} \times \nabla \times \mathbf{u} = \mathbf{u} \times \boldsymbol{\omega}, \qquad \text{(Crocco's law)}$$

showing that the vector gradient of energy per unit mass ($g$ times Head) is equal to the cross product of velocity and vorticity. If we take a scalar product with $\mathbf{u}$ (or with $\boldsymbol{\omega}$),

$$\mathbf{u} \cdot \nabla (gH) = \mathbf{u} \cdot \mathbf{u} \times \boldsymbol{\omega} = 0$$

the right side is zero, as the scalar triple product there has two identical components, remembering that a scalar triple product has the magnitude of the volume of the parallelepiped generated by its three component vectors, and if any two are co-planar the volume is zero. Hence, as $g$ is constant, we have

$$\mathbf{u} \cdot \nabla H = 0,$$

showing that the gradient of the head $H$ is orthogonal to the velocity vector (and to the vorticity vector). That is, in the direction of the velocity vector, along the streamline, by definition, the derivative of $H$ is zero – *even in rotational flow* – so that $H$ is constant along a streamline. This is Bernoulli's theorem.

**Example 6.7** Examine Crocco's Law for the case of the planar channel flow in Example 6.6.

Let the channel have a total depth $d$. At any point of elevation $z$ above the bed, the depth of fluid above the point is $d - z$. As the streamlines are all parallel, the pressure distribution in the flow will be the same as a hydrostatic pressure distribution, $p = \rho g(d - z)$. Evaluating $H$:

$$\begin{aligned} H &= \frac{p}{\rho g} + z + \frac{V^2}{2g} \\ &= \frac{\rho g(d-z)}{\rho g} + z + \frac{U^2(z)}{2g} = d + \frac{U^2(z)}{2g}, \end{aligned}$$

and clearly the head varies across streamlines, giving,

$$\nabla (gH) = \mathbf{i}\frac{\partial (gH)}{\partial x} + \mathbf{j}\frac{\partial (gH)}{\partial y} + \mathbf{k}\frac{\partial (gH)}{\partial z} = \mathbf{k}U(z)U'(z).$$

Now we evaluate $\mathbf{u} \times \boldsymbol{\omega}$:

$$\mathbf{u} \times \boldsymbol{\omega} = \mathbf{i}U(z) \times \mathbf{j}\,U'(z) = \mathbf{k}U(z)U'(z),$$

which is the same as $\nabla (gH)$, so that we have verified Crocco's law in this special case.

## 6.5 Irrotational flow

When we study the dynamics of fluids we will see that if a fluid is not viscous, a so-called *ideal fluid*, then no shear stresses can act on any fluid elements, no moments exist, and any fluid element retains its original (angular momentum / angular velocity / vorticity). A very important case is that of fluid that starts with no vorticity, hence at all times it has no vorticity, and the flow is *irrotational*, *i.e.* $\boldsymbol{\omega} = \nabla \times \mathbf{u} = \mathbf{0}$. It is this model that lies at the heart of the study of hydrodynamics (the mechanics of irrotational incompressible flows) and water waves in coastal and ocean engineering, where the viscosity and vorticity are unimportant.

In irrotational flow $\boldsymbol{\omega} = \mathbf{0}$, and Crocco's law gives $\nabla H = 0$, that is $H$ is constant throughout the fluid, and we can apply Bernoulli's law throughout the fluid. In the more general case of rotational flow, where $H$ varies across streamlines, Crocco's law leads to $\mathbf{u} \cdot \nabla H = 0$, such that $H$ is constant along each streamline, and we can apply Bernoulli's law along each streamline.

An example of an application to irrotational flow is Example 6.3 above, where water which was still, and hence irrotational, drained from a tank. We considered a single typical streamline, but we could have considered any point on the surface and any point at the nozzle leading from the tank.

[13] George K. Batchelor (1920-2000) was an Australian fluid dynamicist who was a professor of applied mathematics at Cambridge University and for many years editor of the *Journal of Fluid Mechanics*. He worked in turbulence and the physics of suspensions.

## 6.6 Summary of applications of the energy equation

In these notes, the hierarchy of problems and methods to be used can be expressed:

| | | |
|---|---|---|
| Control volume has three or more surfaces through which fluid passes | Eqn (6.8) | $\pm Q_1 H_1 \pm Q_2 H_2 \pm Q_3 H_3 \pm \ldots = 0$ where $H = p/\rho g + z + \alpha (Q/A)^2/2g$ |
| Control volume has two surfaces through which fluid passes | Eqn (6.10) | $H_1 = H_2 + \Delta H$ |
| A single streamline can be considered | Bernoulli's law | $H = p/\rho g + z + V^2/2g$ is constant along the streamline |
| Flow is irrotational (not studied in this course) | Bernoulli's law | $H = p/\rho g + z + V^2/2g$ is constant throughout the flow |

In other sources such as textbooks, these are presented in the reverse order, with little accent if any on the integral form of the energy equation. In most cases, the application is referred to as "Bernoulli's equation", even if it is using the energy equation between two points separated by a complicated geometry such as the surface of a reservoir and a garden tap. The use of $\alpha$ seems almost to be unknown.

# 7. Dimensional analysis and similarity

In hydraulics the four basic dimensions are mass M, length L, time T, and temperature $\Theta$. Dimensional analysis can be used to plan experiments and to present data compactly, but it can also be used in theoretical studies as well. It is a method for reducing the number and complexity of variables which affect a physical problem. This can lead to large savings in test programmes.

Dimensional analysis also helps thinking and planning for an experiment or theory. It suggests variables which can be discarded, sometimes immediately, sometimes such that experiment shows them to be unimportant. It also gives insight into the form of the physical relationship we are trying to study. Another benefit is that it provides scaling laws, by which we can experiment on a model and scale the results up to prototype size.

## 7.1 Dimensional homogeneity

The principle of dimensional homogeneity is almost self-evident:

*If an equation expresses a proper relationship between variables in a physical process it will be dimensionally homogeneous, i.e. each of its additive terms will have the same dimensions.*

As an example consider Bernoulli's equation:

$$\frac{p}{\rho g} + z + \frac{V^2}{2g} = \text{Constant along a streamline}$$

$$\frac{\text{MLT}^{-2}/\text{L}^2}{\text{ML}^{-3}\text{LT}^{-2}} = \text{L}, \text{L}, \frac{\left(\text{LT}^{-1}\right)^2}{\text{LT}^{-2}} = \text{L}.$$

The motive behind dimensional analysis is that any dimensionally homogeneous equation can be written in an equivalent non-dimensional form which is more compact. For example we might write Bernoulli's equation by dividing through by a vertical length scale, such as the depth of a river $d$:

$$\frac{p}{\rho g d} + \frac{z}{d} + \frac{V^2}{2gd} = \text{Constant along a streamline,}$$

and if we introduce dimensionless pressure $p_* = p/\rho g d$, dimensionless elevation $z_* = z/d$, and dimensionless velocity $V_* = V/\sqrt{gd}$, then the equation becomes

$$p_* + z_* + \tfrac{1}{2} V_*^2 = \text{Constant.}$$

## 7.2 Buckingham Π theorem

This theorem was proved by E. Buckingham in 1914, and states:

In a physical problem involving $n$ quantities in which there are $m$ dimensions, the quantities can be arranged into $n-m$ dimensionless $\Pi$ parameters, such that the problem can be expressed $f\left(\Pi_1, \Pi_2, \ldots, \Pi_{n-m}\right)=0$, or as $\Pi_1=f_1\left(\Pi_2, \ldots, \Pi_{n-m}\right)$, or $\Pi_2=f_2\left(\Pi_1, \ldots, \Pi_{n-m}\right), \ldots,$

where $f(\ldots)$ indicates a functional relationship – different in each alternative. The dimensionless parameters are expressed as products $\Pi$ of various physical quantities. We select $m$ physical quantities as *repeating variables*, and express each of the $n-m$ dimensionless parameters as a product of powers of these three and one of each of the remaining $n-m$ variables in turn, and solve for the powers such that each parameter is dimensionless. Often these parameters appear as dimensionless values of each of those variables. In many cases the grouping of the quantities is obvious by inspection, such as when two have the same dimension, such as length, and the ratio of these is the $\Pi$ parameter. It is essential that none of the repeating variables can be derived from the other repeating variables.

## 7.3 Useful points

1. If the problem involves a free surface, then gravity is usually very important and viscosity usually has a negligible effect and may be neglected.
2. If the problem involves no free surface, then gravity is not relevant to anything but the pressure if the fluid is incompressible.
3. If head is involved, use $\rho g Q$ times the head, which is the energy flux, more fundamental than head, for the head depends on the local value of $g$, for example.

**Example 7.1** List the quantities governing the head loss in a pipe and arrange them in dimensionless groups so that we obtain an understanding of what is important.

Of relevance are

| | | | |
|---|---|---|---|
| 1 | Head loss $\Delta H$, appearing as the rate of energy loss | $\rho g Q \Delta H$ | $\mathrm{ML^{-3}LT^{-2}L^3T^{-1}L{=}ML^2T^{-3}}$ |
| 2 | Length of pipe | $L$ | L |
| 3 | Flow rate | $Q$ | $\mathrm{L^3T^{-1}}$ |
| 4 | Pipe diameter | $D$ | L |
| 5 | Roughness size on the pipe wall | $d$ | L |
| 6 | Dynamic viscosity of the liquid | $\mu$ | $\mathrm{ML^{-1}T^{-1}}$ |
| 7 | Density of the liquid | $\rho$ | $\mathrm{ML^{-3}}$ |

We have M, L, and T in the variables, so that $m=3$. We choose $Q$, $D$, and $\rho$ as our repeating variables, which involve all 3 dimensions, and as we have $n=7$ physical quantities we will have $n-m=4$ dimensionless variables, based on the dimensional quantities $\rho g Q \Delta H$, $L$, $d$, and $\mu$ in turn:

1. $\Pi_1=Q^{i_1} D^{i_2} \rho^{i_3} \rho g Q \Delta H$ , so that the dimensional equation is

$$\mathrm{M^0L^0T^0}=\left(\mathrm{L^3T^{-1}}\right)^{i_1} \mathrm{L}^{i_2}\left(\mathrm{ML^{-3}}\right)^{i_3} \mathrm{ML^2T^{-3}},$$

and considering the exponent of each dimension in turn,

$$\begin{aligned} \mathrm{M} &: \quad 0=1+i_3 \\ \mathrm{L} &: \quad 0=2+3 i_1+i_2-3 i_3 \\ \mathrm{T} &: \quad 0=-3-i_1, \end{aligned}$$

From this we have immediately $i_1=-3$, $i_3=-1$, and solving the remaining equation, $i_2=4$. Hence we have

$$\Pi_1=\frac{\rho g Q\, \Delta H\, D^4}{\rho Q^3}=\frac{g\, \Delta H\, D^4}{Q^2}.$$

2. $\Pi_2=Q^{j_1} D^{j_2} \rho^{j_3} L$, and from this it is immediately obvious that we can only involve $D$, such that $j_1=j_3=0$, and $j_2=-1$ such that $\Pi_2=L/D$.
3. $\Pi_3=Q^{k_1} D^{k_2} \rho^{k_3} d$, and similarly $\Pi_3=d/D$ and it is obvious that is the only arrangement.
4. $\Pi_4=Q^{l_1} D^{l_2} \rho^{l_3} \mu$, so that the dimensional equation is

$$\mathrm{M^0L^0T^0}=\left(\mathrm{L^3T^{-1}}\right)^{l_1} \mathrm{L}^{l_2}\left(\mathrm{ML^{-3}}\right)^{l_3} \mathrm{ML^{-1}T^{-1}},$$

and considering the exponent of each dimension in turn,

$$\begin{aligned} \mathrm{M} &: \quad 0 = l_3 + 1 \\ \mathrm{L} &: \quad 0 = +3l_1 + l_2 - 3l_3 - 1 \\ \mathrm{T} &: \quad 0 = -l_1 - 1, \end{aligned}$$

which we can easily solve to give $l_3 = -1$, $l_1 = -1$, and $l_2 = 1$, and hence $\Pi_4 = Q^{-1} D \rho^{-1} \mu$.

Summarising, we have

$$\Pi_1 = \frac{g\,\Delta H\, D^4}{Q^2},\ \Pi_2 = \frac{L}{D},\ \Pi_3 = \frac{d}{D},\ \Pi_4 = \frac{\mu D}{Q\rho},$$

and the problem can be written

$$f\left(\frac{g\,\Delta H\, D^4}{Q^2}, \frac{L}{D}, \frac{d}{D}, \frac{\mu D}{Q\rho}\right) = 0,$$

or as the head loss is the main dependent variable, we express it in terms of the other quantities:

$$\frac{g\,\Delta H\, D^4}{Q^2} = f\left(\frac{L}{D}, \frac{d}{D}, \frac{\mu D}{Q\rho}\right).$$

Now, however, we use some physical intuition, that the amount of head loss $\Delta H$ is directly proportional to the length of the pipe $L$, so that we write

$$\frac{g\,\Delta H\, D^4}{Q^2} = \frac{L}{D} \times f\left(\frac{d}{D}, \frac{\mu D}{Q\rho}\right).$$

Re-arranging, we have

$$\frac{\Delta H}{L} = \frac{Q^2}{gD^5} f\left(\frac{d}{D}, \frac{\mu D}{Q\rho}\right). \tag{7.1}$$

It has been found experimentally that this is an excellent way of formulating the problem – that the fundamental law for pipe friction, the Weisbach formula, is exactly of this form, essentially

$$\Delta H = \lambda \frac{L}{D} \frac{U^2}{2g},$$

where $U$ is the mean velocity (proportional to $Q/D^2$), and $\lambda$ is a dimensionless friction coefficient, proportional to the function $f$ in equation (7.1), a function of the relative roughness $d/D$ and the dimensionless viscosity in the form $\nu D/Q$. It will be seen below that this quantity occurs throughout fluid mechanics, usually written upside down, as the Reynolds number.

**Example 7.2** Repeat that example, but instead of rate of energy loss $\rho g Q \Delta H$ use simply head loss $\Delta H$.

Here we will not repeat the analysis, but only the results:

$$\Pi_1 = \frac{\Delta H}{D},\ \Pi_2 = \frac{L}{D},\ \Pi_3 = \frac{d}{D},\ \Pi_4 = \frac{\mu D}{Q\rho}.$$

This is very different from the previous example – using the head loss directly, with its units of length, its corresponding $\Pi$ parameter has appeared simply as a geometric parameter. If we proceeded as before we would obtain, *cf.* equation (7.1),

$$\frac{\Delta H}{L} = f\left(\frac{d}{D}, \frac{\mu D}{Q\rho}\right),$$

which completely misses the important part of the relationship in that earlier equation. This is powerful evidence for the use of rate of energy loss or power dissipation rather than head loss. It is interesting that of the two usually-reliable textbooks (White 2003, Streeter & Wylie 1981), neither mentions the importance of using energy rather than head. *** Just check this in the 2003 edition. Streeter & Wylie (1981, p164) suggested adding $g$ as a parameter (which is also not at all obvious for pipeline problems), and obtained for a smooth pipe ($d/D$ not included) a form equivalent to

$$\frac{\Delta H}{L} = f\left(\frac{Q^2}{gD^5}, \frac{\mu D}{Q\rho}\right),$$

thereby missing the insightful form of equation (7.1).

## 7.4 Named dimensionless parameters

Professor Irmay of the Technion in Israel gave a seminar in Sydney in about 1980 which the lecturer attended, in which he said that "all of the named dimensionless numbers are upside down – and most are also to the wrong power"! We shall see that that is quite a fair statement.

### 7.4.1 Reynolds number

The number was first proposed by Reynolds in 1883.In any problem involving viscosity, with a discharge $Q$ and length scale $D$ such that there is a velocity scale $U = Q/D^2$, a dimensionless viscosity number appears as in the preceding examples:

$$\frac{\mu D}{Q\rho} = \frac{\nu D}{Q} = \frac{\nu}{UD},$$

which is the ratio of viscosity to inertial forces. In most hydraulics literature this quantity is written upside down and is called the Reynolds number:

$$R = \frac{UD}{\nu}.$$

It would have been more satisfying if the number quantifying the relative importance of viscosity had been directly proportional to viscosity! With the traditional definition, high Reynolds number flows are those which are large and/or fast such that the effects of viscosity are small. In hydraulics problems, with, say, a typical length scale of $1\,\mathrm{m}$, a velocity scale of $1\,\mathrm{m\,s^{-1}}$, and a typical value for water at 20° of $\nu = 1 \times 10^{-6}\,\mathrm{m^2\,s^{-1}}$, a typical value of $R = 10^6$ is obtained. Flows which may be laminar for small Reynolds number become turbulent at a Reynolds number of the order of $10^3$, so it can be seen that nearly all flows in hydraulic engineering are turbulent, and the effects of viscosity are not so important. However, we will see that, for example, the resistance coefficient for pipe flows shows significant variation with Reynolds number in commonly-experienced conditions.

### 7.4.2 Froude[14] number

The Froude number is the most important such number in free-surface flows, and is irrelevant if there is no free surface. It is traditionally used in hydraulic engineering to express the relative importance of inertia and gravity forces, and occurs throughout open channel hydraulics. The traditional definition for a flow of velocity $U$, gravitational acceleration $g$ and *depth* $h$ is

$$F = \frac{U}{\sqrt{gh}}.$$

This number usually does not appear in this form – see Professor Irmay's quote above! If we consider an open channel flow and we want to calculate the energy flux, then with an origin on the bottom of the channel, as the depth is the only vertical scale we have,

$$\dot{E} = \rho g Q\left(h + \frac{\alpha}{2g}\frac{Q^2}{A^2}\right),$$

and non-dimensionalising by dividing through by $\rho g Q h$,

$$\frac{\dot{E}}{\rho g Q h} = 1 + \frac{\alpha}{2gh}\frac{Q^2}{A^2} = 1 + \frac{\alpha U^2}{2gh} = 1 + \frac{\alpha}{2}F^2,$$

hence we see that the relative contribution of kinetic energy is $\alpha F^2/2$. Even if we were to consider rather more complicated problems such as the unsteady propagation of waves and floods, and to non-dimensionalise the equations, we would find that the Froude number itself never appeared, but always as $\alpha\mathbf{F}^2$ or $\beta\mathbf{F}^2$, depending on

[14] William Froude (1810-1879) (pronounced "Frood"), British naval architect who proposed similarity rules for free-surface flows.

whether energy or momentum considerations are being used.

Flows which are fast and shallow have large Froude numbers, and those which are slow and deep have small Froude numbers. Generally $\mathbf{F}^2$ is an expression of the wave-making ability of a flow.

We could define an improved Froude number, $F_{\text{improved}} = \alpha U^2/gh$, which explicitly recognises (a) that $U^2/gh$ is more fundamental than $U/\sqrt{gh}$, and (b) that it is the **weighted** value of $u^2$ over the whole section, $\alpha U^2$, which better expresses the importance of dynamic contributions. However, we will use the traditional definition $F = U/\sqrt{gh}$. In the present course outside this section we have little need for it.

### 7.4.3 Other named numbers

These include the Euler number, a dimensionless pressure number; the Weber number, a dimensionless surface tension number (upside down); Mach number – the ratio of the speed of a flow or aircraft to the speed of sound, a compressibility parameter. They are not important in hydraulics.

## 7.5 Physical scale modelling for solving flow problems

Once an experimenter has selected variables and the dimensional analysis performed, he/she seeks to achieve similarity between the model tested and the prototype to be designed. A formal statement is:

Flow conditions for a model test are completely similar if all relevant dimensionless parameters have the same corresponding values for model and prototype.

### 7.5.1 Geometric similarity

A model and prototype are geometrically similar if and only if all body dimensions in all three co-ordinates have the same linear scale ratio.

### 7.5.2 Kinematic similarity

This requires that the model and prototype have the same length-scale ratio and also the same time-scale ratio. The result is that the velocity-scale ratio will be the same for both. Frictionless flows with a free surface, such as in hydraulic models, are kinematically similar if their Froude numbers are equal, as Froude number contains only length and time dimensions:

$$F_{\text{m}} = F_{\text{p}} \text{ or } \frac{U_{\text{m}}}{\sqrt{gh_{\text{m}}}} = \frac{U_{\text{p}}}{\sqrt{gh_{\text{p}}}}.$$

Now, if the model scale is $r = h_{\text{m}}/h_{\text{p}}$, the velocity scale is

$$\frac{U_{\text{m}}}{U_{\text{p}}} = \frac{\sqrt{h_{\text{m}}}}{\sqrt{h_{\text{p}}}} = \sqrt{r},$$

and the time scale is

$$\frac{T_{\text{m}}}{T_{\text{p}}} = \frac{h_{\text{m}}/U_{\text{m}}}{h_{\text{p}}/U_{\text{p}}} = \frac{r}{\sqrt{r}} = \sqrt{r}.$$

Hence, if a water wave model or a river model has a length scale $r$, the wave period, propagation speed, and particle velocities are related by $\sqrt{r}$.

### 7.5.3 Dynamic similarity

Dynamic similarity exists when model and prototype have the same length-scale ratio, time-scale ratio, and force-scale ratio. Geometric similarity is necessary, then dynamic similarity exists, with kinematic similarity, if model and prototype force and pressure coefficients are equal. For incompressible flow with no free surface it is enough to have model and prototype Reynolds numbers equal; with a free surface the Froude number and if necessary the Weber number are correspondingly equal.

Dynamic similarity is very hard to achieve because true equivalence of Reynolds and Froude numbers can only be achieved by dramatic changes in fluid properties, whereas most model testing is done with air or water.

**Hydraulic model testing with a free surface:** if we have obtained Froude similarity as above, then to obtain dynamic similarity we must have

$$R_{\mathrm{m}} = R_{\mathrm{p}} \text{ or } \frac{U_{\mathrm{m}} h_{\mathrm{m}}}{\nu_{\mathrm{m}}} = \frac{U_{\mathrm{p}} h_{\mathrm{p}}}{\nu_{\mathrm{p}}},$$

hence we must have

$$\frac{\nu_{\mathrm{m}}}{\nu_{\mathrm{p}}} = \frac{U_{\mathrm{m}} h_{\mathrm{m}}}{U_{\mathrm{p}} h_{\mathrm{p}}} = r\sqrt{r} = r^{3/2}.$$

If we use a $1:10$ model scale, then we need to find a fluid with a viscosity $0.1^{3/2} = 0.032$ that of water. As the viscosity of air is 15 times that of water, it is ruled out, and so are all other fluids. In practice, water is used for model and prototype, and Reynolds number similarity is unavoidably violated. This is not so bad, as typical values for model and prototype are large, and viscosity effects are relatively small.

There are worse problems in hydraulic models of natural flow systems such as rivers, harbours, and canals, where they have large horizontal dimensions but small vertical dimensions. If we were to scale an estuary model by $1:1000$ the model would be only a few millimetres deep and the Reynolds and Weber numbers would be seriously in error. Hydraulic models usually overcome this by violating geometric similarity by distorting the vertical scale by a factor of 10 or more. In such cases, as deeper channels flow more freely, the model bottom is usually roughened more to correct for the geometric discrepancy. Another problem is when sediment transport is modelled, when one cannot get particles small enough to model prototype sand particles for example. Nevertheless, in this case some interesting corrections can be made by using lighter particles.

# 8. Flow in pipes

The main problem in studying flow in pipes is to obtain the relationship between flow rate and energy loss, so that if frictional characteristics are known, then flow rates can be calculated, given the available head difference between two points.

## 8.1 The resistance to flow

### 8.1.1 Weisbach's equation

In Example 7.1 we used dimensional analysis to obtain the result (equation 7.1):

$$\frac{\Delta H}{L} = \frac{Q^2}{gD^5} f\left(\frac{d}{D}, \frac{\mu D}{Q\rho}\right).$$

for the head loss $\Delta H$ in a pipe of length $L$ and diameter $D$ with a flow rate $Q$, where the roughness size on the pipe wall is $d$, and the physical quantities $g$, $\mu$, and $\rho$ are as usual. This is the basis for Weisbach[15]'s equation for pipes, introduced in the 1840s, which states

$$\Delta H = \lambda \frac{L}{D} \frac{U^2}{2g}, \tag{8.1}$$

where $U$ is the mean velocity, and $\lambda$ is a dimensionless friction coefficient, for which the symbol $f$ or $4f$ is sometimes used, which is a function of relative roughness $\varepsilon = d/D$ and pipe Reynolds number $UD/\nu$. The equation is widely used to calculate friction in pipes, and was at the core of hydraulics research in the first half of the 20th century. Often the equation is called the Darcy-Weisbach equation; some authors do not bother with a name for the equation or for the coefficient $\lambda$. For pipes the gravitational acceleration $g$ plays no role other than that of multiplying $\Delta H$ to give the energy loss per unit mass. The total power loss in the pipe is $\rho g Q \Delta H$.

### 8.1.2 Experimental results

**Nikuradse – uniform sand grains:** The most important developments in the determination of the coefficient $\lambda$ were in the 1930s. Nikuradse[16] measured $\lambda$ in his famous series of experiments on both smooth and

[15] Julius Weisbach (1806-1871), German mathematician and hydraulician.
[16] Johann Nikuradse (1894-1979), Georgian engineer who worked in Germany.

pipes artificially-roughened with uniform sand grains. For fully-rough conditions he concluded that the friction coefficient $\lambda$ was a function only of the relative roughness $\varepsilon = d/D$, where $d$ is the grain diameter, as

$$\frac{1}{\sqrt{\lambda}} = 2.0 \log_{10} \frac{3.7}{\varepsilon}. \tag{8.2}$$

The coefficient 2.0 is usually written as 2, here it will be emphasised that it is experimentally-determined. At the other extreme, for smooth boundaries, or flows of a small Reynolds number such that the viscous layer covers the roughnesses, the Kármán-Prandtl law is

$$\frac{1}{\sqrt{\lambda}} = 2.0 \log_{10} \left(R\sqrt{\lambda}\right) - 0.8, \tag{8.3}$$

where $R$ is the Reynolds number of the pipe flow, $R = UD/\nu$, where $\nu$ is the kinematic coefficient of viscosity, and where the numbers 2.0 and the 0.8 were experimentally obtained by Nikuradse. He subtracted the fully-rough behaviour, equation (8.2), and plotted the quantity

$$F = 2.0 \log_{10} \frac{3.7}{\varepsilon} - \frac{1}{\sqrt{\lambda}} \tag{8.4}$$

as ordinate, such that for fully rough conditions the points tend towards the value $F = 0$. For the abcissa the logarithm of the grain/roughness Reynolds number

$$R_* = \frac{u_* d}{\nu}$$

was used, where $u_*$ is the shear velocity $u_* = \sqrt{\tau_0/\rho}$, in which $\tau_0$ is the boundary shear stress. These are shown on Figure 8-1. In the smooth wall limit and for flows of small Reynolds number such that the viscous boundary layer effectively covers the roughnesses:

$$F = 1.0 - 2.0 \log_{10} R_*, \tag{8.5}$$

such that when $F$ is plotted against $\log_{10} R_*$, as in Figure 8-1 the graph is a straight line of gradient $-2.0$. Nikuradse found that for smooth conditions, his points fell close to this line.

The remarkable result can be seen that all results, smooth and rough, fall on a single curve, giving indeed a single function for the friction factor $\lambda$ in terms of $R_*$ and $\varepsilon$..

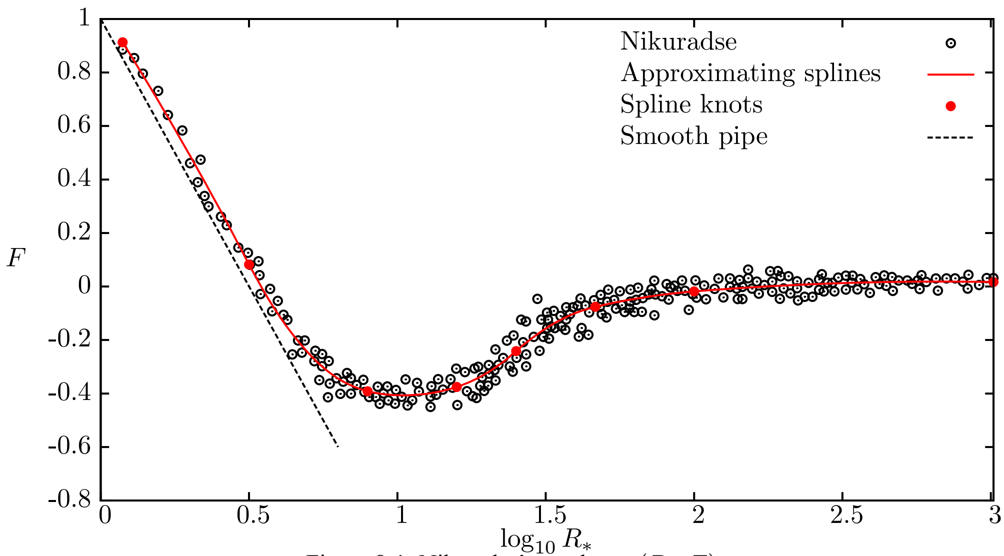


Figure 8-1. Nikuradse's results on $(R_*, F)$ axes.

Nikuradse had found that the experimental points for different values of relative roughness clustered along a single curve, as shown in Figure 8-1, which showed a marked dip in the transition region between the two limits. He had used uniform roughness elements composed of sand grains of the same diameter, such that there was very little protuberance of any above the others. The hydraulic conditions on each grain were similar for each test, and so almost all grains made the transition from laminar to turbulent in the same range of conditions, and so the transition range for the pipe as a whole was relatively limited. Rouse (1937) wrote an interesting article explaining the developments in fluid mechanics of the twentieth century, some of which have been described above. As far as Nikuradse's results were concerned, he wrote:

> *It is to be noted that equation (8.2 in this work) may be expected to apply generally only in the event that the roughness in question is geometrically similar to that of the sand coatings in Nikuradse's investigation. Any departure in the form of roughness will most certainly require different constants in this relationship, and in some cases (waviness) even a different form of equation ... It is with the investigation of other types of roughness in this systematic fashion that laboratories are now engaged , with the ultimate goal of determining the proper functional relationship for major types of commercial pipe.*

In fact, the most important such work is that of Colebrook and White (Colebrook & White 1937, Colebrook 1939), which will now be described, and which has provided the basis for almost all pipe friction calculations.

**Colebrook and White – commercial (variable) roughness:** Of studies of pipes with variable roughness for practical applications, the most comprehensive were those of Colebrook and White. In Colebrook & White (1937) they considered pipes with non-uniform artificial roughness elements: "six different types of roughness were formed from various combinations of two sizes of sand grain, *viz.* $0.035\,\mathrm{cm}$ diam. and $0.35\,\mathrm{cm}$ diam. ... The whole surface was roughened for some of the experiments, while for others part of the surface was left smooth. The fine grains lay in a very uniform manner just touching each other". The large grains were arranged sparsely, in two different configurations. They calculated the $d_s$ the equivalent uniform sand size, from the friction coefficients for fully rough cases. When the results were plotted, using $d = d_s$, on the axes of figure 8-2 here, the results formed a family of curves, all but one showing a dip, like the results of Nikuradse. As the distribution of roughness sizes went from uniform, as Nikuradse, to a mixture of large and small grains, and ultimately to only large grains, each curve of results showed less and less dip together with earlier deviation from the smooth law, so that the transition region became wider and wider. Their case V, for widely-spaced large grains only, showed no dip. They quoted results from tests on galvanised and wrought-iron pipes, which had variable roughness heights, and which showed behaviour similar to their case V, where transition was gradual and "in extreme cases so gradual that the whole working range lies within the transition zone".

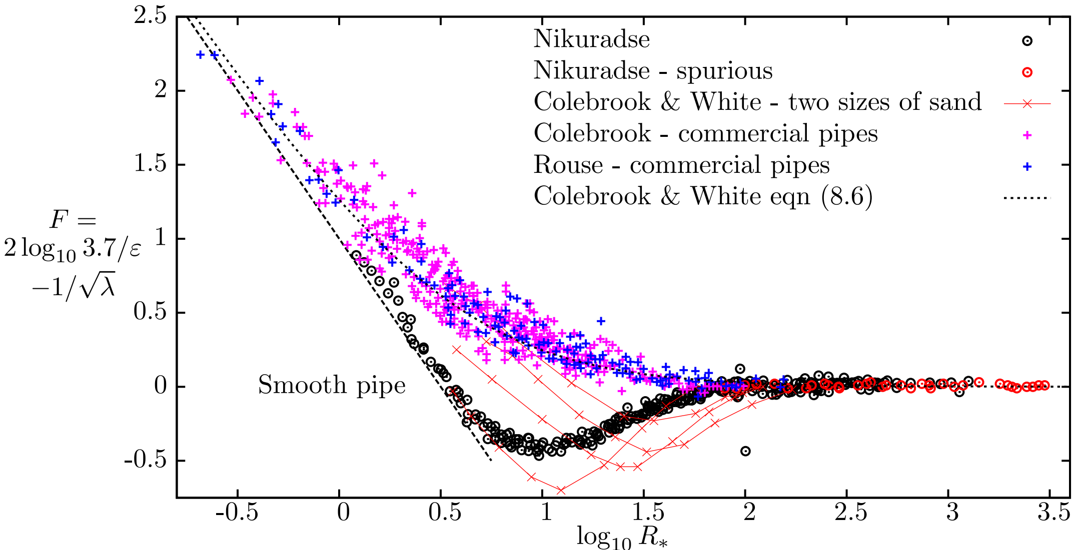


Figure 8-2. Nikuradse's plot, to which results from Colebrook and White for two sand sizes and other results for commercial roughness have been added, the latter showing no dip in the transition zone.

Colebrook (1939) examined results from experiments on commercial pipes of variable roughness – galvanised, tar-coated cast-iron and wrought-iron pipes, and plotted the results on a figure such as 8-2, as has been done here. It can be seen that for each such commercial pipe with non-uniform roughness, *there was no dip* on the diagram, and the transition region was very wide indeed. Colebrook then described how he and White obtained a bridging function between equation (8.4) for small Reynolds number and $F = 0$ for large Reynolds numbers. For computing head loss in turbulent pipe flow Colebrook and White's formula is widely used, expressing the friction factor $\lambda$ as an *implicitly*-defined function of the pipe Reynolds number $R = UD/\nu$ and the relative roughness $\varepsilon = d/D$:

$$\frac{1}{\sqrt{\lambda}} = -2\,\log_{10}\left(\frac{\varepsilon}{3.7} + \frac{2.51}{R\sqrt{\lambda}}\right). \tag{8.6}$$

It is a bridging equation, which goes from one correct limit to the other correct limit. There is nothing special about its validity in the intermediate transition range, other than that it is not very far from the various experimental curves shown. It has no other justification other than that it has the correct behaviour in the two limits. Colebrook did not view the equation as an interpolating function and never expected much of it. He was more of an empirical frame of mind than his successors, and he viewed the different results for the various pipes as being more important than the single equation. In fact, in his conclusions, he stated:

> *The fact that there are considerable variations in the roughness and transition curves in each class of pipe must not be considered a defect in the method of analysis. Such variations are to be expected, since manufacturing conditions are not identical in different plants. For design purposes a series of transition curves for each class is obviously impracticable, so mean curves corresponding to average conditions have been determined.*

Then Colebrook wrote

> *Where it is not possible to determine by experiment the transition curve for any particular type of pipe, the theoretical transition curve (8.6) may be used with very little error provided that the roughness can be determined, and this is not difficult since some reliable experimental data on a few pipes over at least a small range of velocities is usually available.*

In view of the results on the figure here, one might disagree with the ”very little error”. These warnings were repeated by Montes (1998, p109 *et seq.*), who gave a scholarly discussion of the situation and stated, concerning the equation:

> *(it) ... has no other validation than the comparison with data for a particular type of roughness.*

His suggestions and word of warning seem not to have been adopted, at least by authors of textbooks. It provides an approximate solution, which has been extensively used for 60 years. However, it is clear that its progenitors did not believe that it was the complete answer to calculating friction coefficients, and assumed that engineers would use experimental methods much more than they have.

### 8.1.3 Moody (1944) – a graphical presentation of the equation

Possibly the one development which most cemented the Colebrook and White equation into its place as the most widely-used means of calculating friction was the work of Moody (1944) in which he provided a diagram (8-3) here, on which he plotted the Colebrook and White equation (8.6), citing the equation and its originators almost as an afterthought. The diagram showed a number of curves, each for a constant value of the relative roughness $\varepsilon$, with $R$ as abcissa and $\lambda$ as ordinate.

The success of this was caused by the problem in a pre-computer age, that in practical problems, where $\lambda$ has to be calculated for a given Reynolds number and relative roughness, it appears on both sides of the Colebrook and White equation, and the problem becomes one of solving the equation as a nonlinear equation, using methods such as Newton's method, bisection, *etc*.

Many people seem to believe that the Moody diagram has almost magical properties. In fact, all it is is a plot of solutions of the nonlinear transcendental Colebrook and White equation (8.6).

### 8.1.4 Explicit approximations for $\lambda$

There have been several approximations to the equation, giving formulae for $\lambda$ explicitly. There were some early expressions which were not particularly accurate, but in the years 1976-1983 there was a flurry of activity obtaining more accurate approximations that appeared mainly in the chemical engineering literature. Haaland (1983), obtained a relatively simple and useful expression

$$\lambda = \frac{1}{1.8^2}\,\log_{10}^{-2}\left(\left(\frac{\varepsilon}{3.7}\right)^{10/9} + \frac{6.9}{R}\right). \tag{8.7}$$

Haaland made the good point that Colebrook and White's original expression was not exact, and so the level of

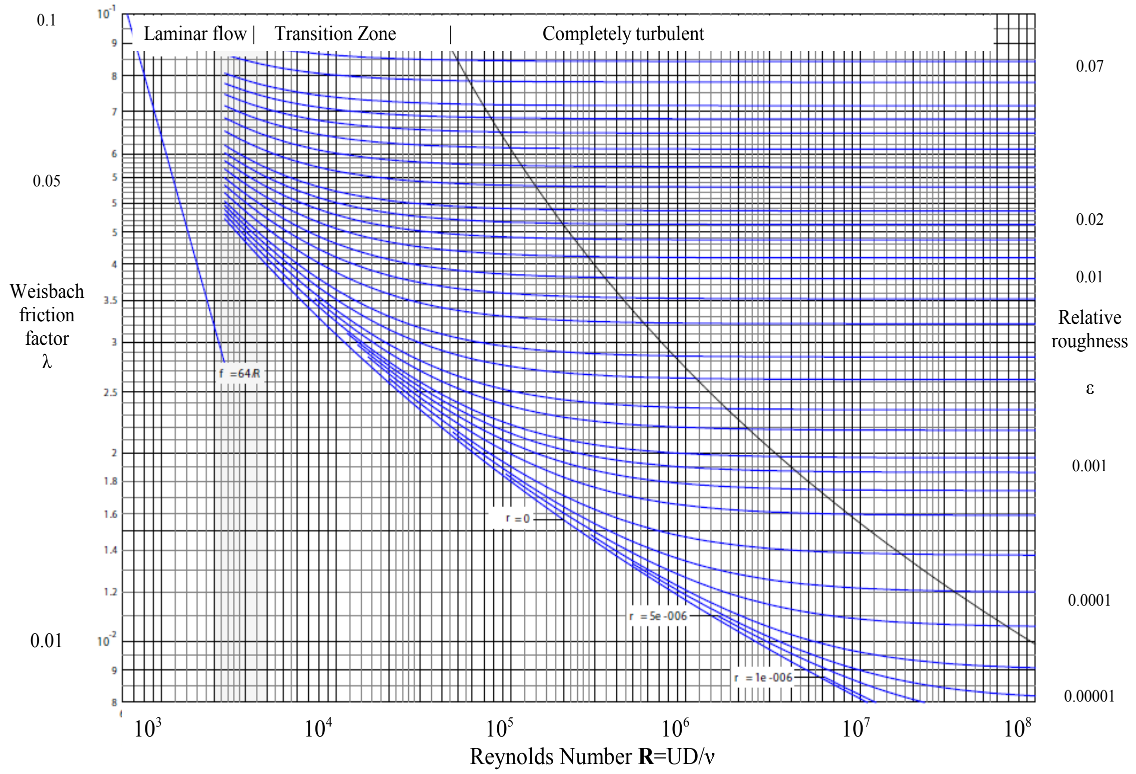


Figure 8-3. The Moody diagram, showing graphically the solution of the Colebrook & White equation for $\lambda$ as a function of $R$ with a parameter the relative roughness $\varepsilon = d/D$.

accuracy of this expression is reasonable. It is accurate to 1% over a wide range of roughnesses and Reynolds numbers. However, as shown above, the Colebrook and White equation is quite a rough approximation anyway. It is surprising that the much simpler explicit equation (8.7) has not been used.

### 8.1.5 Actual physical roughnesses

| Pipe Material | $d$ (mm) |
|---|---|
| Brass, copper, glass, Perspex | 0.003 |
| Plastic | 0.03 |
| Asbestos cement | 0.03 |
| Commercial steel or wrought iron | 0.045 |
| Galvanised iron | 0.15 |
| Cast iron | 0.25 |
| Concrete | 0.3-3.0 |

Table 8-1. Typical absolute roughness values

## 8.2 Practical single pipeline design problems

| Case | Known | To find |
|---|---|---|
| A | Discharge $Q$ and diameter $D$ known | Head loss $\Delta H$ |
| B | Head loss $\Delta H$ and diameter $D$ known | Discharge $Q$ |
| C | Head loss $\Delta H$ and discharge $Q$ known | Diameter $D$ |

Table 8-2. Three cases of pipeline design problems

Here we consider the three types of simple pipe problems, so-called because they are problems where pipe friction is the only loss. Six variables are involved: $Q$, $L$, $D$, $\Delta H$, $\nu$, and $d$. In general the quantities which are known are: length $L$, the temperature and hence the viscosity $\nu$, and $d$ the roughness of the pipe material being considered. the simple pipe problems may then be treated as three types, as shown in Table 8-2.We also have the Weisbach equation (8.1) in terms of more practical quantities

$$\Delta H = \lambda \frac{L}{D} \frac{U^2}{2g} = \lambda \frac{8LQ^2}{g\pi^2 D^5}. \tag{8.8}$$

**A. Determining the head loss, given the pipe details and flow rate:** If the pipe details are known, then $d$, $D$, and $Q$ are known, and the friction factor $\lambda$ may be computed from Haaland's approximation (8.7) to the Colebrook-White equation, and the head loss simply calculated from equation (8.8).

**B. Determining the flow rate, given the head gradient and pipe details:** This has an explicit solution, which is surprising, given how all the variables are implicitly related. It follows from the fact that the quantity $R\sqrt{\lambda}$ occurs in one place, from which $Q$ cancels, leaving an explicit solution. Using equation (8.8) for $\lambda$,

$$R\sqrt{\lambda} = \frac{\sqrt{2igD^3}}{\nu} \quad \text{where } i = \Delta H/L, \text{ the energy gradient.} \tag{8.9}$$

and solving equation (8.8) for $\lambda$ and substituting into the Colebrook-White equation (8.6) gives:

$$Q = -\pi \sqrt{\frac{i\,g}{2}} D^{5/2} \log_{10} \left( \frac{d/D}{3.7} + \frac{2.51\,\nu}{D^{3/2}\sqrt{2\,i\,g}} \right), \tag{8.10}$$

which has been given by Swamee & Jain (1976, eq. (15)).

**C. Determining the size of pipe required, given the flow, the head gradient and pipe roughness:** Rewriting equation (8.10) it can be expressed as a nonlinear transcendental equation, written in a form suitable for an iterative solution:

$$D = \left( -\frac{Q}{\pi} \sqrt{\frac{2}{i\,g}} \log_{10}^{-1} \left( \frac{d/D}{3.7} + \frac{2.51\,\nu}{D^{3/2}\sqrt{2\,i\,g}} \right) \right)^{2/5}. \tag{8.11}$$

such an expression has been given by Swamee & Jain (1976, eq. (11)). An initial value of $D$ is assumed, substituted on the right, and an updated value calculated, which in turn is substituted on the right, until the process converges. Usually only two iterations are necessary.

**D. A modern numerically-based approach:** modern software, especially in the case of spreadsheets, can be conveniently programmed to solve any of the above, with a minimum of programming and details. Some of *Microsoft Excel's* effectiveness for numerical computations comes from a module *Solver*. It was originally designed for optimisation problems, where one has to find values of a number of different parameters such that some quantity is minimised, usually the sum of errors of a number of equations. With this tool one can find such optimal solutions, or solutions of one or many equations, even if they are nonlinear.

In the formulations of the present problems, one just has to take the Colebrook-White equation (8.6):

$$\frac{1}{\sqrt{\lambda}} + 2 \log_{10} \left( \frac{\varepsilon}{3.7} + \frac{2.51}{R\sqrt{\lambda}} \right) = 0, \tag{8.12}$$

and then with $R = 4Q/\nu\pi D$ and the Weisbach equation (8.8) written:

$$\Delta H - \lambda \frac{8LQ^2}{g\pi^2 D^5} = 0, \tag{8.13}$$

the system of equations (8.12) and (8.13) can be numerically solved for $\lambda$ and any other single unknown such as $\Delta H$, $Q$, or $D$ without going to the extent of writing the solutions as we did above.

## 8.3 Minor losses

Losses which occur in pipelines because of bends, elbows, joints, valves, *etc.* are called *minor losses*, although they are just as important as the friction losses we have considered. In almost all cases the minor loss is determined by experiment. A significant exception is the head loss due to a sudden expansion which we will treat below. All such losses are taken to be proportional to the square of the velocity and are expressed as a coefficient times the kinetic head:

$$\Delta H = K\frac{U^2}{2g}. \tag{8.14}$$

## 8.3.1 Pipeline fittings

Values of $K$ for various pipeline fittings are given in Table 8-3, taken from Streeter & Wylie (1981, p245).

| Fitting | $K$ |
|---|---|
| Globe valve (fully open) | 10.0 |
| Angle valve (fully-open) | 5.0 |
| Swing check valve (fully open) | 1.0 |
| Gate valve (fully open) | 0.2 |
| Close return bend | 2.2 |
| Standard T | 1.8 |
| Standard elbow | 0.9 |
| Medium sweep elbow | 0.8 |
| Long sweep elbow | 0.6 |

Table 8-3. Head-loss coefficients $K$ for various fittings

Minor losses may be neglected when they comprise 5% or less of the head losses due to pipe friction. The friction factor, at best, is known to about 5% error, and it is meaningless to try to specify great accuracy. In general, minor losses may be ignored when there is a length of some 1000 diameters between each minor loss.

## 8.3.2 Losses due to sudden expansion in a pipe

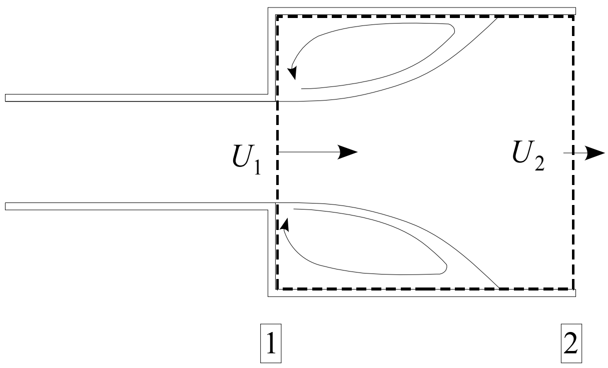


Figure 8-4. Sudden expansion in a pipe

The energy and momentum equations can be used. Consider a control volume which cuts across the pipe at 1 and 2. The momentum equation is applied while assuming that the boundary shear will be small, and assuming that the pressure on the faces at 1 are the same as in the flow, as the radial velocity components of velocity are not large

$$\sum \int_A (\rho \mathbf{u}\, \mathbf{u}\cdot\hat{\mathbf{n}} + p\hat{\mathbf{n}})\; dA = \mathbf{0}$$

$$\mathbf{i}\left(\beta\rho U_1(-U_1)A_1 - p_1 \underbrace{A_2}_{\text{Note}} + \beta\rho U_2(+U_2)A_2 + p_2 A_2\right) = \mathbf{0}.$$

The area $A_2$ was noted as it is multiplied by $p_1$, as it is the area of larger pipe, equal to the smaller pipe plus the expansion (see the figure).

Solving for $p_2 - p_1$:

$$p_2 - p_1 = \beta\rho U_1^2 \frac{A_1}{A_2} - \beta\rho U_2^2. \tag{8.15}$$

The head loss $\Delta H$ due to turbulent eddying in the separation zone will be finite. The energy equation gives

$$\frac{p_1}{\rho g} + \alpha\frac{U_1^2}{2g} = \frac{p_2}{\rho g} + \alpha\frac{U_2^2}{2g} + \Delta H,$$

such that

$$\Delta H = \frac{p_1}{\rho g} - \frac{p_2}{\rho g} + \alpha\left(\frac{U_1^2}{2g} - \frac{U_2^2}{2g}\right).$$

Substituting equation (8.15) gives

$$\Delta H = \beta\frac{U_2^2}{g} - \beta\frac{U_1^2}{g}\frac{A_1}{A_2} + \alpha\left(\frac{U_1^2}{2g} - \frac{U_2^2}{2g}\right),$$

and using mass conservation $U_1 A_1 = U_2 A_2$ to eliminate $U_2$, we have

$$\begin{aligned}\Delta H &= \beta\frac{U_1^2}{g}\left(\frac{A_1}{A_2}\right)^2 - \beta\frac{U_1^2}{g}\frac{A_1}{A_2} + \alpha\left(\frac{U_1^2}{2g} - \frac{U_1^2}{2g}\left(\frac{A_1}{A_2}\right)^2\right) \\ &= \frac{U_1^2}{2g}\left(A_2 - A_1\right)\frac{\alpha A_2 + (\alpha - 2\beta) A_1}{A_2^2},\end{aligned}$$

and for simplicity we assume that $\beta = \alpha$, giving

$$\Delta H = \frac{\alpha}{2g}\left(U_1 - U_2\right)^2 = \frac{\alpha U_1^2}{2g}\left(1 - \frac{A_1}{A_2}\right)^2. \tag{8.16}$$

This is an interesting result, for it shows how excess kinetic energy will be converted to heat, the amount depending on the velocity difference. Also, if $A_1 \ll A_2$ such as a pipe entering a tank, then all the kinetic energy will be converted to heat. In the case of gradual expansions, losses are much less.

### 8.3.3 Sudden contraction

The head loss at the entrance to a pipeline from a tank or reservoir is usually taken as $K = 0.5$ if the opening is square edged. For well-rounded entrances $K = 0.01$ to $0.05$ and may usually be neglected. For re-entrant openings, such as when the pipe extends into the tank beyond the wall, $K = 1$.

## 8.4 Pipeline systems

### 8.4.1 Introduction

One of the most common problems faced by an hydraulic engineer is the analysis and/or design of pipeline systems. In this section we will bring together some sections considered above and apply them to practical problems. In particular, Section 6, the energy equation; Section 8, flow in pipes; and Section 11, fluid machinery. Complex flow problems will be investigated, including systems that incorporate different elements such as pumps and multiple pipeline networks.

There are some warnings to make here:

- Some American books still use the Hazen-Williams equation for pipe friction. It was superseded in the 1930s by the work of the German school.
- For the Weisbach friction factor American books use the symbol $f$. British books tend to use $4f$ instead. To overcome the ambiguity, in this course we have used the European symbol $\lambda$ and Weisbach's formula in the form $\Delta H = \lambda L/D \times U^2/2g$, with no factor of 4 in front of it.

### 8.4.2 Summary of useful results from above for calculating pipe friction

**Continuity equation:** For a control surface, equation (4.3) is

$$\pm Q_1 \pm Q_2 \pm \ldots = 0, \tag{8.17}$$

where the $Q_i$ are the discharges crossing the control surface, where the positive/negative sign is taken for fluid leaving/entering the control volume.

**Integral energy theorem:** The integral energy theorem (equation 6.8) can be written

$$\pm Q_1 H_1 \pm Q_2 H_2 \pm Q_3 H_3 \pm \ldots = 0. \tag{8.18}$$

where the $H_i$ are the corresponding *total head of the flow*, the mean energy per unit mass divided by $g$:

$$H = \frac{p}{\rho g} + z + \frac{\gamma}{2g}\frac{Q^2}{A^2}.$$

**Simple pipe or channel:** For a length of pipe or channel where there are no other entry or exit points for fluid, equation (6.10), explicitly including head loss $\Delta H$, gives:

$$\left(\frac{p}{\rho g} + z + \frac{\gamma}{2g}\frac{Q^2}{A^2}\right)_{\text{in}} = \left(\frac{p}{\rho g} + z + \frac{\gamma}{2g}\frac{Q^2}{A^2}\right)_{\text{out}} + \Delta H \tag{8.19}$$

**Head loss formulae:** Weisbach's equation is

$$\Delta H = \lambda \frac{L}{D}\frac{U^2}{2g}, \tag{8.20}$$

where $\Delta H$ is the head loss in a pipe of length $L$ and diameter $D$, $U$ is the mean velocity, and $\lambda$ is a dimensionless friction coefficient. It can be re-written in terms of more practical quantities using equation (8.13), giving

$$\phi\left(\Delta H, \lambda, Q, D\right) = \Delta H - \lambda \frac{8LQ^2}{g\pi^2 D^5} = 0. \tag{8.21}$$

The value of $\lambda$ is given implicitly by either

**(a) The Colebrook-White equation:** re-written in the form of equation (8.12):

$$\psi_1\left(\lambda, Q, D, d\right) = \frac{1}{\sqrt{\lambda}} + 2\,\log_{10}\left(\frac{\varepsilon}{3.7} + \frac{2.51}{\mathbf{R}\sqrt{\lambda}}\right) = 0, \tag{8.22}$$

where the relative roughness $\varepsilon = d/D$, and the pipe Reynolds number $\mathbf{R} = 4Q/\nu\pi D$, or *explicitly* by

**(b) Haaland's expression:** equation (8.7):

$$\lambda = \frac{1}{1.8^2}\,\log_{10}^{-2}\left(\left(\frac{\varepsilon}{3.7}\right)^{10/9} + \frac{6.9}{\mathbf{R}}\right).$$

Table 8-4 shows typical physical roughnesses.

| Pipe Material | $d$ (mm) |
|---|---|
| Brass, copper, glass, Perspex | 0.003 |
| Plastic | 0.03 |
| Asbestos cement | 0.03 |
| Commercial steel or wrought iron | 0.045 |
| Galvanised iron | 0.15 |
| Cast iron | 0.25 |
| Concrete | 0.3-3.0 |

Table 8-4. Typical absolute roughness values

**Minor losses:** Losses which occur in pipelines because of bends, elbows, joints, valves, *etc.* were described in

#8.3. All such losses are taken to be proportional to the square of the velocity and are expressed as a coefficient times the kinetic head:

$$\Delta H = K\frac{U^2}{2g}. \tag{8.23}$$

Values of $K$ for various pipeline fittings and situations are given in Table 8-5.

| Fitting/Situation | $K$ |
|---|---|
| Globe valve (fully open) | 10.0 |
| Angle valve (fully-open) | 5.0 |
| Close return bend | 2.2 |
| Standard T | 1.8 |
| Elbows | 0.6 – 0.9 |
| Gate valve (fully open) | 0.2 |
| Expansion | $\left(1-\frac{A_1}{A_2}\right)^2$ |
| Sharp contraction | 0.5 |
| Re-entrant contraction | 1.0 |
| Rounded contraction | 0.05 – 0.1 |

Table 8-5. Head-loss coefficients $K$ for various fittings and expansions and contractions

## 8.5 Total head, piezometric head, and potential cavitation lines

### 8.5.1 General considerations

Consider the mean total head at a section across a pipe:

$$H = \frac{p}{\rho g} + z + \frac{\alpha}{2g}\frac{Q^2}{A^2}. \tag{8.24}$$

The pressure $p$ and elevation $z$ will usually vary linearly over the section, such that the *piezometric head* $h = p/\rho g + z$ is a constant over the section, and hence so is $H$. This total head is usually known at control points such as the surface of reservoirs. The amounts lost due to friction and local losses in the system can be calculated.

If $p_v$ is the absolute vapour pressure of the water in the pipe, cavitation will *not* occur if the absolute pressure $p + p_a \geqslant p_v$, where $p_a$ is the atmospheric pressure. Hence, from equation (8.24), for *no* cavitation

$$\frac{p+p_a}{\rho g} = H - z + \frac{p_a}{\rho g} - \frac{\alpha}{2g}\frac{Q^2}{A^2} \geqslant \frac{p_v}{\rho g},$$

giving the condition

$$z \leqslant H + \Delta h_c, \tag{8.25}$$

where $\Delta h_c$ might be called the *cavitation height*

$$\Delta h_c = \frac{p_a}{\rho g} - \frac{p_v}{\rho g} - \frac{\alpha}{2g}\frac{Q^2}{A^2}. \tag{8.26}$$

That is, as $z$ is the elevation of any part of the cross-section, no part of the pipe can have an elevation larger than the magnitude of the local head plus a distance $\Delta h_c$. The limiting condition is for the highest fluid in the pipe at any section, which is just below the soffit (the top of the inside) of the pipeline, such that we can write

> Cavitation will not occur at a section if the soffit of the pipe is lower than a point $\Delta h_c$ above the local total head elevation.

Now consider the quantities which make up the cavitation height $\Delta h_c$ in equation (8.26):

- Atmospheric pressure head $p_a/\rho g$ – typical atmospheric pressures are roughly $990 - 1010\,\mathrm{m\,bar}$, and the density of fresh water is $1000\,\mathrm{kg\,m^{-3}}$ at $5°$ and $958\,\mathrm{kg\,m^{-3}}$ at $100°$, so that $p_a/\rho g$ will vary between 10.1

and 10.8 m. The standard atmosphere of 760 mm of mercury with a value of 10.34 m of water could be assumed without much error.

- Vapour pressure – this shows rather more variation, primarily with temperature. As shown in Figure 8-5 for atmospheric temperatures it is always less than a metre, and for moderate temperatures could be ignored, however as the temperature approaches 100°C it approaches 10.33 m, and $p_a - p_v$ goes to zero such that boiling occurs at atmospheric pressure.

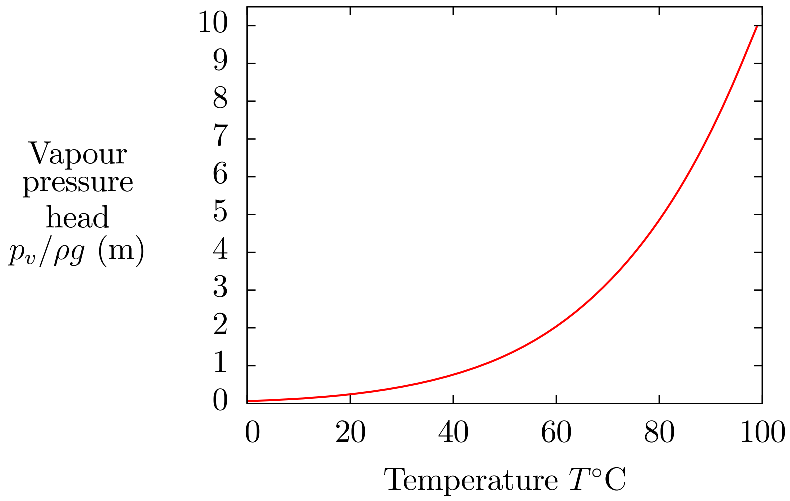


Figure 8-5. Vapour pressure head and its variation with temperature

- Kinetic head – this varies from situation to situation and from pipe to pipe in the same network. For this to be as much as 1 m, the mean fluid velocity in the pipe would be roughly $\sqrt{2 \times 9.8/1.2} \approx 4.0\,\mathrm{m\,s^{-1}}$, which is large.

The manner in which a pipeline is examined for the possibility of cavitation is essentially to plot a graph of $H + \Delta h_c$ (equation 8.25) against horizontal distance along the pipe. If the soffit of the pipe were found to pass above that line, then the absolute pressure in the water would be equal to the vapour pressure there, and it would start to cavitate and disrupt the flow. The calculation is usually done in three stages, giving three lines which are significant to the problem:

**Total head line or "energy grade line":** First calculate the total head $H$ at points such as reservoirs from knowledge of the elevation, then at other points from knowledge of both friction and local losses due to structures, pumps, expansions or contractions. Plotting this line often reveals details of the flow, such as where energy might be reduced due to turbulent mixing and losses destroying kinetic energy. After plotting the total head points, the total head line can be plotted by connecting the known points with straight lines.

**Piezometric head line or "hydraulic grade line":** This is often calculated and plotted, which often helps understanding a problem, but it is not strictly necessary to do so to calculate $H + \Delta h_c$. The piezometric head line joins a series of points showing the piezometric head for each point along a pipe, plotted against horizontal distance. As can be obtained from equation (8.24), the piezometric head $h$:

$$h = H - \frac{\alpha}{2g}\frac{Q^2}{A^2},$$

showing that it is simply plotted a vertical distance equal to the kinetic head $\alpha/2g \times Q^2/A^2$ *below* the total head line. The piezometric head line is parallel to the total head line for each pipe element.

**Potential cavitation line:** Equation (8.25) shows that for no cavitation, $z \leqslant H + \Delta h_c$, where $z$ refers to the soffit of the pipe. This condition can be written

$$z \leqslant \underbrace{H - \frac{\alpha}{2g}\frac{Q^2}{A^2}}_{\text{Piezometric head}} + \underbrace{\frac{p_a - p_v}{\rho g}}_{\text{Almost constant on any one day}}$$

This shows that where points and joining lines are drawn, displaced vertically a distance $(p_a - p_v)/\rho g$ above the piezometric head line, then if the soffit of the pipe ever passes above this "potential cavitation line", cavitation will occur. The additive quantity is a function of atmospheric pressure and water temperature, but for most hydraulic engineering problems varies little.

## 8.5.2 Entry and exit points

**Entry point:** Immediately the flow enters a pipe the total head reduces by an amount $K\,U^2/2g$ (above we saw

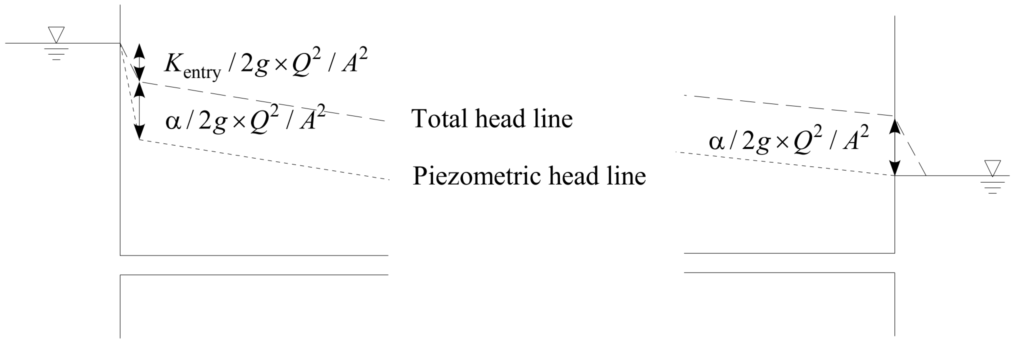


(a) Entry to pipe (b) Exit from pipe to reservoir

Figure 8-6. Behaviour of total and piezometric head lines at entry and exit from pipe into a reservoir

that the head loss coefficient for a square-edged inlet was $K \approx 0.5$). The pressure will further drop by an amount $\alpha\,U^2/2g$, as the kinetic contribution to the head has increased by this amount. This means that the local total head line and piezometric head lines look as in 8-6(a).

**Exit point:** As the flow leaves the pipe and enters a much larger body of water such as a reservoir, all the kinetic energy is destroyed. This can be explained by the theory above leading to equation (8.16) for the case $A_2 = \infty$ or $U_2 = 0$, giving

$$\Delta H = \frac{\alpha U_1^2}{2g}.$$

This means that the piezometric head becomes equal to the head in the reservoir at the exit, and the pressure is the same just inside the pipe as at a point of the same elevation in the reservoir, as shown in Figure 8-6(b).

## 8.5.3 A typical problem

Figure 8-7 shows an example where a pipeline passes from one reservoir to another over a hill, and shows a number of features of total and piezometric head lines. As it is drawn, cavitation will occur, and the actual pressure distribution will be very different. Here, the example is included to demonstrate how one checks for potential cavitation. In practice, if it were found to be likely, then a more complete analysis would be done, incorporating its effects.

- Considering the flow just after the entrance to the pipe, the total head line immediately shows a slight drop because of the losses associated with the sudden contraction, something like 0.1 or 0.5 times $U^2/2g$, according to equation (8.14) and Table 8-1.
- The piezometric line shows an even larger sudden drop because as the fluid has been accelerated into the pipe and now has a finite velocity, the distance between the two curves $\alpha U^2/2g$ is finite.
- As velocity is constant along the pipe, so is the distance between the two curves.
- As the flow approaches the downstream reservoir, the piezometric head in the pipe will be the same as in the reservoir, but the total head contains the kinetic component which is excess – the flow enters the reservoir as a turbulent jet until all the kinetic head is destroyed, as shown in the figure, after which both total and piezometric heads are now equal to the elevation of the still reservoir surface.
- The potential cavitation line can now be simply drawn as a line everywhere a constant distance $(p_a - p_v)/\rho g$ above

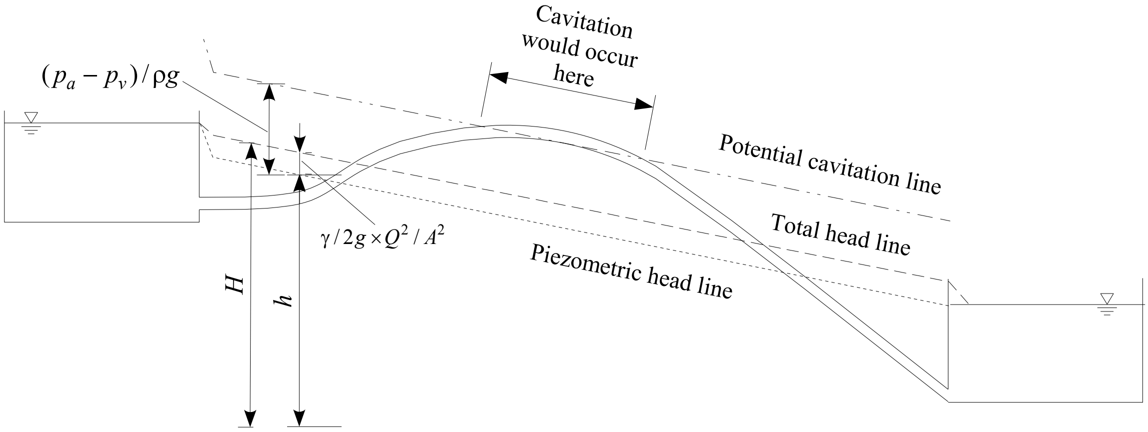


Figure 8-7. Pipeline between two reservoirs passing over a hill showing hydraulic lines and region of cavitation.

the piezometric head line.

- It can be seen that the soffit of the pipe passes above this line, and cavitation will occur wherever it is above. The flow situation will, in fact change, in a manner to be described further below. For present purposes we have shown that cavitation is a problem in this case.

**Example 8.1** (Example #10.1 Streeter & Wylie 1981)

Consider the pipeline emerging from a tank, passing through a valve, and finally the flow emerges into the atmosphere *via* a nozzle. Determine the elevation of hydraulic and energy grade lines at points A-E. The energy loss due to the nozzle is $0.1 \times U_E^2/2g$. In this case we take a value of $\alpha = 1.3$.

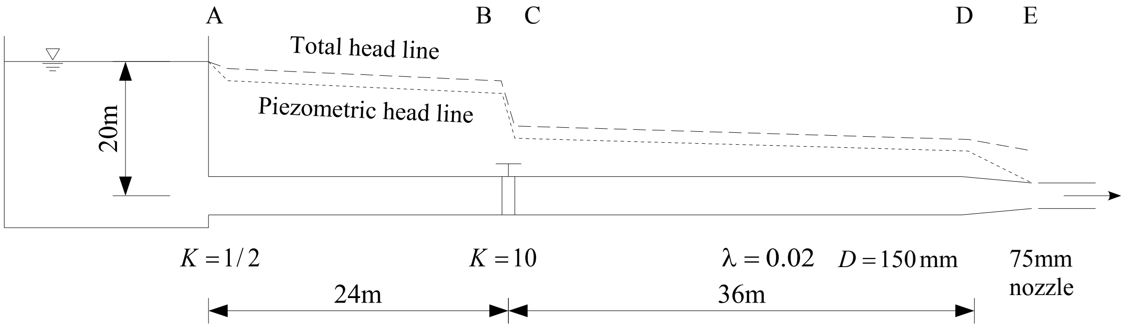


Figure 8-8. Tank, pipeline and nozzle, with total head and piezometric head lines

First we apply the integral energy equation for a control surface around all the sides of the tank, the pipe, and across the nozzle.

$$\left(\frac{p}{\rho g} + z + \frac{\alpha}{2g}\frac{Q^2}{A^2}\right)_{\text{in}} = \left(\frac{p}{\rho g} + z + \frac{\alpha}{2g}\frac{Q^2}{A^2}\right)_{\text{out}} + \Delta H$$

which gives

$$\begin{aligned} 0 + 20 + 0 \quad &= \quad 0 + 0 + \frac{\alpha}{2g}\frac{Q^2}{\underbrace{\left(\pi\left(D/2\right)^2/4\right)^2}_{\text{Note: Diameter of nozzle}}} + \frac{Q^2}{2g\left(\pi D^2/4\right)^2}\left(\underbrace{\frac{1}{2}}_{K_A} + \underbrace{10}_{K_{BC}} + \underbrace{\frac{0.02 \times 60}{0.15}}_{\text{Friction: } fL/D}\right) \\ &\quad +0.1 \times \frac{Q^2}{2g \times \underbrace{\left(\pi\left(D/2\right)^2/4\right)^2}_{D/2 \text{ diameter of nozzle}}} \end{aligned}$$

$$20 = \frac{Q^2}{2g\left(\pi D^2/4\right)^2}\left(\alpha\times 16+\tfrac{1}{2}+10+8+0.1\times 16\right)$$

With $\alpha = 1.3$, we obtain a discharge of $Q = 0.0547$, while with $\alpha = 1$, $Q = 0.0582$. The difference of 6% seems enough to warrant using the more realistic value. Hence, our basic quantity is

$$\frac{U^2}{2g} = \frac{Q^2}{2g\left(\pi D^2/4\right)^2} = \frac{0.0547^2}{2\times 9.8\times\left(\pi 0.15^2/4\right)^2} = 0.489,$$

to be used in local loss formulae, while the kinetic head term to be used is

$$\alpha\frac{U^2}{2g} = 1.3\times 0.489 = 0.636.$$

Now we apply the energy equation between the surface of the tank and just after A, and then between each of the subsequent points:

$H_A = 20 - 0.5\times 0.489 = 19.76$ $\quad h_A = 19.76 - 0.64 = 19.12$
$H_B = 19.76 - \frac{0.02\times 24}{0.15}\times 0.489 = 18.20$ $\quad h_B = 18.20 - 0.64 = 17.56$
$H_C = 18.2 - 10\times 0.489 = 13.31$ $\quad h_C = 13.31 - 0.64 = 12.67$
$H_D = 13.31 - \frac{0.02\times 36}{0.15}\times 0.489 = 10.96$ $\quad h_D = 10.96 - 0.64 = 10.32$
$H_E = 10.96 - 16\times 0.1\times 0.489 = 10.18$ $\quad h_E = 10.18 - 16\times 0.64 = -0.06$

The final value of the piezometric head at E should have been zero, but accumulated round-off error by working to two places only, has caused the error. These results are plotted in Figure 8-9.

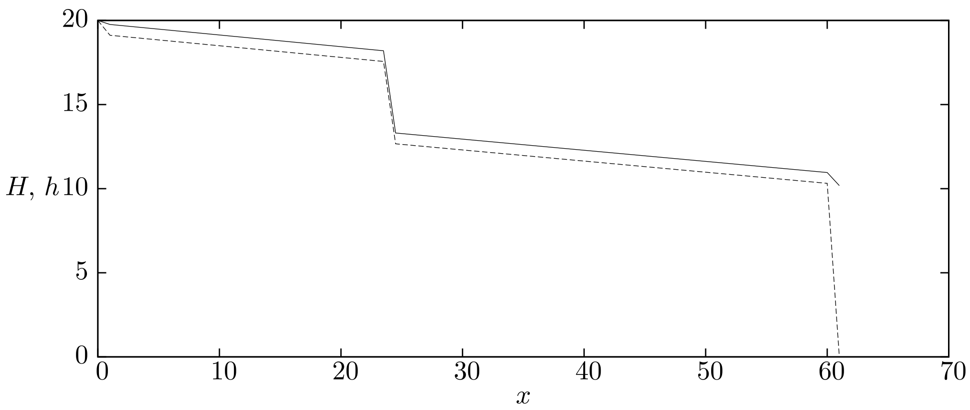


Figure 8-9. Total and piezometric head lines for example

**Example 8.2** Consider a single pipe of length $L = 1000\,\mathrm{m}$ connecting two reservoirs with a head difference $\Delta H = 10\,\mathrm{m}$. It has a diameter of $D = 300\,\mathrm{mm}$, roughness height $d = 0.3\,\mathrm{mm}$; it has a square-edged entry, $K_0 = 0.5$, and with $\alpha = 1.3$ in the pipe. Calculate the flow in the pipe.

$$0+\Delta H+0 = 0+0+0+\frac{Q^2}{2g\left(\pi D^2/4\right)^2}\left(K_0+\frac{\lambda L}{D}+\alpha\right)$$

We will solve the problem by iteration using Haaland's approximation for $\lambda$, which is a weakly-varying function of $Q$, so that the equation is an implicit equation for $Q$:

$$Q = \frac{\pi D^2/4}{\sqrt{K_0+\lambda L/D+\alpha}}\sqrt{2g\Delta H}, \tag{8.27}$$

and we will start with the fully-rough approximation for $\lambda$.

For $\varepsilon = d/D = 0.3/300 = 0.001$,

$$\lambda = \frac{1}{1.8^2}\frac{1}{\left(\log_{10}\left(\left(\frac{0.001}{3.7}\right)^{10/9}\right)\right)^2} = 0.0196.$$

Hence from (8.27)

$$Q = \frac{\pi \times 0.3^2/4}{\sqrt{0.5 + 0.0196 \times 1000/0.3 + 1.3}} \sqrt{2 \times 9.8 \times 10} = 0.121\,\mathrm{m}^3\,\mathrm{s}^{-1},$$

This is our first estimate. Here we calculate $R$ as a function of $Q$:

$$R = \frac{UD}{\nu} = \frac{QD}{A\nu} = \frac{4Q}{\pi D\nu} = \frac{4}{\pi \times 0.3 \times 10^{-6}} Q \quad \text{or} \quad \frac{1}{R} = \frac{2.36 \times 10^{-7}}{Q}$$

and so from Haaland, equation (8.7)

$$\lambda = \frac{1}{1.8^2} \frac{1}{\left(\log_{10}\left(\left(\frac{0.001}{3.7}\right)^{10/9} + 6.9/R\right)\right)^2} = \frac{1}{1.8^2} \frac{1}{\left(\log_{10}\left(\left(\frac{0.001}{3.7}\right)^{10/9} + \frac{1.63 \times 10^{-6}}{Q}\right)\right)^2},$$

and so, using $Q = 0.121\,\mathrm{m}^3\,\mathrm{s}^{-1}$ we get $\lambda = 0.0202$. Substituting again into (8.27)

$$Q = \frac{\pi \times 0.3^2/4}{\sqrt{0.5 + 0.0201 \times 1000/0.3 + 1.3}} \sqrt{2 \times 9.8 \times 10} = 0.119\,\mathrm{m}^3\,\mathrm{s}^{-1},$$

And repeating, we get $\lambda = 0.0202$, hence it has converged sufficiently. The discharge is $0.119\,\mathrm{m}^3\,\mathrm{s}^{-1}$.

### 8.5.4 Compound pipe systems

**Pipes in series:** When two pipes of different sizes or roughnesses are so connected that fluid flows through

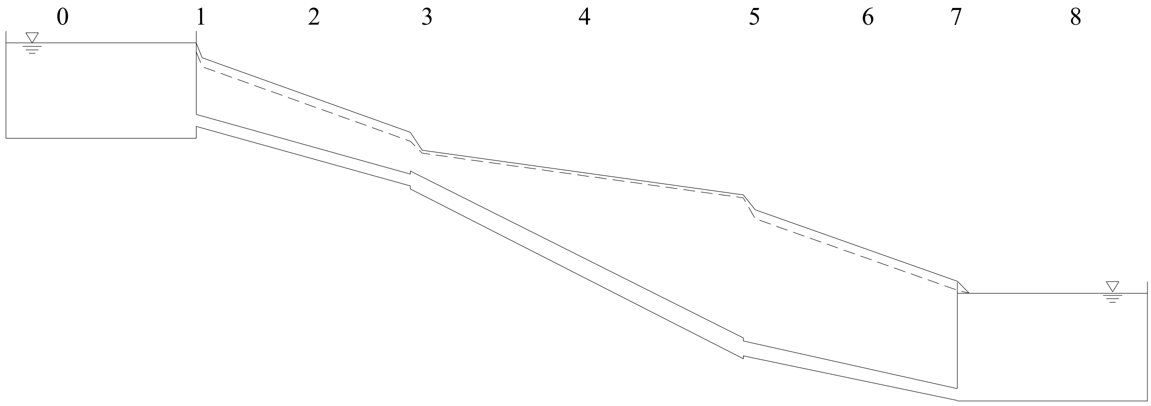


Figure 8-10. Compound pipe system – in series, joining two reservoirs

one pipe and then through the other. Consider Figure 8-10, where we apply the energy integral equation between the surface of the two reservoirs:

$$\begin{aligned}\left(\frac{p}{\rho g} + z + \frac{\gamma}{2g}\frac{Q^2}{A^2}\right)_{\text{in}} &= \left(\frac{p}{\rho g} + z + \frac{\gamma}{2g}\frac{Q^2}{A^2}\right)_{\text{out}} + \Delta H \\ 0 + z_0 + 0 &= 0 + z_8 + 0 + K_1 \frac{Q^2/A_1^2}{2g} + \lambda_2 \frac{L_2}{D_2}\frac{Q^2/A_2^2}{2g} + \ldots + \lambda_6 \frac{L_6}{D_6}\frac{Q^2/A_6^2}{2g} + \gamma \frac{Q^2/A_7^2}{2g}\end{aligned}$$

Hence we obtain

$$z_0 - z_8 = \frac{Q^2}{2g}\left(\frac{K_1}{A_1^2} + \frac{\lambda_2 L_2/D_2}{A_2^2} + \ldots + \frac{\lambda_6 L_6/D_6}{A_6^2} + \frac{\gamma}{A_7^2}\right) = \frac{Q^2}{2g}\sum_{i=1}^{N}\frac{K_i}{A_i^2}, \tag{8.28}$$

where for the friction loss in a length of pipe, $K_i = \lambda_i L_i/D_i$, and usually, if the kinetic head is destroyed at the end of the pipe, $K_N = \gamma$. The Colebrook-White equation

$$\frac{1}{\sqrt{\lambda}} + 2\log_{10}\left(\frac{\varepsilon}{3.7} + \frac{2.51}{\mathbf{R}\sqrt{\lambda}}\right) = 0$$

shows us that $\lambda_i$ is an implicit function of relative roughness $\varepsilon_i = d_i/D_i$ of a pipe and the Reynolds number of the pipe flow in the form

$$\frac{1}{\mathbf{R}_i} = \frac{\nu}{U_i D_i} = \frac{\nu \pi D_i}{4Q}.$$

Substituting gives

$$\frac{1}{\sqrt{\lambda_i}} + 2\,\log_{10}\left(\frac{\varepsilon_i}{3.7} + \frac{1.97\nu D_i}{Q}\frac{1}{\sqrt{\lambda_i}}\right) = 0. \tag{8.29}$$

We now have a system of nonlinear equations to solve: equation (8.28) is an equation for $Q$ and all of the $\lambda_i$ (and any $K_i$ which depend on the Reynolds number), while for each pipe segment, equation (8.29) is a single equation in the common $Q$ and a single $\lambda_i$. There are precisely as many equations as unknowns, and a solution seems possible. Any one of a number of different methods such as Newton's method for a system of equations, or optimisation methods are possible, which might be quite complicated. In this case, however, the structure of the system is simple, because in each of the Colebrook-White equations the term involving $\lambda_i$ is weakly varying, which suggests using a *direct iteration method*.

As noted in Section 8.2, there are three types of practical pipeline design problems:

**A. Determining the head loss, given the pipe details and flow rate:** In this case it is possible to solve the problem sequentially through the pipes, and to proceed by a process of direct iteration for the $\lambda$.

**Example 8.3** Here we consider an example of a single pipe of length $L = 1000\,\mathrm{m}$, with a diameter of $D = 300\,\mathrm{mm}$, roughness height $d = 0.3\,\mathrm{mm}$, and discharge $Q = 0.05\,\mathrm{m^3\,s^{-1}}$; it has a square-edged entry, $K_0 = 1$, and with $\gamma = 1.3$ in the pipe. We use the Colebrook-White equation in the form of a reworked version of equation (8.29) so that we can use direct iteration to solve for a solution, starting with $\lambda = 0.02$ as an initial estimate:

$$\begin{aligned}
\frac{1}{\sqrt{\lambda}} &= -2\,\log_{10}\left(\frac{\varepsilon}{3.7} + \frac{1.97\nu D}{Q}\frac{1}{\sqrt{\lambda}}\right)\\
&= -2\,\log_{10}\left(\frac{0.001}{3.7} + \frac{1.97\times 1\times 10^{-6}\times 0.3}{0.05}\times\frac{1}{\sqrt{0.02}}\right) = 6.902\\
&= -2\,\log_{10}\left(\frac{0.001}{3.7} + \frac{1.97\times 1\times 10^{-6}\times 0.3}{0.05}\times 6.902\right) = 6.907
\end{aligned}$$

Hence it has converged sufficiently in just two steps, giving $\lambda = 1/6.907^2 = 0.0210$. Now we determine the head loss directly. We have an entry loss and an exit loss, as well as the frictional loss. As we have a single pipe we can factor $A$ out:

$$\begin{aligned}
H &= \frac{Q^2}{2gA^2}\left(K_0 + \frac{\lambda L}{D} + \gamma\right)\\
&= \frac{0.05^2}{2\times 9.8\times(\pi\times 0.3^2/4)^2}\left(0.5 + \frac{0.0210\times 1000}{0.3} + 1.3\right)\\
&= 1.83\,\mathrm{m}.
\end{aligned}$$

**B. Determining the flow rate, given the head gradient and pipe details:** This requires a certain amount of iterative solving, as we have seen in Example 8.3. An equation similar to (8.28) is written, and then as many Colebrook-White equations as there are pipes, each of which is solved iteratively, the whole procedure being iterated until converged.We will show an example here, and subsequently show how a numerical optimisation approach enables a rather more automatic approach.

**Example 8.4** (Example 10.4 of Streeter & Wylie 1981) We consider two pipelines, the first with $K_0 = 0.5$, $L_1 = 300\,\mathrm{m}$, $D_1 = 600\,\mathrm{mm}$, $d_1 = 2\,\mathrm{mm}$. The second has $L_2 = 240\,\mathrm{m}$, $D_2 = 1000\,\mathrm{mm}$, $d_2 = 0.3\,\mathrm{mm}$, $\nu = 3\times 10^{-6}\,\mathrm{m^2\,s^{-1}}$, and $H = 6\,\mathrm{m}$. Use $\gamma = 1$. Find the flow.

From the energy equation (8.28):

$$H = \frac{Q^2}{2g}\left(\frac{K_0}{A_1^2} + \frac{\lambda_1 L_1/D_1}{A_1^2} + \underbrace{\left(\frac{1}{A_1} - \frac{1}{A_2}\right)^2}_{\text{Expansion loss, Table 8-1}} + \frac{\lambda_2 L_2/D_2}{A_2^2} + \frac{\gamma}{A_2^2}\right),$$

and substituting numerical values

$$6=\frac{Q^2}{2g}\quad\left(\frac{0.5}{\left(\pi/4\times0.6^2\right)^2}+\frac{\lambda_1\times300/0.6}{\left(\pi/4\times0.6^2\right)^2}+\left(\frac{1}{\pi/4\times0.6^2}-\frac{1}{\pi/4\times1^2}\right)^2\right.$$
$$\left.+\frac{\lambda_2\times240/1}{\left(\pi/4\times1^2\right)^2}+\frac{1}{\left(\pi/4\times1^2\right)^2}\right),$$

from which we obtain

$$Q=\frac{\sqrt{6}}{\sqrt{0.663\,27+319.\,1\lambda_1+19.\,851\lambda_2}} \tag{8.30}$$

This is in a form ready for direct iteration. Now we use the Colebrook-White equation in the form,

$$\lambda=\frac{1}{2^2}\log_{10}^{-2}\left(\frac{\varepsilon}{3.7}+\frac{1.97\nu D}{Q}\frac{1}{\sqrt{\lambda}}\right),$$

from which we obtain

$$\lambda_1 = \frac{1}{4}\log_{10}^{-2}\left(\frac{2/600}{3.7}+\frac{1.97\times3\times10^{-6}\times0.6}{Q}\frac{1}{\sqrt{\lambda_1}}\right) \tag{8.31}$$
$$\lambda_2 = \frac{1}{4}\log_{10}^{-2}\left(\frac{0.3/1000}{3.7}+\frac{1.97\times3\times10^{-6}\times1}{Q}\frac{1}{\sqrt{\lambda_2}}\right) \tag{8.32}$$

Now we evaluate the three equations (8.30)-(8.32) iteratively – this should be stable, as all the left sides are slowly varying functions of all the variables. Initially $\lambda_1=\lambda_2=0.02$, giving the sequence of results

| Iteration | $Q$ | $\lambda_1$ | $\lambda_2$ |
|---|---|---|---|
| 0 | – | 0.02 | 0.02 |
| 1 | 0.8979 | 0.0272 | 0.0165 |
| 2 | 0.7878 | 0.0272 | 0.0168 |
| 3 | 0.7880 | | |

The process has converged quickly. This could be programmed on a spreadsheet, however it is simpler to use the automatic facility in *Microsoft Excel* which will be described below. Not every variable in every equation is as dominant as they were here.

**C. Determining the size of pipe required, given the flow, the head gradient and pipe roughness:** The diameter $D$ of the pipe is embedded deeply in the equations – a more general technique than iteration is required.

**A numerically-based approach:** Modern software, especially in the case of spreadsheets, can be conveniently programmed to solve any of the above, with a minimum of programming and details. Some of *Microsoft Excel's* effectiveness for numerical computations comes from a module *Solver*. It was originally designed for optimisation problems, where one has to find values of a number of different parameters such that some quantity is minimised, usually the sum of errors of a number of equations. With this tool one can find such optimal solutions, or solutions of one or many equations, even if they are nonlinear.

Let our system of equations be $\mathbf{f}(\mathbf{x})=\mathbf{0}$, where $\mathbf{f}$ and $\mathbf{x}$ are vectors such that

$$\mathbf{f}(\mathbf{x})=\left[f_i(x_j,\,j=1,\ldots,N)=0,\,i=1,\ldots,M\right],$$

namely we have a system of $M$ equations $f_i$ in $N$ unknowns $x_j$. If the equations are linear, a number of linear algebra methods such as matrix inversion, *etc.* are possible. In the more general case, if the equations are nonlinear, then nonlinear optimisation methods are suggested. In this process, $\varepsilon$, the sum of the squares of the errors for all the equations are evaluated:

$$\varepsilon=\sum_{i=1}^{M}f_i^2(x_j),$$

and the values of the $x_i$ found such that $\varepsilon$ will be a minimum. If $M=N$ it should be possible to find a solution such that $\varepsilon=0$ and the equations are solved. If there are fewer variables than equations, $N<M$, then it will not

be possible to solve the equations, but minimising $\varepsilon$ produces a useful solution anyway. This is particularly so in the case of finding approximating functions.

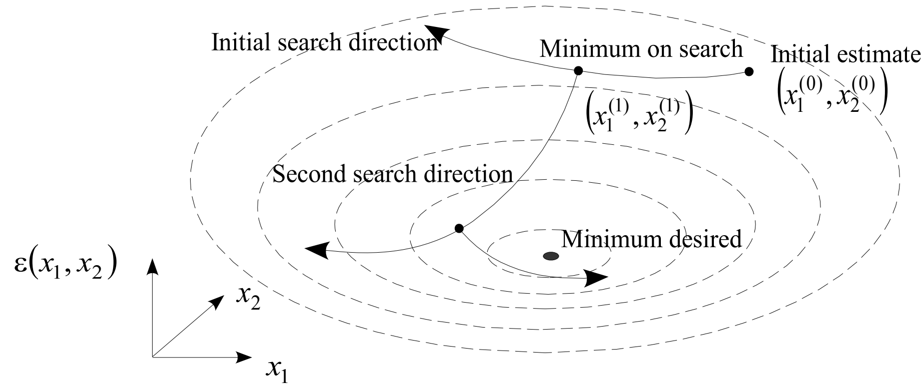


Figure 8-11. Representation of typical search method for the minimum of a function of two variables

In the formulations of the present problems, we have to write all the equations with all terms taken over to one side, and then to implement an optimisation procedure such as *Solver*. It does not matter how complicated the equations are – it is just necessary to be able to evaluate them. Most methods for minimising $\varepsilon$ are gradient methods, such that in the $N$-dimensional solution space, a direction is determined, and the minimum of the error function in that direction found, at the minimum a new direction found, usually orthogonal to the previous one, and so on. For two dimensions it can be shown as finding the minimum value of a surface, as in Figure 8-11; the three dimensional case can be imagined as finding the hottest point in a room by successively travelling in a number of different directions, finding the maximum in each, and then setting off at right angles, and so on. In either case the gradients are not obtained analytically but numerically by evaluating the functions at different values.

This procedure usually means that we have simply to write down the equations, with initial trial values of the unknowns, and call the optimising routine. It is very general and powerful, and we can usually write down the equations in the simplest form, so that no algebraic manipulation is necessary or favourable. As an example, refer to **URL:** *http://johndfenton.com/Lectures/Hydraulics/Pipesolver.xls*. This contains solutions to Examples 8.3 and 8.4 above. It can be seen that it works rather more simply, and no attention has to be paid to the solution process.

### 8.5.5 Parallel pipelines

If the flow is divided among two or more pipes and then is joined again, it is a *parallel-pipe system*. In pipes in series the same fluid flows through all the pipes and the head losses are cumulative, but in parallel pipes the head losses are the same in any of the lines and the discharges are cumulative.

Two types of problem occur:

- With the heads known at the ends of the pipes, find the discharge. This is just the separate solution of simple pipe problems for discharge, since the head loss is known for each.
- With the discharge known, find the distribution of flow and the head loss. This is more complicated, as the losses are nonlinear, and for different flows the fraction of flow in each pipe will change.

  Consider the case where there are three pipes. The equations are, from (8.28) but assuming just frictional resistance,

$$H = \lambda_1 \frac{L_1}{D_1} \frac{Q_1^2}{2gA_1^2} = \lambda_2 \frac{L_2}{D_2} \frac{Q_2^2}{2gA_2^2} = \lambda_3 \frac{L_3}{D_3} \frac{Q_3^2}{2gA_3^2}, \text{ and } Q = Q_1 + Q_2 + Q_3,$$

  and adding a Colebrook-White equation for each pipe gives us a total of seven equations in the seven unknowns $H$, $\lambda_1$, $Q_1$, $\lambda_2$, $Q_2$, and $\lambda_3$, $Q_3$. They are nonlinear. It would seem simplest to use *Solver* again.

### 8.5.6 Branching pipelines

There are two different cases:

**The dividing flow type:** this is the more usual case, where a pipeline bifurcates or enters a manifold, from which flow leaves *via* a number of different exits. Examples include the bifurcating nature of a water supply system and diffusers for disposal of sewage or heated effluents into large bodies of water. There is no reason to expect unusual losses, and a simple energy balance equation can be written, including conventional coefficients associated with bends *etc.* at the bifurcation.

**The combining flow type:** in this case where two or more pipes combine, it is possible that there will be some finite energy losses associated with two different streams of different energies per unit mass and different mass flow rates combining and leaving with the same energy per unit mass. This seems not to be treated in text books, but it is possible that an analysis based on momentum might yield results.

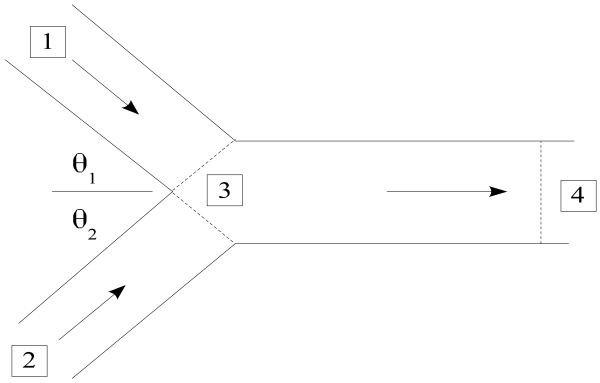


Figure 8-12. Pipe junction, showing control surface dashed

Consider two pipes joining as in Figure 8-12, where a flow 1 and flow 2, with the assumed directions of flow shown, join at 3, and it is assumed that in general some losses will occur before a station 4. The control surface is shown by a dashed line. The mass conservation equation gives

$$-Q_1 - Q_2 + Q_4 = 0, \tag{8.33}$$

the momentum conservation equation gives, where it is assumed that at the entry to the control volume, the pressure in both pipes is $p_3$, and that frictional forces between 3 and 4 are negligible,

$$-\cos\theta_1\left(\frac{p_3}{\rho}A_1 + \frac{\beta_1 Q_1^2}{A_1}\right) - \cos\theta_2\left(\frac{p_3}{\rho}A_2 + \frac{\beta_2 Q_2^2}{A_2}\right) + \frac{p_4}{\rho}A_4 + \frac{\beta_4 (Q_1+Q_2)^2}{A_4} = 0, \tag{8.34}$$

where it is been assumed that due to turbulent mixing of the streams, that $\beta_4 = 1$ and $\gamma_4 = 1$. The energy conservation equation gives

$$-Q_1\left(\frac{p_1}{\rho} + \frac{\gamma_1}{2}\left(\frac{Q_1}{A_1}\right)^2\right) - Q_2\left(\frac{p_2}{\rho} + \frac{\gamma_2}{2}\left(\frac{Q_2}{A_2}\right)^2\right) + Q_4\left(\frac{p_4}{\rho} + \frac{1}{2}\left(\frac{Q_4}{A_4}\right)^2\right) - Q_4 g\,\Delta H = 0, \tag{8.35}$$

where $-g\Delta H$ is the change in head between 3 and 4 such that $\Delta H$ is a positive quantity. Eliminating $p_4$ between equations (8.34) and (8.35) gives

$$\begin{aligned} g\Delta H = {} & \frac{p_3}{\rho}\left(1 - \frac{A_1}{A_4}\cos\theta_1 - \frac{A_2}{A_4}\cos\theta_2\right) - \frac{\beta_1 Q_1^2}{A_4 A_1}\cos\theta_1 - \frac{\beta_2 Q_2^2}{A_4 A_2}\cos\theta_2 \\ & + \frac{1}{2}\frac{(Q_1+Q_2)^2}{A_4^2} + \frac{1}{2}\frac{\gamma_1 Q_1^3}{(Q_1+Q_2)A_1^2} + \frac{1}{2}\frac{\gamma_2 Q_2^3}{(Q_1+Q_2)A_2^2}. \end{aligned} \tag{8.36}$$

This has an important counterpart in the hydraulic jump, the turbulent phenomenon in open channels which takes a shallow high-speed stream to a deep low-speed state with no momentum loss, but with intense turbulence causing a loss in energy.

It is interesting that in this case, unlike losses due to fittings and bends, the pressure also plays a role.

To obtain an idea of the magnitude of the losses, consider two pipes of the same area $A_1 = A_2$ carrying the same discharge $Q_1 = Q_2$, which enter a larger pipe at angles of $\pm 45°$. From the Weisbach equation it can be shown that, for the same head gradient, that discharge is proportional to the pipe diameter to the power $5/2$, hence we can say that $D_4/D_1 = (Q_4/Q_1)^{2/5} = 2^{2/5}$, or that $A_4/A_1 = 2^{4/5}$. As a first approximation we will set all the $\beta$ and $\gamma$ to 1, and so substituting into equation (8.36),

$$\begin{aligned} g\Delta H &= \frac{p_3}{\rho}\left(1 - 2\times 2^{-4/5}\,2^{-1/2}\right) - 2\times\frac{Q_1^2}{2^{4/5}A_1^2}\frac{1}{\sqrt{2}} + \frac{1}{2}\frac{(2Q_1)^2}{2^{8/5}A_1^2} + \frac{2}{2}\frac{Q_1^2}{2\,A_1^2} \\ &= 0.188\,\frac{p_3}{\rho} + 0.348\,\frac{Q_1^2}{A_1^2}. \end{aligned} \tag{8.37}$$

Now we calculate the effective local loss coefficient $K_{\text{junction}}$ such that $\Delta H = K_{\text{junction}} \times U_4^2/2g$, giving

$$K_{\text{junction}} = \frac{2g\Delta H}{(Q_4/A_4)^2} = \frac{2g\Delta H}{(2Q_1/A_1/2^{4/5})^2} = 1.52\times\frac{g\Delta H}{(Q_1/A_1)^2},$$

and substituting back into (8.37)

$$K_{\text{junction}} = 1.52\left(0.188\,\frac{p_3}{\rho U_1^2} + 0.348\right) = 0.284\frac{p_3}{\rho U_1^2} + 0.527,$$

hence for negligible pressure, we obtain a value of 0.53, typical of such local losses. However the pressure contribution might be quite large. Let us take $p_3/\rho g \approx 100\,\mathrm{m}$ and $U_1 = 1\,\mathrm{m\,s^{-1}}$, giving

$$K_{\text{junction}} = 0.284\,\frac{9.8\times 100}{1} + 0.527 \approx 280,$$

which seems a remarkably high value, and may cause a re-evaluation of the role of junctions in a network.

### 8.5.7 Branching pipe systems

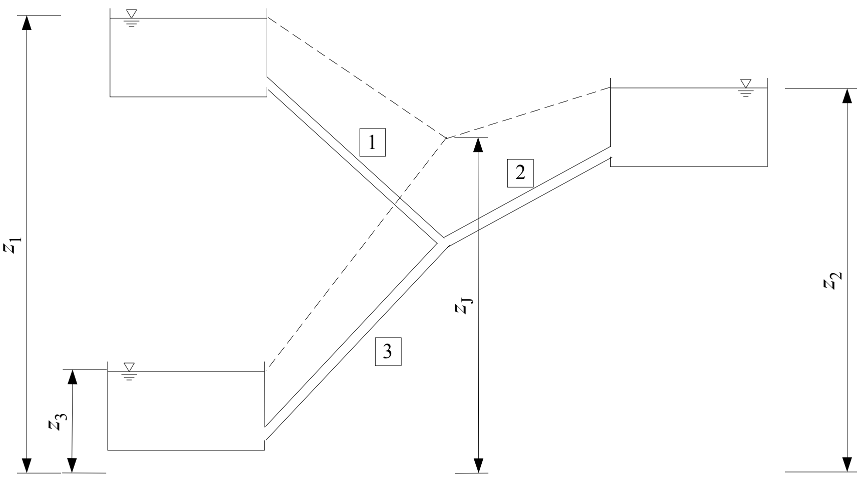


Figure 8-13. Three interconnected reservoirs

A simple branching pipe system is shown in Figure 8-13, where the total energy lines – ignoring all local losses – are shown dashed. In a typical problem, the flow through each pipe is wanted when the reservoir elevations are given. The Darcy-Weisbach equation is written for each pipe, a pipe-friction law also, and continuity at the pipe junction must be satisfied. Hence we have the equation for pipe $i$, bringing terms to one side:

$$z_{\text{J}} - z_i + \lambda_i\frac{L_i}{D_i}\frac{Q_i\,|Q_i|}{2gA_i^2} = 0, \quad \text{for} \quad i = 1,2,3, \tag{8.38}$$

written, instead of $Q_i^2$, with $Q_i\,|Q_i|$ with the convention that $Q_i$ is positive if it is from $i$ to J, in which case $z_{\text{J}} < z_i$, and, of course, if $Q_i$ is negative, then $z_{\text{J}} > z_i$. The $\lambda_i$ are given by the Haaland approximation , equation (8.7):

$$\lambda_i = \frac{1}{1.8^2}\,\log_{10}^{-2}\left(\left(\frac{\varepsilon_i}{3.7}\right)^{10/9} + \frac{6.9}{\mathbf{R}_i}\right),\ \text{where } \mathbf{R}_i = \frac{4\,|Q_i|}{\nu\pi D_i}, \quad \text{for} \quad i = 1,2,3,$$

where we must take the Reynolds number as a positive quantity as shown, using $|Q_i|$. The remaining equation is that of mass-conservation at the junction J:

$$Q_1 + Q_2 + Q_3 = 0. \tag{8.39}$$

Hence, if we know the reservoir elevations, the pipe diameters, roughnesses, and lengths, then we have four nonlinear equations (8.38) and (8.39) in the four unknowns $Q_1, Q_2, Q_3$ and $z_{\mathrm{J}}$. *Solver* can be used to solve this system. However a useful system for hand solution which works is to assume the elevation of the total head line $z_{\mathrm{J}}$ at the junction, and calculate the resistances from the Haaland equations, initially neglecting the Reynolds number term, then from each Darcy-Weisbach equation compute the discharge, then by how much the mass-conservation equation is violated at the junction, and the $z_{\mathrm{J}}$ adjusted there, and the process repeated. To do this we re-arrange equation (8.38) in a form which also incorporates the direction of the flow:

$$Q_i = A_i \sqrt{\frac{2gD_i}{\lambda_i L_i}} \times \frac{z_i - z_{\mathrm{J}}}{\sqrt{|z_i - z_{\mathrm{J}}|}}, \quad \text{for} \quad i = 1, 2, 3, \tag{8.40}$$

such that if $z_{\mathrm{J}} > z_i$ then $Q_1$ is negative and flow is away from the junction.

Note that we have neglected all local losses.

**Example 8.5** (Example 10.7 of Streeter & Wylie 1981): Find the discharges at 20°C ($\nu = 1 \times 10^{-6}\,\mathrm{m^2\,s^{-1}}$) for three reservoirs connected by pipes with the following data:

| | Pipe 1 | Pipe 2 | Pipe 3 |
|---|---|---|---|
| Length $L$ | $3000\,\mathrm{m}$ | $600\,\mathrm{m}$ | $1000\,\mathrm{m}$ |
| Diameter $D$ | $1\,\mathrm{m}$ | $0.45\,\mathrm{m}$ | $0.6\,\mathrm{m}$ |
| Area $A$ | $0.785\,\mathrm{m}^2$ | $0.159\,\mathrm{m}^2$ | $0.283\,\mathrm{m}^2$ |
| Relative roughness $\varepsilon$ | 0.0002 | 0.002 | 0.001 |
| Reservoir surface level $z$ | $30\,\mathrm{m}$ | $18\,\mathrm{m}$ | $9\,\mathrm{m}$ |

Assume elevation of total energy line at J: $23\,\mathrm{m}$. Initially neglect Reynolds number terms in equations for $\lambda_i$:

$$\lambda_1 \approx \tfrac{1}{1.8^2}\log_{10}^{-2}\left(\left(\tfrac{0.0002}{3.7}\right)^{10/9}\right) = 0.0137 \quad Q_1 = 0.785\sqrt{\tfrac{2\times 9.8\times 1}{0.0137\times 3000}} \times \tfrac{30-23}{\sqrt{30-23}} = 1.433$$
$$\lambda_2 \approx \tfrac{1}{1.8^2}\log_{10}^{-2}\left(\left(\tfrac{0.002}{3.7}\right)^{10/9}\right) = 0.0234 \quad Q_2 = 0.159\sqrt{\tfrac{2\times 9.8\times 0.45}{0.0234\times 600}} \times \tfrac{18-23}{\sqrt{|18-23|}} = -0.282$$
$$\lambda_3 \approx \tfrac{1}{1.8^2}\log_{10}^{-2}\left(\left(\tfrac{0.001}{3.7}\right)^{10/9}\right) = 0.0196 \quad Q_3 = 0.283\sqrt{\tfrac{2\times 9.8\times 0.6}{0.0196\times 1000}} \times \tfrac{9-23}{\sqrt{|9-23|}} = -0.819$$
$$Q_1 + Q_2 + Q_3 = 1.433 - 0.282 - 0.819 = 0.332$$

Hence the inflow is greater than the outflow, so we will increase $z_{\mathrm{J}}$ to be $25\,\mathrm{m}$. Now we iterate again, however we believe that the friction factors are already satisfactory.

$$\lambda_1 = \tfrac{1}{1.8^2}\log_{10}^{-2}\left(\left(\tfrac{0.0002}{3.7}\right)^{10/9} + 6.9\tfrac{10^{-6}\pi\times 1}{4\times 1.433}\right) = 0.0142 \quad Q_1 = 0.785\sqrt{\tfrac{2\times 9.8\times 1}{0.0142\times 3000}}\tfrac{30-25}{\sqrt{|30-25|}} = 1.190$$
$$\lambda_2 = \tfrac{1}{1.8^2}\log_{10}^{-2}\left(\left(\tfrac{0.002}{3.7}\right)^{10/9} + 6.9\tfrac{10^{-6}\pi\times 0.45}{4\times 0.282}\right) = 0.0236 \quad Q_2 = 0.159\sqrt{\tfrac{2\times 9.8\times 0.45}{0.0236\times 600}} \times \tfrac{18-25}{\sqrt{|18-25|}} = -0.332$$
$$\lambda_3 \approx \tfrac{1}{1.8^2}\log_{10}^{-2}\left(\left(\tfrac{0.001}{3.7}\right)^{10/9} + 6.9\tfrac{10^{-6}\pi\times 0.6}{4\times 0.82}\right) = 0.0198 \quad Q_3 = 0.283\sqrt{\tfrac{2\times 9.8\times 0.6}{0.0198\times 1000}} \times \tfrac{9-25}{\sqrt{|9-25|}} = -0.872$$
$$Q_1 + Q_2 + Q_3 = 1.190 - 0.332 - 0.872 = -0.014$$

which is close enough to zero, and the process seems to have converged quickly, with a somewhat lucky guess as to $z_{\mathrm{J}}$.

All this is rather more simply done using *Solver*: **URL:** *http://johndfenton.com/Lectures/Hydraulics/Pipesolver.xls*.

### 8.5.8 Networks of pipes

**Hardy-Cross method (1936):** The following conditions must be satisfied in a network of pipes:

1. The algebraic sum of the head drops around each circuit must be zero.
2. The net flow at a junction must be zero.
3. The Weisbach equation must be satisfied in each pipe.

To solve the resulting set of equations, methods of successive approximation have been traditionally used. The Hardy Cross method is one in which flows are assumed for each pipe so that continuity is satisfied at every junction. A correction to the flow in each circuit is then computed in turn and applied to bring the circuits into closer balance.

This is suited to hand computation, but seems to require some arbitrariness and monitoring. The following method seems better for computer applications.

**An alternative approach:** Consider the Weisbach equation for head loss which we will write in slightly more general form, allowing local losses and for the direction of flow being in the direction of head loss:

$$\Delta H = -\frac{1}{2gA^2}\left(\frac{\lambda L}{D} + \sum K\right) Q\,|Q|\,,$$

where the negative sign and the modulus symbol has been introduced so that if $Q$ is positive, then $\Delta H$ is negative, head loss occurring in the direction of flow. We re-write this in terms of the flow from a node $i$ to a node $j$, for which we use the symbol $Q_{ij}$:

$$H_j - H_i = -\frac{1}{2gA_{ij}^2}\left(\frac{\lambda_{ij} L_{ij}}{D_{ij}} + \sum_{\text{Local losses}} K_{ij}\right) Q_{ij}\,|Q_{ij}|\,,$$

which we write as

$$H_i - H_j = \Omega_{ij}^2\, Q_{ij}\,|Q_{ij}|\,. \tag{8.41}$$

This notation is suggested by the electrical analogy, where there is a linear relationship

Potential difference = Resistance × Current.

In equation (8.41) the resistance-like quantity $\Omega_{ij}$ is defined by

$$\Omega_{ij}^2 = \frac{1}{2gA_{ij}^2}\left(\frac{\lambda_{ij} L_{ij}}{D_{ij}} + \sum_{\text{Local losses}} K_{ij}\right).$$

and solving the "quadratic" equation (8.41) for $Q_{ij}$, which is not so trivial because of the modulus sign, we obtain

$$Q_{ij} = \frac{1}{\Omega_{ij}}\,\mathrm{sign}\,(H_i - H_j)\,\sqrt{|H_i - H_j|}, \tag{8.42}$$

and sign$(H_i - H_j)$ means take the sign of the head difference. In this way, if $H_i > H_j$, then $Q_{ij}$ is positive, with flow from $i$ to $j$, which is correct..

We can use the Colebrook-White equation or the Haaland approximation for $\lambda$, equation (8.7), for each pipe, here modified slightly in terms of $|Q_{ij}|$:

$$\lambda_{ij} = \frac{1}{1.8^2}\,\log_{10}^{-2}\left(\left(\frac{\varepsilon_{ij}}{3.7}\right)^{10/9} + \frac{6.9}{\mathbf{R}_{ij}}\right),\ \text{where } \mathbf{R}_{ij} = \frac{4\,|Q_{ij}|}{\nu\pi D_{ij}}, \tag{8.43}$$

and mass-conservation at the junction $J$:

$$\sum_i Q_{iJ} = 0, \tag{8.44}$$

where summation is over all the pipes meeting at $J$. As in both these equations the discharge can be expressed in terms of the heads from equation (8.42), the resulting system of equations is in terms of the heads at the nodes and the friction factors in each of the pipes. *Excel Solver* can be used to solve these nonlinear equations.

Hence, the suggested procedure is:

1. Write a mass-conservation equation (8.44) at each junction of the network,
2. Write a law for the friction parameter such as equation (8.43) for each pipe in the network,
3. Equations (8.42) can be substituted for every occurrence of $Q_{ij}$ so that the equations are only in terms of the unknown heads at the nodes and the unknown friction factors of the pipes, as well as the known characteristics of pipes and fittings.

4. Use a nonlinear equation solver such as *Excel Solver* to solve the equations.

**Example 8.6** Consider the pipe network shown in Figure 8-14, where the friction factors are presumed known, giving the $\Omega$ shown.Hence the equations we have are:

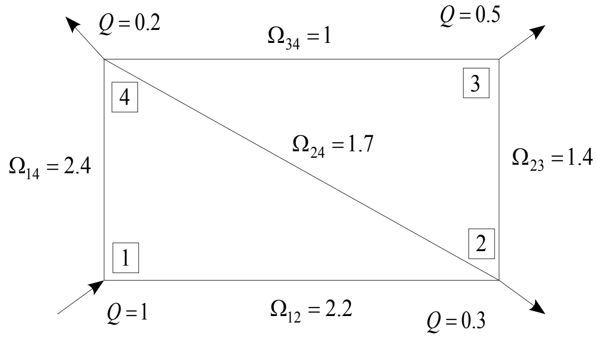


Figure 8-14. Simple network

| | |
|---|---|
| Junction 1 | $Q_{12} + Q_{14} - 1 = 0$ |
| Junction 2 | $-Q_{12} + Q_{24} + Q_{23} + 0.3 = 0$ |
| Junction 3 | $-Q_{23} + Q_{34} + 0.5 = 0$ |
| Junction 4 | $-Q_{34} - Q_{24} - Q_{14} + 0.2 = 0$ |

where

$$Q_{12} = \frac{1}{2.2} \operatorname{sign}(H_1 - H_2) \sqrt{|H_1 - H_2|}, \text{ and so on.}$$

Substituting these expressions we have 4 equations in the 4 unknowns $H_1, \ldots, H_4$. However, we believe that one of the junction equations is redundant and that we are free to specify one value of $H = 10$ for example, leaving three equations in three unknowns.

# 9. Discharge measurement in pipes

Pipeline flow can be measured in many ways. Selection of a particular installation depends upon specific local situations. The accuracy of flow measurements in pipelines can be very high.

## 9.1 Differential head meters – Venturi, nozzle and orifice meters

This class of flowmeters includes venturi, nozzle, and orifice meters. These meters have a potential accuracy of 1%. They have no moving parts but use some form of constriction. Heads are measured upstream where the meter is the size of the approach pipe and downstream where the area is reduced to a minimum. Energy relationships are used to obtain the discharge in terms of the difference of head between the two locations. However in practice the results are modified by the use of discharge coefficients so that the results agree more with experiment.

Venturi meters are one of the most accurate type of flow measuring device that can be used in a water supply system. They contain no moving parts, require very little maintenance, and cause very little head loss. Venturi meters are often used in the laboratory to calibrate other closed conduit flow measuring devices. The effective discharge coefficient for venturi meters ranges from 0.9 to about unity. As venturi meters have smoothly varying flow boundaries, they have been used for measuring sewage and flow carrying other materials.

### 9.1.1 Venturi meters

On page 53 we analysed a Venturi meter using the energy theorem, but without describing how the pressures were to be measured. Consider the gradual constriction in the pipe in Figure 9-1, where there are pressure tapping points in the pipe at point 1 before the constriction and point 2 in the constriction.

We use a control volume crossing the pipe at 1 and 2 and apply equation (6.10), the integral energy theorem for a

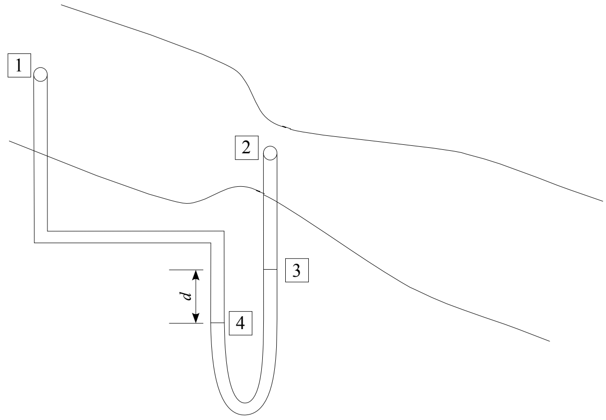


Figure 9-1. Venturi meter, showing constriction, tapping points, and manometer

single inlet and outlet:

$$\frac{p_1}{\rho g} + z_1 + \frac{\gamma}{2g}\frac{Q^2}{A_1^2} = \frac{p_2}{\rho g} + z_2 + \frac{\gamma}{2g}\frac{Q^2}{A_2^2}.$$

This can be written more simply in terms of piezometric heads $h_1$ and $h_2$:

$$h_1 + \frac{\gamma}{2g}\frac{Q^2}{A_1^2} = h_2 + \frac{\gamma}{2g}\frac{Q^2}{A_2^2},$$

and solved for $Q$:

$$Q = \sqrt{\frac{1}{\gamma}\frac{2g\,(h_1 - h_2)}{1/A_2^2 - 1/A_1^2}} = \frac{1}{\sqrt{\gamma}} A_1 A_2 \sqrt{\frac{2g\,(h_1 - h_2)}{A_1^2 - A_2^2}}. \tag{9.1}$$

It is interesting that it has been possible to express the discharge so simply in terms of the piezometric head difference. Usual practice is to write this equation as

$$Q = C A_1 A_2 \sqrt{\frac{2g\,(h_1 - h_2)}{A_1^2 - A_2^2}}, \tag{9.2}$$

where, it is said, $C$ is a "coefficient determined experimentally", which ranges from 0.9 to about unity. Comparison with our expression (9.1) shows that $C = 1/\sqrt{\gamma}$, and so, if we assume a value of $\gamma = 1.3$, we obtain $C = 1/\sqrt{1.3} = 0.88$, and so it is possible that our incorporation of $\gamma$ in these lectures has provided an explanation for the values of $C$, without having to invoke energy losses.

### 9.1.2 Nozzle Meters

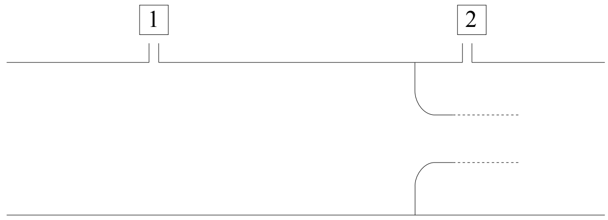


Figure 9-2. Nozzle meter

In effect, the flow nozzle is a venturi meter that has been simplified and shortened by eliminating the gradual downstream expansion (Figure 9-2). The streamlined entrance of the nozzle causes a straight jet without contraction, so its effective discharge coefficient is nearly the same as the venturi meter. Flow nozzles allow the jet to expand of its own accord. This feature causes a greater amount of turbulent expansion head loss than the loss that occurs in venturi meters, which suppress exit turbulence with a gradually expanding tube boundary.

The effective coefficient of discharge for flow nozzles in pipelines varies from 0.96 to 1.2 for turbulent flow and increases as the throat-to-pipe-diameter ratio increases.

Frequently, the upstream pressure connection is made through a hole in the wall of the conduit at a distance of about one pipe diameter upstream from the starting point of the flare of the nozzle. Thus, the pressure is measured before it curves to enter the nozzle, while the downstream pressure connection may be made through the pipe wall just above the end of the nozzle tube.

### 9.1.3 Orifice Meter

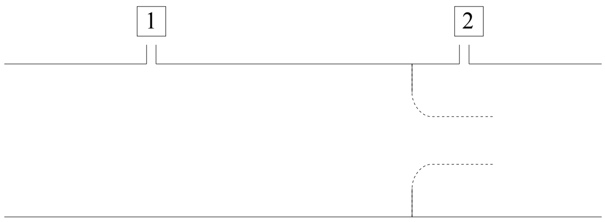


Figure 9-3. Orifice meter

The most common differential-pressure type flowmeter used in pipelines is the sharp-edged orifice plate (Figure 9-3). Applications with proper water quality, careful attention to installation detail, and proper operation techniques make these flowmeters capable of producing accuracy to within 1%.

Advantages of the orifice plate are its simplicity and the ability to select a proper calibration on the basis of the measurements of the geometry. Disadvantages of the orifice plate include long, straight pipe length requirements and the limited practical discharge range ratio of about one to three for a single orifice hole size. However, the location of the range can be shifted by using sets of plates for changing orifice hole sizes. This shift, in effect, provides a range ratio increase. Calibrations based on tap locations relative to pipe diameter, rather than orifice diameter, make this feasible because the same tap locations can be used for different orifice plate hole sizes.

It should be noted that the orifice plate installation in the Sexton Laboratory is not of this type, for the downstream measurement point is considerably further downstream such that the jet will have diffused through the flow and there will have been energy losses. In this case the coefficient $C$ is purely empirically determined.

### 9.1.4 Measurement of piezometric head difference

For applications where continuous monitoring and control are necessary the pressure elevation heads will be measured and recorded digitally. However the U-tube manometer provides a simple way of doing this manually, as in Figure 9-1 where a U-tube manometer measures an elevation difference of $d$.

Consider the hydrostatic pressure equation

$$\frac{p}{\rho g} + z = \text{Constant} = h,$$

hence we see that the hydrostatic pressure equation is simply a statement that in a fluid at rest, the piezometric head $h$ is constant. In the present context we can simply say that $h_1 = h_4$ and that $h_2 = h_3$. Hence the piezometric head difference $h_1 - h_2$ in equations (9.1) and (9.2) is simply $h_4 - h_3$. It is this quantity that the manometer measures. Now we can write for the quantity $h_1 - h_2$ that we need in equation (9.2):

$$\begin{aligned} h_1 - h_2 &= h_4 - h_3 \\ &= \frac{p_4}{\rho g} + z_4 - \frac{p_3}{\rho g} - z_3, \end{aligned}$$

and we can obtain $p_4 - p_3$ by using the hydrostatic pressure equation in the manometric fluid where the density is $\sigma\rho$:

$$\frac{p_4}{\sigma\rho g} + z_4 = \frac{p_3}{\sigma\rho g} + z_3, \qquad \text{giving} \qquad \frac{p_4}{\rho g} - \frac{p_3}{\rho g} = \sigma\left(z_3 - z_4\right),$$

and substituting gives

$$h_1 - h_2 = (\sigma - 1)\left(z_3 - z_4\right) = (\sigma - 1)\, d.$$

Equation (9.2) becomes

$$Q = CA_1A_2\sqrt{\frac{2(\sigma-1)\,gd}{A_1^2-A_2^2}},$$

and we see that the discharge is obtained simply by measuring the elevation difference across the manometer. It is not surprising that the relative density appears as $\sigma - 1$, as on one side of the manometer there is a fluid column of relative density $\sigma$ and on the other side one of 1. It is convenient that the elevations of the tapping points are unimportant – the only elevation to measure is $d$ the height difference across the manometer.

## 9.2 Acoustic flow meters

Now we consider rather more modern technologies by considering non-mechanical, non-intrusive devices which are capable of measuring discharge in open channels or pipes with considerable accuracy. It will be seen that in practice this accuracy is seldom realised.

1. Transit-time acoustic flow meters

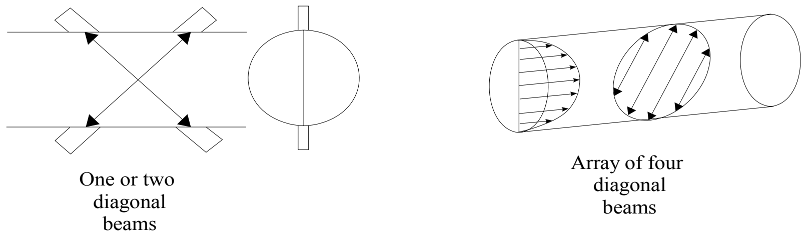


Figure 9-4. Ultrasonic flow meters – one, or two crossed beams, or four or more beams.

Transit-time acoustic (ultrasonic) flowmeters are based on the principle that transit time of an acoustic signal along a known path is altered by the fluid velocity. A high frequency acoustic signal sent upstream travels slower than a signal sent downstream. By measuring the transit times of signals sent in both directions along a diagonal path, the average path velocity can be calculated. Then the average axial velocity can be computed.

Manufacturers and users make claims for the accuracy (0.5-3%) of a multi-beam installation, but this is exaggerated, as an inaccurate numerical integration method is used to incorporate the data from the beams (Fenton 2002).

2. Doppler-type acoustic flow meter

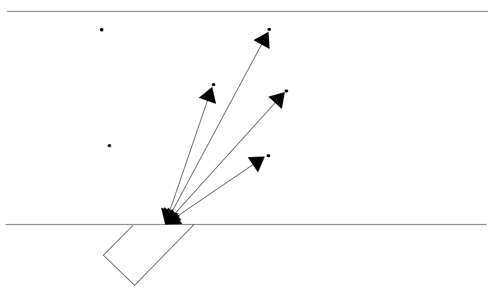

Figure 9-5. Doppler-type acoustic flow meter showing beams reflected from individual particles.

The Doppler flowmeter measures the velocity of particles moving with the flowing fluid (Figure 9-5). Acoustic signals of known frequency are transmitted, reflected from particles, and are picked up by a receiver. The received signals are analysed for frequency shifts, and the resulting mean value of the frequency shifts is supposed to be directly related to the mean velocity of the particles moving with the fluid. System electronics are used to reject stray signals and correct for frequency changes caused by the pipe wall or transducer protective material.

Doppler flowmeter performance is highly dependent on physical properties such as the liquid's sonic conductivity, particle density, and flow profile. Likewise, non-uniformity of particle distribution in the pipe cross section results in a computed mean velocity that is incorrectly weighted. Therefore, the meter accuracy is sensitive to velocity profile variations and to distribution of acoustic reflectors in the measurement section.

Unlike other acoustic flowmeters, Doppler meters are affected by changes in the liquid's sonic velocity. As a result, the meter is sensitive to changes in density and temperature.

These problems make Doppler flowmeters unsuitable for highly accurate measurements, however they are widely used and believed in flow measurements in streams. They should not be.

3. Acoustic Doppler Current Profilers (ADCP)

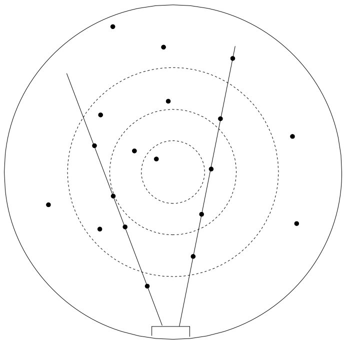

Figure 9-6. Acoustic Doppler Current Profiler showing isovels, beams and backscattering particles.

These are a recent (1997) development, and take the previous Doppler method rather further. Figure 9-6 shows a typical profiler installation for measuring flow in a pipe. A transducer assembly is mounted on the invert of a pipe or channel. Piezoelectric ceramics emit short pulses along narrow acoustic beams pointing in different directions. Echoes of these pulses are backscattered from material suspended in the flow. As this material has motion relative to the transducer, the echoes are Doppler shifted in frequency. Measurement of this frequency shift enables the calculation of the flow speed.

The Profiler divides the return signal into discrete regular intervals which correspond to different depths in the flow. Velocity is calculated from the frequency shift measured in each interval. The result is a profile, or linear distribution of velocities, along the direction of the beam. Each of the small black circles in Figure 9-6 represent an individual velocity measurement in a small volume known as a cell.

Usually there are actually two beams for each of those shown – one pointing upstream and the other downstream. The data from one beam pair are averaged to generate one profile, and a beam pair on the opposite side of the transducer assembly generates the other. It can be inferred from the diagram that the sampling does not give a particularly good coverage of the whole flow. When operated as a vertical beam from a moving boat, the results can be accurate, but for the installation shown we do not expect great accuracy.

## 9.3 Magnetic Flowmeters

The operation of magnetic flowmeters is based upon the principle that a voltage is induced in an electrical conductor moving through a magnetic field. In the case of magnetic flowmeters, the conductor is the flowing water being measured. For a given field strength, the magnitude of the induced voltage is proportional to the mean velocity of the conductor, giving the discharge. This is actually a method which, unlike all the previous methods, automatically integrates the velocity over the pipeline.

The meter consists of a nonmagnetic and nonelectrical conducting tube or pipe through which the water flows. Two magnetic coils are used, one on each side of the pipe. Two electrodes in each side of the insulated pipe wall sense the flow-induced voltage. The meter has electrical circuits to transform the induced voltage into a rate-of-flow indication on a meter dial. The electrical sensing system and uniform flow-through passage allow the magnetic flowmeter to measure flow in both directions.

A source of electrical power is needed to activate the magnetic field, and a transmitter is used to record or send the rate-of-flow signals to desired stations. The water needs sufficient conductivity, but other properties such as temperature, viscosity, density, or solid particles do not change calibration. However, dissolved chemicals can deposit on the electrodes and cause accuracy errors. Some of these meters are provided with wipers or electrolytic or ultrasonic electrode cleaners.

Head losses through the meter are negligible, and accuracy of measurement in the upper half of the meter's rated capability is usually good. Later model electromagnetic meters can have good accuracy (+/-1.0%) for a range of minimum to maximum discharge.

# 10. Pressure surges in pipes

## 10.1 Introduction

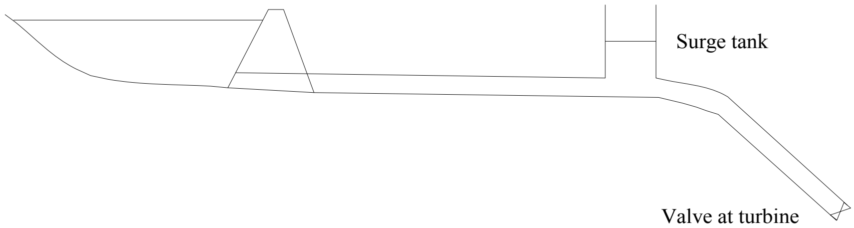


Figure 10-1. Reservoir, pipeline, surge tank, penstock and turbine valve system

Unsteady flow in pipelines when compressibility effects are not important are referred to as surge. When the flow passage suddenly closes, partly or completely, the water decelerates and compressibility of the fluid and elasticity of the pipe walls must be considered, this is called *water hammer*. As one means of eliminating water hammer, the water may be allowed to surge into a tank as shown. The valve at the end of a pipeline may be controlled by a turbine governor, and may quickly stop if the generator loses its load. To destroy all momentum in the long pipe system quickly would require high pressure and a costly pipeline. With a surge tank as near the valve as possible, although surge will occur between the reservoir and surge tank, development of high pressures in this part is prevented. It would still be necessary to design the pipeline between surge tank and valve to withstand water hammer.

Closed surge tanks which operate under air pressure are used in certain case, for example, after a reciprocating pump, but are uneconomical for large pipelines.

Detailed analysis of surge tanks requires solution of the equation of motion and continuity for the liquid in the pipeline, but in this course we will concentrate on water hammer, including compressibility of the liquid and elasticity of the pipeline.

## 10.2 The phenomenon of water hammer

Water hammer may occur in a pipeline when there is a sudden retardation or acceleration of the flow, such as the closing of a valve on the line. If the change is gradual, calculations may be carried out by surge methods, considering the liquid incompressible and the pipeline rigid. Water hammer is produced by a sudden change in the velocity of flow in a conduit, when the head on the upstream side of the valve is increased and causes a pulse of high pressure to propagate upstream at the sonic wave speed $c$. Examples include Sharp (1981, page 1):

- The stopping and starting of pumps
- The turning off of a tap at a wash basin
- The sudden flow demand of an automatic fire sprinkler system
- A resonance in a liquid supply line
- Mechanical failure of an item such as a valve – a casualty of age or wear from repeated use.

Water hammer is a wave motion which is very rapid – changes may propagate at $1200\,\mathrm{m\,s^{-1}}$, while liquid velocities are usually no greater than $6\,\mathrm{m\,s^{-1}}$. When water hammer is produced it is transmitted to all parts of the connected system, where it is modified by changes in geometry and the conduit properties and boundary conditions. A sudden change of $1\,\mathrm{m\,s^{-1}}$ can be accompanied by a pressure change of $100\,\mathrm{m}$. Valve controls and all pipework should be designed so that they can survive the water hammer without damage.

The assembly of data and an understanding of the properties of wave transmission and reflection are the first steps. Once a system has been analysed, the maximum and minimum (for cavitation and rupture of the water column is also possible) pressures are known and the system may be modified and re-analysed.

## 10.3 Sequence of events following sudden valve closure

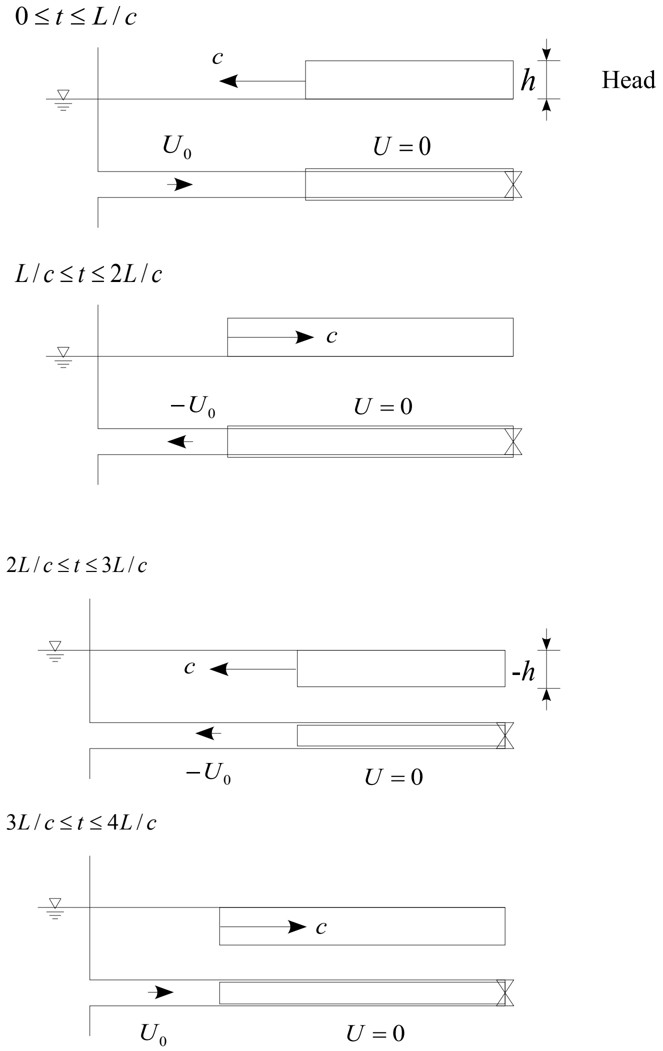


Figure 10-2. Four stages of one cycle of sudden closure of a valve

The following description and Figure 10-2 have been taken from Streeter & Wylie (1981, #12.4):

---

Consider a valve in a pipeline which is suddenly closed. Friction is neglected in this discussion. At the instant of valve closure $t = 0$ the fluid nearest the valve is compressed and brought to rest and the pipe wall is stretched as shown in the first figure. As soon as the first layer is compressed, the process is repeated for the next layer of fluid particles. The fluid upstream from the valve continues to move downstream at the original speed as there has been no time for any sound waves to have reached it and informed it. This continues until successive layers have been compressed back to the reservoir. The high pressure moves upstream as a wave, bringing the fluid to rest as it passes, compressing it and expanding the pipe. When the wave reaches the upstream end of the pipe at $t = L/c$, all the fluid is under the extra head $h$, all the momentum has been lost, and all the kinetic energy has been converted into elastic energy.

Now there is an unbalanced condition at the reservoir end at the instant of arrival of the pressure wave, as the reservoir pressure is unchanged. The fluid starts to flow backward, beginning at the reservoir. This flow returns the pressure to the value before closure, the pipe wall returns to normal, and the fluid has a velocity $-U_0$. This process of conversion travels downstream toward the valve at the speed of sound $c$ in the pipe. At the instant $2L/c$ the wave arrives at the valve, pressures are back to normal, but the velocity in the pipe everywhere is $-U_0$. Since the valve is closed, no fluid is available to maintain the flow at the valve and a low pressure $-h$ develops such that the fluid is brought to rest. This low-pressure wave travels upstream at a speed $c$ and everywhere brings the fluid to rest, causes it to expand because of the lower pressure, and allows the pipe walls to contract. If the static pressure in the pipe is not sufficiently high to sustain the head $-h$ the liquid cavitates, vaporises and continues to move backward over a longer period of time.

At the instant the negative pressure wave arrives at the reservoir end, $3L.c$ after closure, the fluid is at rest but at head $-h$. This leaves an unbalanced condition at the reservoir and fluid flows into the pipe, acquiring a velocity $+U_0$ and returning the pipe and fluid to normal conditions as the wave travels down the pipe at speed $c$. At the instant this wave reaches the valve, conditions are exactly the same as at the instant of closure, $4L/c$ earlier.

This process is repeated every $4L/c$. The action of fluid friction and imperfect elasticity of fluid and pipe wall is to damp out the motion and eventually to cause the fluid to come to a state of rest. Closure of a valve in less than $2L/c$ is called *rapid closure*; *slow closure* is obvious.

## 10.4 Derivation of fundamental relationship using steady momentum theorem

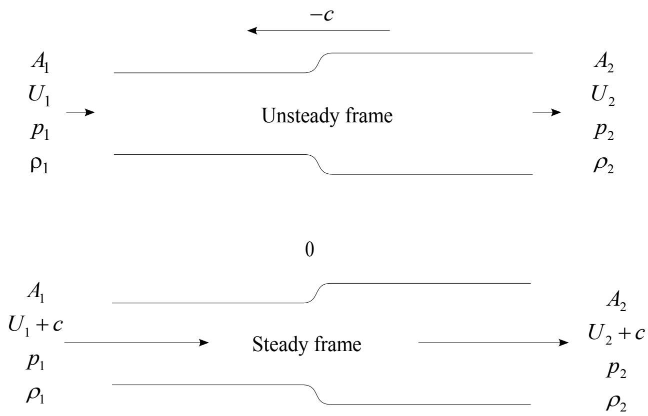


Figure 10-3. Propagating wave in pipe showing wave velocity and fluid velocities – in the physical unsteady frame and in a frame travelling with the wave.

Consider the motion in the two frames as shown in Figure 10-3. The first is the physical frame, through which the wave moves at a velocity of $-c$. To make motion steady we superimpose a velocity of $+c$, so that the wave is now motionless, but the horizontal velocities with which the fluid moves through the system have increased by $+c$. Now we apply principles of mass and momentum conservation in the steady frame. Mass conservation gives

$$-\rho_1 (U_1 + c) A_1 + \rho_2 (U_2 + c) A_2 = 0. \tag{10.1}$$

Now to apply momentum conservation we note that there will be an additional horizontal force of the pipe on the fluid where the pipe suddenly expands. As the pressure there is $p_2$, just as at the exit of area $A_2$, it seems simplest to assume that the force contribution there is $p_2$ times the area of the annulus, which is $p_2 (A_2 - A_1)$. So, applying the integral momentum theorem (5.2), using $\beta = 1$ in the fluid momentum terms, because the Galilean transformation of $+c$ applies to all the fluid, and taking the horizontal component we have

$$-\rho_1 A_1 (U_1 + c)^2 - p_1 A_1 + \rho_2 A_2 (U_2 + c)^2 + p_2 A_2 = \underbrace{p_2 (A_2 - A_1)}_{\text{Force of annular bulge on fluid}} .$$

Collecting like terms gives

$$-\rho_1 A_1 (U_1 + c)^2 + \rho_2 A_2 (U_2 + c)^2 + A_1 (p_2 - p_1) = 0. \tag{10.2}$$

Multiplying equation (10.1) by $U_2 + c$, subtracting from equation (10.2), and cancelling common factors gives:

$$p_2 - p_1 + \rho_1 (c + U_1) (U_2 - U_1) = 0.$$

If we make the sensible approximation that as $U_1 \ll c$, that we replace $U_1 + c$ by $c$:

$$p_2 - p_1 = \rho_1 c (U_1 - U_2) ,$$

and dividing by $\rho g$ gives an expression for the head rise in terms of the velocity change:

$$\Delta h = \frac{c}{g}\left(-\Delta U\right).$$

Here we have not considered all the mechanics of the pipeline system, and have not derived an expression for the wave speed $c$. If we had we would have obtained the relationship

$$c = \sqrt{\frac{K/\rho}{1 + \frac{DK}{Ew}}}, \tag{10.3}$$

where $c$ is the propagation speed of compressible disturbances in elastic pipes, $K$ is the bulk modulus of the fluid, such that

$$dp = K\frac{d\rho}{\rho},$$

$E$ is the Young's modulus of the pipe wall, $D$ is pipe diameter and $w$ is pipe wall thickness. If we had rigid thick walls such that $E \gg K$, then $DK/Ew \to 0$, and we obtain $c = \sqrt{K/\rho}$ the propagation speed of sound waves in the fluid. Finite values of $DK/Ew$ mean that the speed of waves in the combined pipe/water system will be less.

This derivation gives some physical insight into the basic mechanism of water hammer. The extra head is caused by the piling up of fluid with higher momentum into a region of lower momentum, with the compressibility of the fluid and elasticity of the pipeline softening the blow. While water hammer might be thought of as a nuisance, it is a good thing that the compressibility does come into play. Otherwise, if we had a rigid pipeline $E \to \infty$ and an incompressible fluid $K \to \infty$, then from equation (10.3) then the velocity of waves (the propagation of information) in the pipeline would be infinite, and hence so would be the increase in head. We can imagine the effect of a long solid bar of stone crashing against an immoveable barrier. With compressibility, the time for the fluid to slow is finite, and so is the extra pressure caused.

## 10.5 Practical considerations

Some of the following has been taken from the useful introduction to water hammer of Sharp (1981).

### 10.5.1 Rupture of the water column

Rupture or separation of the water column occurs frequently in pipelines, as negative pressures can easily be induced by wave reflection. Unlike some aspects of system behaviour that are conservative when neglected, this phenomenon in general increases the problems and severity of water hammer. It is too complex to treat here.

### 10.5.2 Resonance

It is quite possible that the abrupt nature of water hammer, which contains a large number of Fourier components, can excite the natural frequencies of a system, and a full analysis should bear this in mind.

### 10.5.3 Protection methods

The use of some form of protection device is largely a matter of economics. It is physically possible to design a pipeline capable of withstanding any surge or shock so that failure does not occur. However it is more reasonable to design a pipeline for pressures only slightly in excess of normal steady operating values. If occasional large shocks must be provided for, it will generally cost less to prevent them from reaching the rest of the pipe system, by some form of protective device.

- Flywheels – Install a flywheel on rotating machinery such that in the event of failure the velocity changes are not so rapid, and so the water hammer is reduced.
- Open surge tank – hydroelectric installations use an open surge tank often, although there are stability problems in the case of turbine load fluctuations. In pumping schemes it is seldom possible to install an open surge tank on the delivery side, and closed surge tanks are used, which depend upon air pressure. It is necessary to provide as generous a connection as possible between the pipeline and the surge tank, otherwise rather more water hammer passes the surge tank.
- Bypass methods may be used – since the development of water hammer is due to sudden changes in the

velocity of flow, protection may be achieved by slowly decelerating the liquid. For example, when flow reverses towards a pump a bypass may be opened allowing water to flow to the suction side. The bypass valve may then be closed slowly with only a small overpressure developing. Similarly in a hydroelectric system, when regulation requires a sudden decrease in output a bypass may open rapidly in concert with the flow reduction through the turbine. An example is the deflector plate/needle valve combination at a Pelton wheel.

In the same category are pressure relief valves which open very rapidly as warning of an excessive pressure increase occurs.

- Other methods for protection

  - One way surge tank – when pressures less than atmospheric occur in a pipe, a surface reservoir isolated by a non-return valve can automatically discharge into a pipeline, which is the reverse of the bypass method.
  - Controlled closing of a non-return valve - using a control or damping mechanism
  - Anti-vacuum valves - air may be admitted when pressures are less than atmospheric and prevent low pressures from occurring. This has the disadvantage that the air has subsequently to be removed.
  - Valve stroking – deliberate phasing of the degree of opening of a valve so as to control the ultimate water hammer pressures. This assumes a detailed knowledge of the valve characteristics.

### 10.5.4 Typical values

As a general rule, for a large steel water pipeline, a typical value of $c$ is $1000\,\mathrm{m\,s^{-1}}$. For other situations $c$ can vary between the speed of sound in water, typically $1500\,\mathrm{m\,s^{-1}}$, down to some $200\,\mathrm{m\,s^{-1}}$ for plastic lines. The bulk modulus $K = 2.2$ GPa at 20°C.

| Material | $E$ (GPa) |
|---|---|
| Aluminium alloy | 70 |
| Asbestos cement | 24 |
| Concrete | 20 |
| Copper | 120 |
| Glass | 70 |
| Iron | 100 |
| Plastic | 0.8-3 |
| Steel | 210 |
| Rock - Granite | 50 |
| Rock - Sandstone | 3 |

# 11. Pumps and turbines

To move fluid from one point to another in a pipe, it is necessary to supply a driving force. In some cases, gravity can be used to supply the driving force (*i.e.* when there is a difference in elevations). In most cases, however, pumps or fans must be used to supply the driving force that is required to move the fluid. Different types of pumps can be used to accomplish different tasks. For example, the energy that is transferred from a pump to the fluid may be used to increase the velocity, pressure, or elevation of the fluid. Going in the other direction, hydraulic turbines are used all around the world to extract power from water. In this course we will deal mainly with pumps.

It is interesting that fluid machinery is one of the best applications of dimensional analysis, as the machines are so complicated that theory can do very little, whereas dimensional analysis provides some very practical help indeed.

## 11.1 Introduction to pump types

Pumps move mainly incompressible fluids (like water) and fans move compressible fluids (gases like air). There are many types of pumps. The main ones are

- Rotodynamic pumps, which are the main ones of interest to us, use rotating elements such as impellers or blades. The lower the head required and the greater the flow required the more axial the pump or turbine should be for efficient operation, hence for high heads a fast-rotating relatively small element is used, while for low heads a larger fan-type of design is used.

- Centrifugal - fluid is spun around and ejected by centrifugal action. These are the most common pumps used in industry,
- Positive displacement or force pumps – a set volume of fluid is physically moved, often by a piston. These pumps are less common, and are used for thick and viscous fluids under high pressure or where the delivery flow must be precise,
- Others such as the Hydraulic Ram, suitable for remote locations, and the Archimedean Screw, which is useful for low heads.

## 11.2 Hydraulic ram pumps

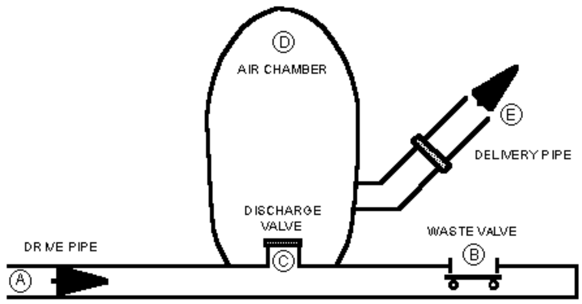


Figure 1. Hydraulic ram pump components.

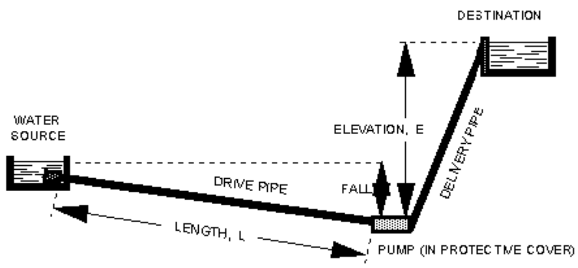


Figure 2. Hydraulic ram pump system layout

Figure 11-1. Hydraulic ram pump – components and system layout

An hydraulic ram pump[17] is a simple, motorless device for pumping water at low flow rates. It uses the energy of flowing water to lift water from a stream, pond, or spring to an elevated storage tank or to a discharge point. It is suitable for use where small quantities of water are required and power supplies are limited, such as for household, garden, or livestock water supply. A hydraulic ram pump is useful where the water source flows constantly and the usable fall from the water source to the pump location is at least 1 metre. They can be particularly useful in the developing world in the wet tropics.

### 11.2.1 Principles of Operation

Components of a hydraulic ram pump are illustrated in Figure 11-1(a). Its operation is based on converting the kinetic energy in flowing water into potential energy of a smaller quantity of fluid. Water flows from the source through the drive pipe (A) and escapes through the waste valve (B) until it builds enough pressure to suddenly close the waste valve. Water then surges through the interior discharge valve (C) into the air chamber (D), compressing air trapped in the chamber. When the pressurised water reaches equilibrium with the trapped air, it rebounds, causing the discharge valve (C) to close. Pressurised water then escapes from the air chamber through a check

[17] These notes and the accompanying figure were prepared by Gregory D.Jennings, Agricultural Engineering Extension Specialist, North Carolina Cooperative Extension Service, USA.

valve and up the delivery pipe (E) to its destination. The closing of the discharge valve (C) causes a slight vacuum, allowing the waste valve (B) to open again, initiating a new cycle.

The cycle repeats between 20 and 100 times per minute, depending upon the flow rate. If properly installed, a hydraulic ram will operate continuously with a minimum of attention as long as the flowing water supply is continuous and excess water is drained away from the pump.

### 11.2.2 System Design

A typical hydraulic ram pump system layout is illustrated in Figure 11-1(b). Each of the following must be considered when designing a hydraulic ram pump system:

1. Available water source
2. Length and fall of the drive pipe for channelling water from the source to the pump
3. Size of the hydraulic ram pump
4. Elevation lift from the pump to the destination
5. Desired pumping flow rate through the delivery pipe to the destination.

## 11.3 Centrifugal Pumps

A centrifugal pump, in its simplest form, consists of an impeller rotating inside a casing. The impeller imparts kinetic energy to the fluid. The velocity head, which is created by moving fluid from the low-velocity centre to the high-velocity edge of the impeller, is converted into a pressure head when the fluid leaves the pump. In the volute of the centrifugal pump, the cross section of the liquid path is greater than in the impeller, and in an ideal frictionless pump the drop from the high velocity in the impeller to the lower velocity is converted according to the energy equation, to an increased pressure. This is the source of the discharge pressure of a centrifugal pump.

Figure 11-2. Typical centrifugal pump

**Advantages of centrifugal pumps:**

- Simple to construct,
- Low cost,
- Fluid is delivered at uniform pressure without shocks or pulsations,
- The discharge line may be throttled (partly shut off) or completely closed without damaging the pump,
- Able to handle liquids with large amounts of solids,
- Can be coupled directly to motor drives,
- There are no valves involved in the pump operation, and
- Lower maintenance costs than other types of pumps.

**Disadvantages of centrifugal pumps:**

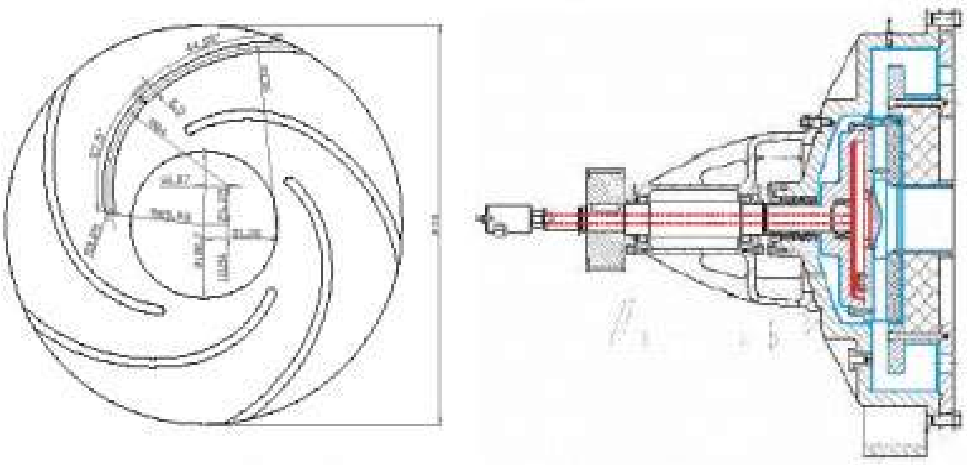

Figure 11-3. Centrifugal pump: impeller and housing

- Cannot be operated at high heads,
- Subject to air binding and usually must be primed (the supply line must be filled with water),
- The maximum efficiency for a pump holds over a fairly narrow range of conditions, and
- Do not handle highly-viscous fluids efficiently.

## 11.4 Pump Performance Curves/Characteristic Curves

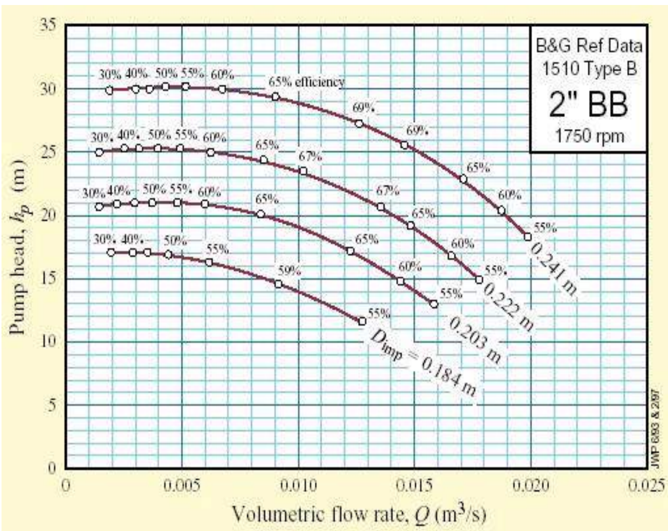


Figure 11-4. Typical characteristic curves for a family of pumps.

Pump manufacturers often produce graphs, such as that in Figure 11-4, for fixed pump size and fixed operating speed. Changing the size of the pump $L$ or the operating speed of rotation $N$ changes the conditions for optimum operation. The desired size of pump and operating speed can be inferred from similitude. There are many different factors which determine the actual performance characteristics of a pump. For this reason, it is best to use the actual experimental performance of the pump for determining the size that is required. The performance characteristics of a pump can be measured in-house, or they can be obtained from the pump manufacturer.

The performance characteristics of pumps and fans are most often presented in a graphic form called ’characteristic curves’. These curves describe characteristics of available head (pressure) and efficiency and power consumption, from zero to maximum flow. A family of performance curves can exist for various impeller diameters.

The performance curves which are supplied by the pump manufacturer will typically show plots of:

- Developed head (pressure) *vs* discharge (flow rate),
- Efficiency *vs* discharge, and
- Power *vs* discharge,

for various pump speeds. These plots are typically given for water, but for low viscosity fluids the plots will not change much.

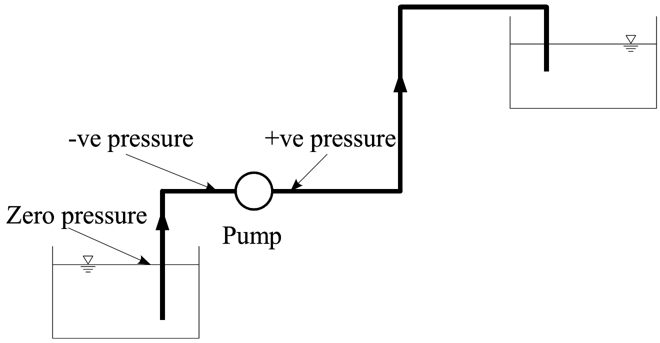


Figure 11-5. Simple pump line showing how negative pressures arise in the suction line.

On the suction side (*i.e.* upstream) the pressure may be negative (see Figure 11-5). Although it is often not possible, one should try to avoid negative pressures. Certainly one should try to minimise the length of negative pressure to avoid leakage of air into the pipe and pipe collapse (circular pipes are stronger under positive pressure – no buckling). Thus, we try to locate pumps as close as possible to the water level on the suction side.

The power output of a pump is $\rho g Q H$, where $Q$ is the flow through the pump and $H$ is the head across the pump. If the power required to drive a pump is $P$, and $\eta$ is the efficiency of the pump, then

$$\eta = \frac{\rho g Q H}{P}$$

## 11.5 Dimensional analysis

The actual performance characteristics of rotating machines have to be determined by experimental testing, and different machines have different characteristics. Furthermore, machines belonging to the same family may run at different speeds. Each size and speed combination will produce a unique set of characteristics, so that for one family of machines the number of characteristics to be determined is impossibly large. The problem is solved by the application of dimensional analysis. The dimensionless groups obtained provide the similarity laws governing the relationships between the variables within one family of geometrically-similar machines.

The variables to be considered are:

| Symbol | Variable | Dimensions |
|---|---|---|
| $Q$ | Volumetric flow rate through machine | $\mathrm{L}^3\mathrm{T}^{-1}$ |
| $H$ | Head difference across machine, as energy per unit mass, $gH$ | $\mathrm{L}^2\mathrm{T}^{-2}$ |
| $N$ | Rotational speed of machine (revolutions per second) | $\mathrm{T}^{-1}$ |
| $D$ | Length scale of machine, possibly diameter of impeller | L |
| $\rho$ | Density of fluid handled | $\mathrm{ML}^{-3}$ |
| $\mu$ | Dynamic viscosity of fluid | $\mathrm{ML}^{-1}\mathrm{T}^{-1}$ |
| $K$ | Bulk modulus of elasticity of the fluid | $\mathrm{ML}^{-1}\mathrm{T}^{-2}$ |
| $d$ | Absolute roughness of machine's internal passages | L |

Now we do the dimensional analysis. We have 8 variables and 3 dimensions, giving 5 dimensionless groups from the Buckingham $\Pi$ theorem. We choose $\rho$, $N$, and $D$ as the repeating variables, and not $Q$ as it is an output of the system.

1. $\Pi_1 = N^{i_1} D^{i_2} \rho^{i_3} gH$, so that the dimensional equation is

$$\mathrm{M}^0\mathrm{L}^0\mathrm{T}^0 = \left(\mathrm{T}^{-1}\right)^{i_1} \mathrm{L}^{i_2} \left(\mathrm{ML}^{-3}\right)^{i_3} \mathrm{L}^2\mathrm{T}^{-2},$$

and considering the exponent of each dimension in turn,

$$\begin{array}{ccl} \mathrm{M} & : & 0 = i_3 + 0 \\ \mathrm{L} & : & 0 = i_2 - 3i_3 + 2 \\ \mathrm{T} & : & 0 = -i_1 - 2, \end{array}$$

From this we have immediately $i_1 = -2$, $i_3 = 0$, and solving the remaining equation, $i_2 = -2$. Hence we have

$$\Pi_1 = \frac{gH}{N^2 D^2}.$$

2. $\Pi_2 = N^{j_1} D^{j_2} \rho^{j_3} Q$, so that the dimensional equation is

$$\mathrm{M}^0\mathrm{L}^0\mathrm{T}^0 = \left(\mathrm{T}^{-1}\right)^{j_1} \mathrm{L}^{j_2} \left(\mathrm{ML}^{-3}\right)^{j_3} \mathrm{L}^3\mathrm{T}^{-1},$$

and considering the exponent of each dimension in turn,

$$\begin{array}{ccl} \mathrm{M} & : & 0 = j_3 + 0 \\ \mathrm{L} & : & 0 = j_2 - 3j_3 + 3 \\ \mathrm{T} & : & 0 = -j_1 - 1, \end{array}$$

From this we have $j_1 = -1$, $j_3 = 0$, and solving the remaining equation, $j_2 = -3$. Hence we have

$$\Pi_2 = \frac{Q}{ND^3}.$$

3. $\Pi_3 = N^{k_1} D^{k_2} \rho^{k_3} \mu$, so that the dimensional equation is

$$\mathrm{M}^0\mathrm{L}^0\mathrm{T}^0 = \left(\mathrm{T}^{-1}\right)^{k_1} \mathrm{L}^{k_2} \left(\mathrm{ML}^{-3}\right)^{k_3} \mathrm{ML}^{-1}\mathrm{T}^{-1},$$

and considering the exponent of each dimension in turn,

$$\begin{array}{ccl} \mathrm{M} & : & 0 = k_3 + 1 \\ \mathrm{L} & : & 0 = k_2 - 3k_3 - 1 \\ \mathrm{T} & : & 0 = -k_1 - 1, \end{array}$$

From this we have immediately $k_1 = -1$, $k_3 = -1$, and solving the remaining equation, $k_2 = -2$. Hence we have

$$\Pi_3 = \frac{\mu}{\rho N D^2}.$$

4. $\Pi_4 = N^{l_1} D^{l_2} \rho^{l_3} K$, so that the dimensional equation is

$$\mathrm{M}^0\mathrm{L}^0\mathrm{T}^0 = \left(\mathrm{T}^{-1}\right)^{l_1} \mathrm{L}^{l_2} \left(\mathrm{ML}^{-3}\right)^{l_3} \mathrm{ML}^{-1}\mathrm{T}^{-2},$$

and considering the exponent of each dimension in turn,

$$\begin{array}{ccl} \mathrm{M} & : & 0 = l_3 + 1 \\ \mathrm{L} & : & 0 = l_2 - 3l_3 - 1 \\ \mathrm{T} & : & 0 = -l_1 - 2, \end{array}$$

From this we have immediately $l_1 = -2$, $l_3 = -1$, and solving the remaining equation, $l_2 = -2$. Hence we have

$$\Pi_4 = \frac{K}{\rho N^2 D^2}.$$

5. $\Pi_5 = N^{m_1} D^{m_2} \rho^{m_3} d$, so that we can write the group by inspection

$$\Pi_5 = \frac{d}{D}.$$

Hence we have the relationship

$$\frac{gH}{N^2 D^2} = f\left(\frac{Q}{ND^3}, \frac{\mu}{\rho N D^2}, \frac{K}{\rho N^2 D^2}, \frac{d}{D}\right).$$

In fact, the quantity $K_H = gH/N^2D^2$ is the *head coefficient*, and $K_Q = Q/ND^3$ is the *flow coefficient*. As $ND$ has units of velocity, the quantity $\mu/\rho N D^2 = \nu/ND^2$ is $1/\mathbf{R}$, where $\mathbf{R}$ is the Reynolds number based on impeller diameter. The quantity $\varepsilon = d/D$ is the *relative roughness* of the machine's internal passages. It can be shown that the speed of sound in water $c = \sqrt{K/\rho}$, so that the remaining dimensionless number $K/\rho N^2 D^2 = c^2/(ND)^2 = 1/\mathbf{M}^2$, where $\mathbf{M}$ is the *Mach number* of flow in the machine. Hence we now can write

$$\frac{gH}{N^2 D^2} = f\left(\frac{Q}{ND^3}, \mathbf{R}, \mathbf{M}, \varepsilon\right). \tag{11.1}$$

Now consider the power required to drive the pump $P = \rho Q g H/\eta$. This gives

$$P = \rho Q N^2 D^2/\eta \times f\left(Q/ND^3, \mathbf{R}, \mathbf{M}, \varepsilon\right),$$

and replacing $Q \times f(Q/ND^3, \ldots)$ by $ND^3 \times f_1(Q/ND^3, \ldots)$, where $f_1$ is a different function of the same variables, this gives

$$\frac{P\eta}{\rho N^3 D^5} = f_1\left(Q/ND^3, \mathbf{R}, \mathbf{M}, \varepsilon\right),$$

the *power coefficient* $K_P$. The functional relationships between $gH/N^2D^2$, $Q/ND^3$, and $P/\rho N^3 D^5$ are determinable by experiment and constitute a set of performance characteristics which are the same shape as the $H$ and $P$ versus $Q$ characteristics, but represent the whole family of geometrically similar machines and are identical for all such machines if $\mathbf{R}$, $\mathbf{M}$, and $\varepsilon$ are the same. In general, of course, they are not, but it is a convenient approximation that the functions are weakly dependent on them.

## 11.6 Similarity laws

For all machines belonging to one family and operating under dynamically similar conditions, each of the dimensionless coefficients are the same, and so we have

$$\frac{Q}{ND^3} = \text{constant}, \tag{11.2}$$

$$\frac{gH}{N^2D^2} = \text{constant, and} \tag{11.3}$$

$$\frac{P}{\rho N^3 D^5 \eta} = \text{constant}. \tag{11.4}$$

With these relationships we can obtain the performance of a machine operating under different conditions from those which are known. This will be an estimate of course, as we have ignored the effects of the other variables.

Hence if we keep the same pump size ($D$ fixed)

$$Q_2 = Q_1 \frac{N_2}{N_1} \quad \text{and} \quad H_2 = H_1 \left(\frac{N_2}{N_1}\right)^2.$$

Hence if we know the new head $H_2$ we can calculate the required speed and hence the flow.

Often we need to consider pumps of different sizes. Thus operating at maximum efficiency for which the manufacturer's data gives us the values of

$$\frac{gH}{N^2D^2} \quad \text{and} \quad \frac{Q}{ND^3},$$

we have

$$\frac{gH_1}{N_1^2 D_1^2} = \frac{gH_2}{N_2^2 D_2^2} \quad \text{and} \quad \frac{Q_1}{N_1 D_1^3} = \frac{Q_2}{N_2 D_2^3}.$$

If we want to use this type of pump to deliver 5 times the flow and 2 times the head that the manufacturer chose to illustrate the performance of the pump, such that $Q_2 = 5Q_1$ and $H_2 = 2H_1$, then we can solve this pair of equations for $D_2/D_1$ and $N_2/N_1$:

$$\frac{N_2^2 D_2^2}{N_1^2 D_1^2} = 2 \quad \text{and} \quad \frac{N_2 D_2^3}{N_1 D_1^3} = 5, \text{ such that}$$

$$\frac{D_2}{D_1} = \left(\frac{25}{2}\right)^{1/4} \approx 1.9 \quad \text{and} \quad \frac{N_2}{N_1} = \left(\frac{8}{25}\right)^{1/4} \approx 0.75,$$

hence we need a pump about twice the size (linear dimension) of the one in the manufacturer's literature, which would operate at $3/4$ of the speed.

**Type number or specific speed:** The performance of machines belonging to different families may be compared by plotting their dimensionless characteristics on the same graph. Detailed comparison may then be achieved by analysing the various aspects of the sets of curves. A simpler method of machine classification is the use of *type number* or *specific speed*.

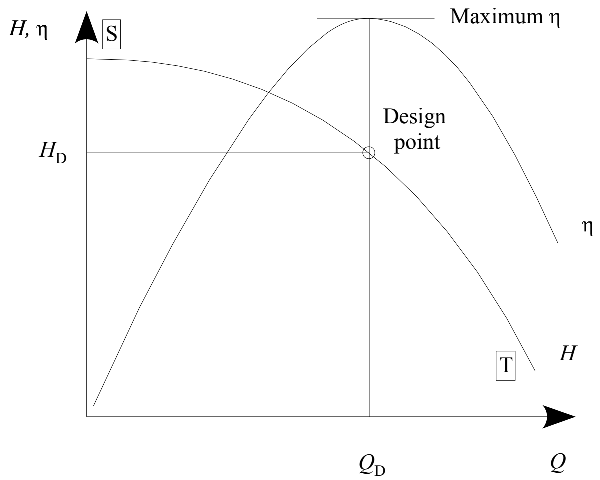


Figure 11-6. Design point on a pump characteristic.

Every machine is designed to meet a specific duty, usually referred to as the *design point* on its basic performance characteristic usually associated with the maximum efficiency of the machine. It is thus informative to compare machines by quoting the values of $K_H$, $K_Q$, and $K_P$ corresponding to their design points. for pumps $K_H$ and $K_Q$ are the two most important parameters, their relative size indicates the suitability of a particular pump for large or small volumes relative to the head developed. If their relative size is calculated such that the impeller diameter is eliminated from it, the comparison becomes independent of machine size. This is the type number $n_s$. Hence we write

$$n_s = \frac{\left(Q/ND^3\right)^i}{\left(gH/N^2D^2\right)^j},$$

and we choose the powers $i$ and $j$ such that $N$ appears to the power 1 and $D$ to the power zero, such that it disappears. Hence, $-i + 2j = 1$ and $-3i + 2j = 0$, with solution $i = 1/2$ and $j = 3/4$:

$$n_s = \frac{NQ^{1/2}}{(gH)^{3/4}}.$$

A value of type number can be calculated for any point on the characteristic curve. It will be equal to zero at point S on Figure 11-6 because there the flow is zero and will become large at T as the head is small. Such values are of no practical interest, and only *the* type number at the design point is used for classification, comparison, and design.

## 11.7 Series and parallel operation

Pumps may be arranged in series or parallel to achieve the effect required.

**Series arrangement – see Figure 11-7**

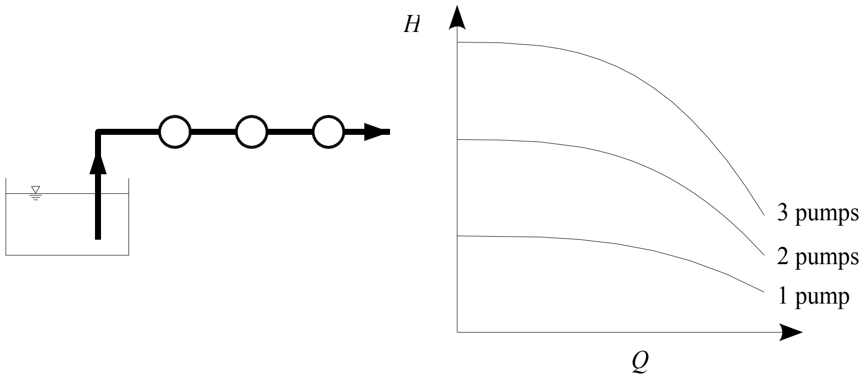


Figure 11-7. Three pumps in *series* and the characteristic curves of 1, 2, and all 3 pumps.

**Parallel arrangement – see Figure 11-8**

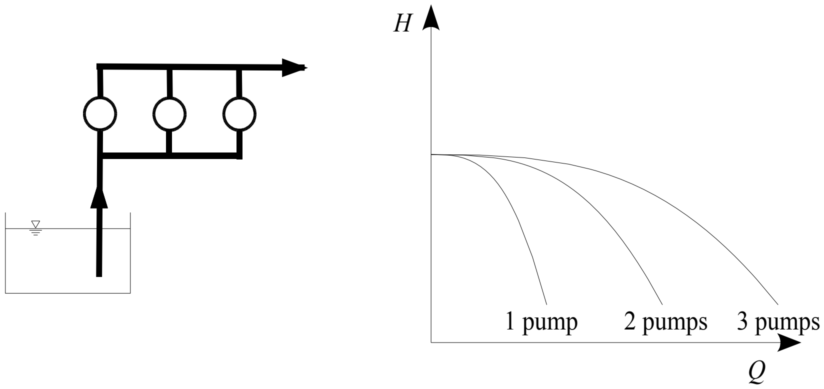


Figure 11-8. Three pumps in *parallel* and the characteristic curves of 1, 2, and all 3 pumps.

## 11.8 Euler equation for a rotor (impeller)

We have seen Conservation of Mass and Volume, Energy, and Momentum (three components) – now we have Conservation of Moment of Momentum (often called Angular Momentum), which also has three components, but it is rare that more than one of these equations is needed. A one-dimensional (radial) approximation is used which simplifies the problem very much. Consider the centrifugal impeller shown in Figure 11-9, rotating with angular velocity $\omega$:

- Flow enters the impeller at 1, where the radius is $r_1$, and then flows along a typical streamline shown dashed (in the steady frame of the impeller) to point 2, radius $r_2$, where it leaves the impeller and enters, possibly, another cascade of vanes.
- The absolute velocity at 1 is $v_1$, the tangential velocity of the impeller is $u_1$ so that the velocity of the fluid relative to the impeller is $v_{r_1}$, tangential to the impeller blades. The angle between the absolute velocity $u_1$ and a tangent to the impeller is $\alpha_1$. In this basic velocity triangle the absolute velocity is resolved into two components, one the radial direction velocity of flow $v_{f_1}$ and the other the velocity of whirl $v_{w_1}$.
- Similarly the outlet velocity triangle at 2 is constructed as shown. The relative velocity $v_{r_2}$ is now parallel to the rear of the blades, while the absolute velocity is parallel to a stationary outer cascade of vanes if they are present. It can be seen that the vanes in the impeller and in the outer cascade have very different angles, but

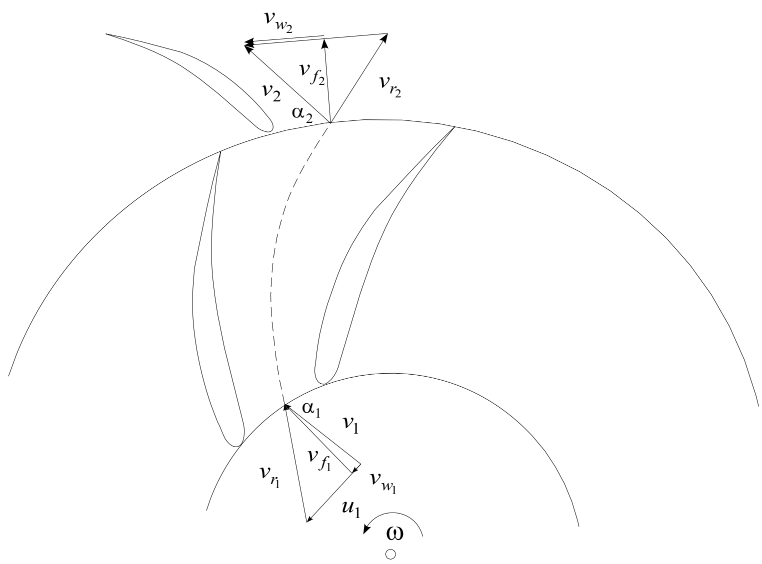


Figure 11-9. One-dimensional flow through a centrifugal impeller.

in each case the relative velocity is parallel to them.

The general expression for the energy transfer between the impeller and the fluid, usually referred to as Euler[18]'s turbine equation can now be obtained.

From Newton's second law applied to angular motion,

Torque $=$ rate of change of moment of momentum
Moment of momentum $=$ mass $\times$ tangential velocity $\times$ radius
Moment of momentum entering the impeller per second $= \dot{m} v_{w_1} r_1$
Moment of momentum leaving the impeller per second $= \dot{m} v_{w_2} r_2$,

where $\dot{m}$is the mass flow rate. Therefore

$$\text{Rate of change of moment of momentum} = \text{Torque transmitted} = \dot{m}\left(v_{w_2} r_2 - v_{w_1} r_1\right),$$

hence the rate of work being applied to the water is the product of torque and angular velocity:

$$\text{Work done per second} = \dot{m}\omega\left(v_{w_2} r_2 - v_{w_1} r_1\right),$$

but $u_2 = \omega r_2$ and $u_1 = \omega r_1$, hence

$$\text{Work done per second} = \dot{m}\left(v_{w_2} u_2 - v_{w_1} u_1\right),$$

and the rate of energy transfer per unit mass of fluid flowing is $v_{w_2} u_2 - v_{w_1} u_1$, and so dividing by $g$ to bring to units of head, we find that the theoretical head developed is:

$$H = \frac{u_2 v_{w_2} - u_1 v_{w_1}}{g},$$

which is Euler's equation. It is useful to express Euler's head in terms of the absolute fluid velocities rather than components. We have

$$v_{w_1} = v_1 \cos\alpha_1 \quad \text{and} \quad v_{w_2} = v_2 \cos\alpha_2,$$

so that

$$H = \frac{u_2 v_2 \cos\alpha_2 - u_1 v_1 \cos\alpha_1}{g}.$$

[18] Leonhard Euler (1707-1783), Swiss mathematician and physicist, remarkable genius.

However, from the cosine rule,

$$v_{r_1}^2 = u_1^2 + v_1^2 - 2u_1 v_1 \cos\alpha_1,$$

so that $u_1 v_1 \cos\alpha_1 = \frac{1}{2}\left(u_1^2 - v_{r_1}^2 + v_1^2\right)$, with a similar result for 2, giving

$$H = \underbrace{\frac{v_2^2 - v_1^2}{2g}}_{\text{A}} + \underbrace{\frac{u_2^2 - u_1^2}{2g}}_{\text{B}} + \underbrace{\frac{v_{r_1}^2 - v_{r_2}^2}{2g}}_{\text{C}}.$$

Term A denotes the increase of kinetic energy of the fluid in the impeller. Term B represents the energy used in setting the fluid in circular motion about the impeller axis. Term C is the regain of static head due to a reduction of relative velocity in the fluid passing through the impeller.

## 11.9 Water turbines

Turbines are used to extract energy from water – the reverse of pumps. A typical hydro-electric power station will have several, each directly coupled to an electric generator There are three main types, the Pelton wheel, which is an *impulse turbine*, and the Francis turbine and the axial flow Kaplan turbine, both of which are *reaction turbines*. Below are presented three photographs of turbines and of one pump in the Michell Hydraulics Laboratory at Melbourne University, with thanks to Ms Pam Doughty, Webmaster of the Civil and Environmental Engineering Department and Mr Joska Shepherd, Technician in Charge of the Laboratory.

(a) Francis turbine

(b) Francis turbine from other side

(c) Pelton wheel, including deflector vane

(d) Submersible de-watering pump & Joska Shepherd

Table 11-1. Examples of rotating machines in the Michell Laboratory

### 11.9.1 Reaction turbines

**Francis turbines:** In reaction turbines, such as the Francis turbine in (a) and (b) of Table 11-1, the fluid first passes around the snail-shell like volute around the periphery of the turbine (see (a)), and then through a ring of stationary guide vanes or *wicket gate* (see (b)) in which only part of the head is converted into kinetic energy. The guide vanes discharge onto the runner along the whole of its periphery such that the fluid entering the runner has pressure as well as kinetic energy. The pressure energy is converted into kinetic energy in the runner (the passage running full). In fact, the situation looks very similar to the centrifugal pump vanes shown in Figure 11-9, but where everything runs in reverse. Examples are most of the power stations in the Kiewa scheme in Victoria, or the Snowy Mountains scheme.

**Axial-flow or Kaplan turbines:** Another common type of reaction turbine which is used in lower-head installations, is the Kaplan or axial-flow turbine, which looks rather like a large air-fan with wide blades, but which also acts in reverse. These are typically used in power stations which are in dams across a river, such as at Yarrawonga on the Murray River or stations on the Derwent River in Tasmania.

## 11.9.2 Impulse turbines

In impulse turbines, such as the Pelton wheel, as in entry (c) in Table 11-1, the total head available is first converted into kinetic energy in one or more nozzles operating at atmospheric pressure. The jet(s) of water strike ”buckets” of elliptical shape attached to the periphery of a rotating wheel. The jet of water strikes the bucket, is split symmetrically so that there is no extra thrust along the axis of the wheel, and is deflected back roughly in the direction whence it came, thereby imparting momentum to the bucket and the wheel. The total head available at the nozzle is equal to the gross head less losses in the pipeline leading to the nozzle. These are used for high-head installations.

Since a Pelton wheel which drives an electrical generator should rotate at constant speed, the only way to control it and increase or decrease load when required is to control the discharge $Q$, which is done by means of a needle (spear) valve in the nozzle. The water will still emerge at the same speed, but the power provided will be different. For cases of sudden load removal, because it is not possible to close the valve quickly without causing high-pressure surges in the penstock or supply line, deflector plates are used so that the jet of water can be quickly deflected from the wheel but without causing damaging transients in the supply line. Gradually the needle valve will move to the new position and the deflector returns to its original position, not interfering with the flow.

| | Pelton | Francis | Kaplan |
|---|---|---|---|
| Type number $n_s$(using $N$ in $\mathrm{rad\,s^{-1}}$) | 0.05 – 0.4 | 0.4 – 2.2 | 1.8 – 4.6 |
| Operating head ($\mathrm{m}$) | 100 – 1700 | 80 – 500 | Up to 400 |
| Maximum power output (MW) | 55 | 40 | 30 |
| Best efficiency ($\eta$%) | 93 | 94 | 94 |
| Regulation mechanism | Spear valve & deflector plate | Guide vanes, surge tanks | Blade feathering |

Table 11-2. Comparison of water turbines

Table 11-2 shows a comparison of the three types of turbines which are used to drive electric generators.